Reversible Deficiencies in Flagellar Beating and Axonemal Assembly

Mei Wei
Marquette University

REVERSIBLE DEFICIENCIES IN FLAGELLAR BEATING
AND AXONEMAL ASSEMBLY

by

Mei Wei, B.S.

A Dissertation submitted to the Faculty of the Graduate School,
Marquette University,
in Partial Fulfillment of the Requirements for
the Degree of Doctor of Philosophy

Milwaukee, Wisconsin

December 2010

ABSTRACT
REVERSIBLE DEFICIENCIES IN FLAGELLAR BEATING
AND AXONEMAL ASSEMBLY

Mei Wei, B.S.

Marquette University, 2010

Axonemal complexes in flagella are largely prepackaged in the cell body. As such, one mutation often results in the absence of the co-assembled components and permanent motility deficiencies. For example, a *Chlamydomonas* mutant defective in RSP4 in the radial spoke, which is critical for bend propagation, has paralyzed flagella that also lack the paralogue RSP6 and three additional radial spoke proteins. Intriguingly, recent studies showed that several mutant strains contain a mixed population of swimmers and paralyzed cells despite their identical genetic background. Here we report a cause underlying these variations. Two new mutants lacking RSP6 swim processively and other components appear normally assembled in early log phase indicating that, unlike RSP4, this paralogue is dispensable. However, swimmers cannot maintain the typical helical trajectory and reactivated cell models tend to spin. Interestingly the motile fraction and the spoke head content dwindle during stationary phase. Chemical cross-linking supports a model that RSP4/6 paralogues and the pair of the MORN-motif proteins in the spoke head form a symmetric module. These results suggest that (1) intact radial spokes are critical for maintaining the rhythm of oscillatory beating and thus the helical trajectory; (2) the symmetric module could guide tilt-return cycles of the spoke head against the central apparatus; (3) assembly of the axonemal complex with subtle defects is less efficient and the inefficiency is accentuated in compromised conditions, leading to reversible dyskinesia. Consistently, several organisms only possess one RSP4/6 gene. Gene duplication in *Chlamydomonas* enhances radial spoke assembly to maintain optimal motility in various environments.

ACKNOWLEDGEMENTS

Mei Wei, B.S.

I would like to express my great appreciation to Dr. Yang for her invaluable instructions and support during the past five years. I have been amazingly fortunate to have her as my advisor. She is so insightful in both doing research and training students. This dissertation could not have been possible without her encouragement and constant guidance. I will never forget the advice she gave me and our discussions on experiments, projects, life and my future career.

I would also like to thank all my committee members, Dr. Waring, Dr. Schläppi, Dr. Stuart and Dr. Eddinger for their very precious advice on my research and dissertation. Their suggestions make my research follow the right track and also greatly open my mind to think broadly and deeply.

I would like to acknowledge Dr. David R Mitchell for offering two *Chlamydomonas* strains and our lab members Dr. Chun Yang, Dr. Radhika Gopal, Priyanka Sivadas, Stephanie Davis and Anjali Gupta for their cooperation and support.

My deepest gratitude goes to my family for their love and support throughout my life. I would like to thank my parents for their faith in me and allowing me to pursue my dreams thousands of miles away from home. Particularly, I would like to thank my husband Xintong Wang for his understanding, patience and love during the past few years.

TABLE OF CONTENTS

LIST OF TABLES

LIST OF FIGURES

Chapter 1: Introduction

1.1 Significance of Motile Cilia and Flagella

Motile cilia and flagella play crucial roles for eukaryotes. They enable simple organisms to execute directed movement that is critical for survival like feeding, mating and avoiding hazardous environment. The motility is also integral to normal functions of several vital systems in multicellular organisms. For example, a flagellum propels sperm to reach the egg. In the respiratory system, motile cilia sweep away mucus along with the trapped debris and pathogens. In the brain ventricles, ependymal cilia propel cerebral spinal fluid, guiding neuroblasts to migrate with the fluid flow (Sawamoto et al., 2006). Defective motility may lead to symptoms including infertility, chronic lung infection and hydrocephaly. These symptoms are collectively referred to as primary ciliary dyskinesia (PCD) (Lie and Ferkol, 2007). Identifying the key components and elucidating the motility mechanism are necessary to better understand this incredible biological machine and diagnose PCD, a serious yet rather common polygenic disorder due to the defect of this biological machine.

1.2 The Motile Machinery: 9+2 Axonemes

The majority of motile cilia and flagella are supported by a 9+2 axoneme, a highly conserved microtubule scaffold associated with remarkably elaborate molecular complexes (Figure 1-1). In the 9+2 axoneme, a central pair of singlet microtubules is surrounded by nine double microtubules, which form an elongated cylinder protruding from the basal body in the cell body. The dynein motor complexes anchor on the A

A
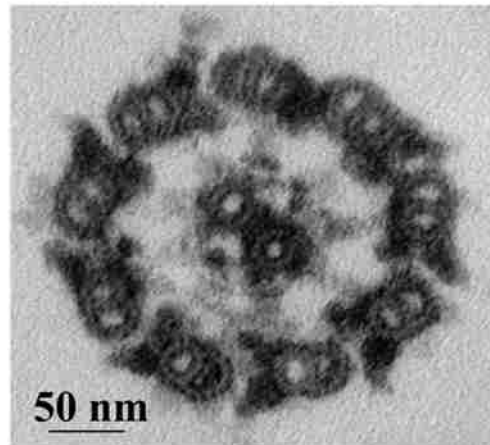
B
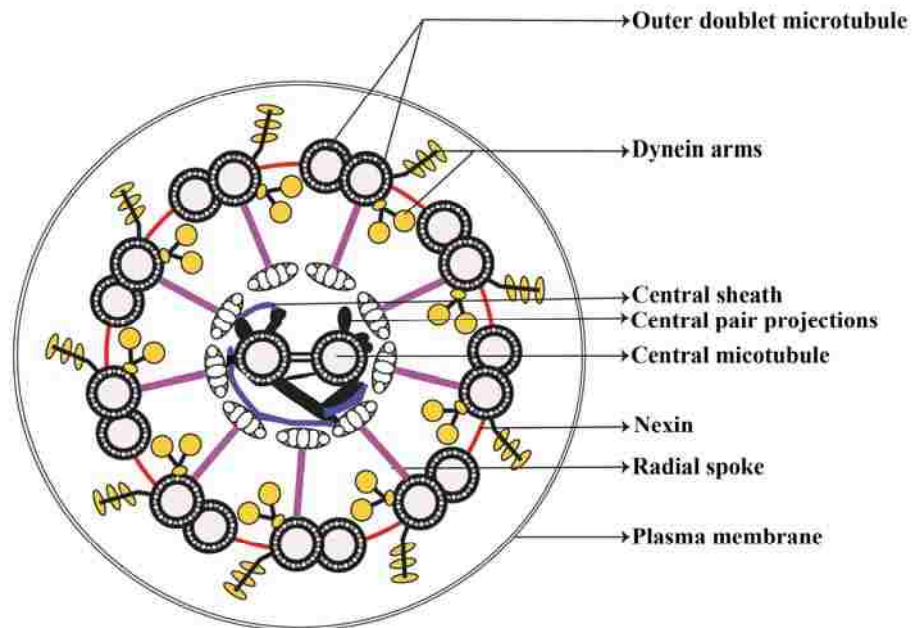
Figure 1-1. The cross section of the 9+2 axoneme.
Electron microscopy (EM) of *Chlamydomonas* axoneme and the
schematic diagram.

tubule of each outer doublet and project toward the neighboring outer doublet. In addition, the radial spoke, also anchored on the A tubule, projects inward toward the central apparatus. These axonemal complexes are positioned at precise locations in each 96-nm repeat.

The oscillatory beating of motile cilia is based on the dynein-driven inter doublet sliding (Summer and Gibbons, 1971). The motors engage the adjacent outer doublet and walk toward the minus end of the outer doublet while hydrolyzing ATP. The dynein-driven movement results in sliding between adjacent outer doublets. Constrained by the attachment to the basal body and by structural linkers between the doublets, the inter-doublet sliding is converted to bending and ultimately oscillatory beating (Smith and Yang, 2004).

In contrast to the motors, the mechanisms of radial spokes and the central apparatus are less clear. The central apparatus is composed of C1 and C2 microtubules and several associated projections interconnected by a barely visible central sheath (Figure 1-1B). The radial spoke, mostly appearing like a T or drumstick shaped, consists of a thin stalk that is anchored to the doublet microtubule, adjacent to dynein motors, and a bulbous head seeming juxtaposed to the central pair projections (Figure 1-1). Depending on the organism, radial spokes are present in doublets or triplets in each 96 nm repeat along each outer doublet microtubule (Warner and Satir, 1974). Radial spokes and the central apparatus are crucial for the motility of 9+2 axonemes. Mutants lacking a significant portion of either structure are paralyzed (Witman et al., 1978). Consistently, they are retained in most motile cilia and flagella. Defects in these complexes have been found in a fraction of PCD patients.

1.3 The Role of the Central Apparatus and Radial Spokes

In theory, dyneins on the 9 outer doublets are regulated to generate typical ciliary and flagellar bending. There are thousands of motors along the length and around the circumference of the axonemes. If all of the dynein motors simultaneously undergo a power stroke, the flagella will become rigid. Only sequential activation of the motors can allow bend formation and propagation.

Independent lines of evidence suggest that the central apparatus and radial spokes are regulatory complexes. One is the study of suppressor mutants. Although *Chlamydomonas* mutants missing radial spokes or the central apparatus are paralyzed, additional mutations rescue the paralysis of these mutants without restoring either structure (Huang et al., 1982). Importantly, the suppressor mutations occur in genes encoding outer dyneins (Huang et al., 1982; Porter et al., 1994), inner dyneins (Porter et al., 1992) or polypeptides from dynein regulatory complex that are located near the radial spoke and dynein motors (Piperno et al., 1992, 1994). It was predicted that absence of the central apparatus or radial spokes results in the inhibition of the dynein activity, while the suppressor mutations bypass the inhibition to restore motility (Huang et al., 1982; Piperno et al., 1992, 1994). Yet, flagellar waveform of these suppressor mutants is more symmetric, contrary to the asymmetric waveform of wild type (WT) flagella. It was postulated that the central apparatus and radial spokes convert symmetric waveform for backward swimming to asymmetric waveform for forward swimming (Brokaw et al., 1982).

Secondly, the paralyzed *Chlamydomonas* axoneme missing the central pair apparatus or radial spokes can be reactivated to beat in vitro as WT axonemes. However,

the reactivation conditions have to be modified such as reduction of ATP concentration from ~1 mM to μM level or applying ATP analogs (Yagi and Kamiya, 2000; Frey et al., 1997; Omoto et al., 1996). Furthermore, 9+0 axoneme in nodal cilia or even those with 3+0 axoneme are motile (Nonada et al., 1998; Prensier and Vivier, 1980). Yet the movements of 9+2 and 9+0 cilia and flagella differ. Nodal cilia lacking the central apparatus and radial spokes beat with low frequency with primitive 3-dimensional waveforms of shallow amplitude (Okada et al., 1999). Similarly the movement of reactivated paralyzed flagella is slow and less asymmetric (Omoto et al., 1996), while 9+2 cilia and flagella tend to beat with planar waveforms of larger amplitude and at high frequency.

Different beating may serve distinct purposes. High frequency beating with a planner waveform could sweep cell body or mucus. However, the powerful movement may be inappropriate for nodal cilia, which may establish a morphogen gradient that determines the development of left-right asymmetry (Nonaka et al., 2002).

These collective findings suggest that the central apparatus and radial spokes operate as a higher-order system to control the primitive movements driven by the dynein motors on the 9 outer doublets (Kamiya, 2002).

1.4 The Radial Spoke, a Postulated Mechano-transducer
Several hypotheses are proposed to explain the control mechanism of the axoneme. Thin section electron microscopy (EM) of instantly fixed beating cilia showed that in the straight regions, the radial spokes are perpendicular to outer doublets and appear to attach to the central pair projections while at the region of bend, the radial spokes appear tilted.

Distal to the bend, the spokes heads appear reattaching to a more distal region of central pair projections while the base of spoke stalk always attaches to the outer doublet (Warner and Satir, 1974). It was predicted that radial spokes tilt against the central apparatus along the longitudinal axis of the axoneme as cilia bend. These morphological studies predict that the central apparatus transiently interacts with the radial spokes to regulate the bend formation and propagation.

Interestingly, the asymmetric central apparatus rotates once per beat in many, but not all, motile cilia and flagella (Tamm and Tamm, 1981; Omoto et al., 1999). The rotation of the asymmetric central apparatus with different projections may induce spoke tilting relative to the circumferential axis as well, providing additional regulatory mechanism for the fine control of flagellar motility (Smith and Yang, 2004). The cycles of detachment and reattachment of the radial spokes with the central apparatus accompanying with the radial spoke tilting longitudinally and circumferentially may control dynein activity to generate a wide range of motility.

As the only structure within axonemes that exhibits obvious asymmetry, the asymmetric central apparatus may specify dynein activity on subsets of doublet microtubules. Using in vitro microtubule sliding assay in *Chlamydomonas*, Wargo and Smith, 2003 showed that the C1 central microtubule is oriented toward the position of active microtubule sliding. This correlation is abolished in radial spoke mutants, suggesting that the C1 central microtubule regulates dynein activity on specific subsets of doublet microtubules through interactions with the radial spokes. The relationship between flagellar bends and orientation of the central apparatus is also revealed by observation of EM of rapidly fixed *Chlamydomonas* cells (Mitchell, 2003). In a similar

way, the central apparatus is parallel to the bend plane throughout the principal bends in both power stroke and recovery stroke of the beat cycle. C1 central microtubule always faces the outer edge of the curve.

Taken together, it was postulated that transient interaction between the asymmetric central apparatus and radial spokes transduces mechanical signals to activate dynein motors in specific subsets of outer microtubules (Smith and Yang, 2004). The mechanical signals may physically pull or push dynein motors and the outer doublets (Sakakibara et al., 2004).

1.5 The Radial Spoke, a Postulated Chemical-transducer

The central apparatus and radial spokes are also involved in the alteration of flagellar motility triggered by second messengers. Calcium and cNMP regulate ciliary and flagellar beating universally (Smith and Yang, 2004). For example, cAMP inhibits reactivation of *Chlamydomonas* axonemes (Hasegawa et al., 1987) while different calcium concentrations trigger distinct motility changes. In the presence of 10^{-8} M calcium, reactivated axonemes beat with a highly asymmetric and planar waveform. When the calcium concentration is increased from 10^{-8} to 10^{-4} M, the movement becomes quiescent followed by a switch from asymmetric waveform to symmetric waveform (Bessen et al., 1980; Kamiya and Witman, 1984). Since isolated axonemes are sensitive to second messengers, it is predicted that the regulatory elements responsive to the second messengers are built into the axoneme. The putative regulatory molecules include second-messenger dependent kinases and phosphatases, such as PKA (cAMP-dependent

Protein Kinase A), PKG (cGMP-dependent Protein Kinase), calmodulin and calcium-binding proteins.

The microtubule sliding assay of paralyzed axonemes revealed that some regulatory elements are located in the radial spokes. Despite the paralyzed axoneme of *Chlamydomonas* radial spoke mutants, these axonemes undergo dynein-driven microtubule sliding in the presence of protease. However the velocity is greatly reduced compared to WT axonemes (Smith and Sale, 1992; Smith, 2002).

Interestingly, the reduced microtubule sliding velocity is restored upon reconstitution with dyneins from WT axonemes or addition of kinase inhibitors. PKA and casein kinase 1(CK1) inhibitors restore WT dynein activity to the axonemes from radial spoke mutants (Yang and Sale, 2000; Howard et al., 1994). These experiments predict that these kinases inhibit dynein activity and radial spokes function to release the inhibition. These findings are consistent with the observation that cAMP, the major activator of PKA, inhibits the reactivation of WT axonemes (Hasegawa and Kamiya, 1987). Conversely, inhibitors against protein phosphatase 1 (PP1) and protein phosphatase 2A (PP2A) reverse the effect of PKA and CK1 (Habermacher et al., 1996; Yang and Sale, 2000). The prediction is supported by the discoveries that these two phosphatases were stably associated with the axonemes (Yang et al., 2000).

The discovery of an A-kinase anchor protein (AKAP) in the radial spoke further supports the notion that radial spokes modulate dynein activities via PKA. It was found that radial spoke protein 3 (RSP3) binds to RII, the regulatory subunit of PKA in an overlay assay designed to reveal AKAPs (Gaillard et al., 2001). Furthermore, the PKA inhibitor improves the motile fraction of reactivated axonemes with mutations in the PKA

binding domain of RSP3 (Gaillard et al., 2006). The study predicts that the unanchored kinase inhibits the dynein motors and inhibition of the kinase rescues the motility. However, although much evidence suggested the presence of PKA in *Chlamydomonas* axoneme (Hasegawa et al., 1987; Howard et al., 1994; Yang and Sale, 2000; Smith 2002), the precise axonemal locations remained unknown.

Several substrates of phosphoenzymes have been identified. Most of them are subunits in dynein motor complexes. In *Paramecia*, cAMP-mediated phosphorylation of one dynein chain significantly increases the swimming velocity in vitro (Hamasaki et al., 1991; Smith and Yang, 2004). In *Tetrahymena*, phosphorylation of dynein motors greatly improves in vitro microtubule translocation velocity compared with its unphosphorylated counterpart. (Christensen et al., 2001; Smith and Yang, 2004).

In *Chlamydomonas*, the activity of inner dynein arm subform I1, located adjacent to the radial spoke, is required for phosphoregulation of microtubule sliding (Porter and Sale, 2000). Although kinase inhibitors restore the slow sliding of radial spoke defective axonemes, these inhibitors do no affect the axonemes defective in both radial spokes and I1(Yang and Sale, 2000; Habermacher and Sale, 1997). Furthermore, IC138, an intermediate chain subunit of I1, is hyper-phosphorylated and I1 activity is inhibited in radial spoke mutants (Habermacher and Sale, 1997; Hendrickson et al., 2004). Mutants with hyper-phosphorylated IC138 or defective I1 is defective in photoresponse, a motility change due to the light stimulus and subsequent increased concentrations of calcium (King and Dutcher, 1997; Perrone et al., 2000). Taken together, these studies indicate that the radial spokes modulate dynein motors, I1 and IC138 in particular, via coupling a network of phosphoenzymes anchored to the axonemes.

Aside from the cAMP-dependent signaling, radial spokes and the central apparatus are implicated in calcium-dependent motility changes. In microtubule sliding assays, high calcium restores dynein activity of central pair defective axonemes, not radial spokeless mutants, to WT level (Smith, 2002). Consistently, calmodulin inhibitors reverse the effect of high calcium. Biochemical studies reveal calmodulin, a calcium binding protein, is a constitutive subunit in the radial spokes and central apparatus (Yang et al., 2001; Dymek et al., 2002). In addition, two spoke proteins, RSP2 and RSP23, contain calmodulin binding motifs and bind to calmodulin in a calcium-dependent and – independent manner in vitro (Yang et al., 2004; Patel-King et al., 2004). In parallel, the central apparatus is also involved in the calcium-dependent regulation in the flagella of sea urchin sperm (Bannai et al., 2002; Nakano et al., 2003). These observations imply that calcium alters dynein-driven microtubule sliding and the central apparatus and radial spokes are involved in this calcium signaling pathway (Smith EF, 2002). Collectively, these independent lines of evidence support a model that radial spokes and the central apparatus modulate dynein activity via a network of phosphoenzymes and calcium sensors (Smith and Sale, 1992; Smith and Yang, 2004).

In summary, these studies suggest that the radial spoke is a structure complex that transduces mechanical and chemical signals for modulating dynein-driven flagellar beating. The physical contact between the central apparatus and radial spokes appears to specify dyneins activity on specific subsets of double microtubules to generate oscillatory and planar waveforms typical of eukaryotic cilia and flagella. Specific signals may change the property of the radial spokes by phosphorylation and calcium binding to modulate flagellar motility.

1.6 The Composition and Assembly of *Chlamydomonas* Radial Spokes

Elucidation of the mechanisms of motile cilia and flagella largely relied on

Chlamydomonas reinhardtii, a biflagellate unicellular green alga. The combined

experimental advantages have made *Chlamydomonas* as an unparalleled model organism

to study motile cilia and flagella.

Biochemical approaches that are possible for *Chlamydomonas* were taken to

reveal the constituents in the radial spoke. Comparison of a two-dimensional (2-D) map

of axonemal proteins prepared from WT and radial spoke mutants as well as isolated

radial spokes have revealed that the radial spoke contains at least 23 proteins (Table 1-1)

(Piperno et al., 1977, 1981; Yang et al., 2001; Patel-King et al., 2004). Comparison of the

missing components in the mutant lacking the bulbous spoke head and the entire spoke

complex concluded that five of these proteins (RSP1, 4, 6, 9, 10) are located in the spoke

head whereas the rest are present in the stalk (Piperno et al., 1977; Huang et al., 1981).

Within the radial spoke head, there are two pairs of homologous spoke head

proteins. RSP1 and RSP10 share common MORN (for "membrane occupation and

recognition nexus") motifs and the former contains an extended C-terminus. RSP4 and

RSP6 are encoded by tandomly aligned duplicated genes. They are highly similar,

sharing 46% amino acid identity and are evolutionally conserved (Figure1-2) (Curry and

Rosenbaum, 1992). They do not contain obvious known molecular domains. The two

pairs of homologues are consistent with the ultrastructure revealed by freeze-etch EM of

Tetrahymena cilia (Goodenough and Heuser, 1985). The ciliate's spoke head appears to

be a tetrameric module consisting of two central globules and two lateral hooks (Figure

1-3).

Table 1-1. *Chlamydomonas* **radial spoke proteins.**

RSP*	pI/Mr (2D-NEPHGE)	pI/Mr (Theroetical)	Mutants
RSP1	5.2/ 123	4.55/ 78.6	
RSP2	5.0/ 118	4.48/ 77.4	*pf*24
RSP3	5.5/ 86	4.85/ 56.8	*pf*14
RSP4	5.1/ 76	4.58/ 49.8	*pf*1
RSP5	5.1/ 69	4.68/ 55.9	
RSP6	5.1/ 67	4.53/ 48.8	*pf*26
RSP7	5.1/ 58	4.54/ 55	
RSP8	6.5/ 40	5.76/ 40.5	
RSP9	5.7/ 26	5.02/ 29.5	*pf*17
RSP10	5.6/ 24	5.02/ 23.5	
RSP11	4.8/ 22	4.53/ 21.5	*pf*25
RSP12	6.3/ 20	5.46/ 19.7	
RSP13	6.3/ 98		
RSP14	6.8/ 41	5.84/28.3	
RSP15	5.7/ 38		
RSP16	7.1/ 34	6.78/ 39.0	
RSP17	6.2/ 124	5.56/ 98.5	
RSP18	5.4/ 210		
RSP19 (β-tubulin)	5.5/ 140	4.82/ 49.6	
RSP20 (calmodulin	4.3/ 18	4.3/ 18.3	
RSP21	6.2/ 16		
RSP22 (LC8)	6.8/ 8	6.89/ 10.3	
RSP23	5.4/ 102	4.67/ 61	

* Radial spoke head proteins are indicated by white charcters on a black background

Figure 1-2. The alignment of amino acid sequences of RSP4 and RSP6 orthologues.
Identical residues, in black shade; residues with similar properties, in gray shade.
CRRSP4 and CRRSP6, *Chlamydomonas* RSP4 and RSP6; HS294004 and HS110412, two human orthologues.

A
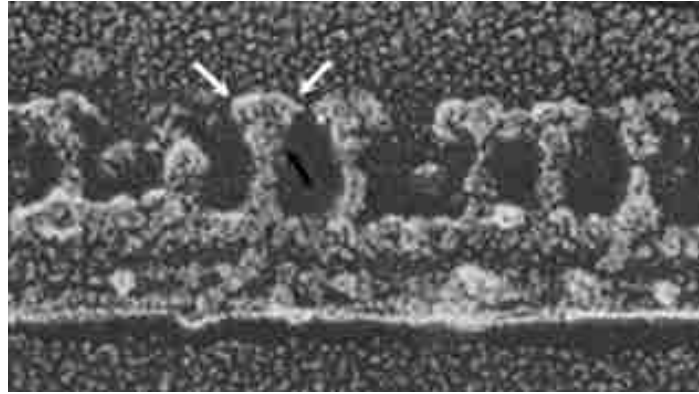
B
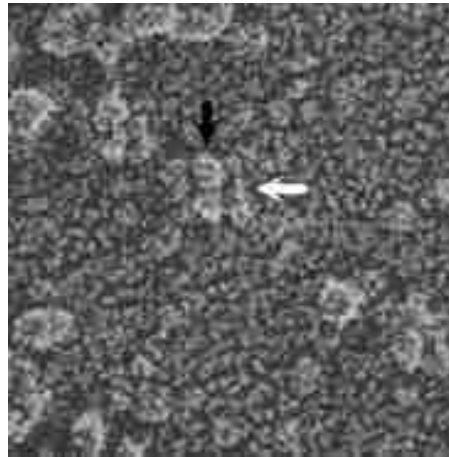
Figure 1-3. Freeze-etch EM of spoke heads in *Tetrahymena* cilia.
(A) The image of the longitudinal fracture of the axoneme showed that each spoke head has a central domain (black arrow) and two lateral domains (white arrow). (B) In *en face* view, the spoke head appeared as a tetramer with two central globular units (black arrow) flanked by two lateral units (white arrow) (modified from Goodenough and Heuser, 1985).

Among the stalk proteins, RSP2, 5, 16, 23 are postulated to reside adjacent to the spoke head. In the RSP2 mutant *pf24*, RSP2, RSP16 and 23 are diminished while spoke head proteins are reduced (Huang et al., 1981). In contrast, the rest of the spoke stalk proteins are present in normal amounts. This suggests that RSP2, 16, 23 are located near the junction between the radial spoke head and spoke stalk. The prediction for RSP5 is based on the observation that RSP5 is coextracted with spoke head proteins by low ionic solution (Piperno et al., 1981). The rest of the spoke stalk proteins including RSP3, are proposed to be located toward the base of the spoke stalk. RSP3 is involved in binding radial spokes to the outer doublets. For example, *pf14*, a mutant defective in the RSP3 gene, lacks the entire radial spoke (Piperno et al., 1981). Recombinant RSP3 binds to radial spokeless axonemes and the binding site is mapped to its N-terminus (Diener et al., 1993).

Molecular domains that are involved in the predicted chemical signaling of radial spokes are exclusively located in the spoke stalk (Figure 1-4). For example, RSP2 and RSP23 contain calmodulin-binding motifs. RSP23 also has an NDK domain that converts NDP to NTP. RSP8 and 14 have armadillo repeats that function in protein-protein interactions. Interestingly, the RIIa domain responsible for targeting RII and PKA to AKAPs are found in two radial spoke proteins, RSP7 and RSP11, yet they do not contain other signature features for cAMP binding or kinase catalysis. Nonetheless, RSP11 binds to recombinant RSP3 (Yang and Yang, 2006). Thus although RSP3 binds PKA RII in vitro, the mechanism that radial spokes regulate dynein activity via PKA is not straight forward. The molecular composition in the radial spoke suggests that the radial spoke head is a structural complex specialized for the transient interaction with the
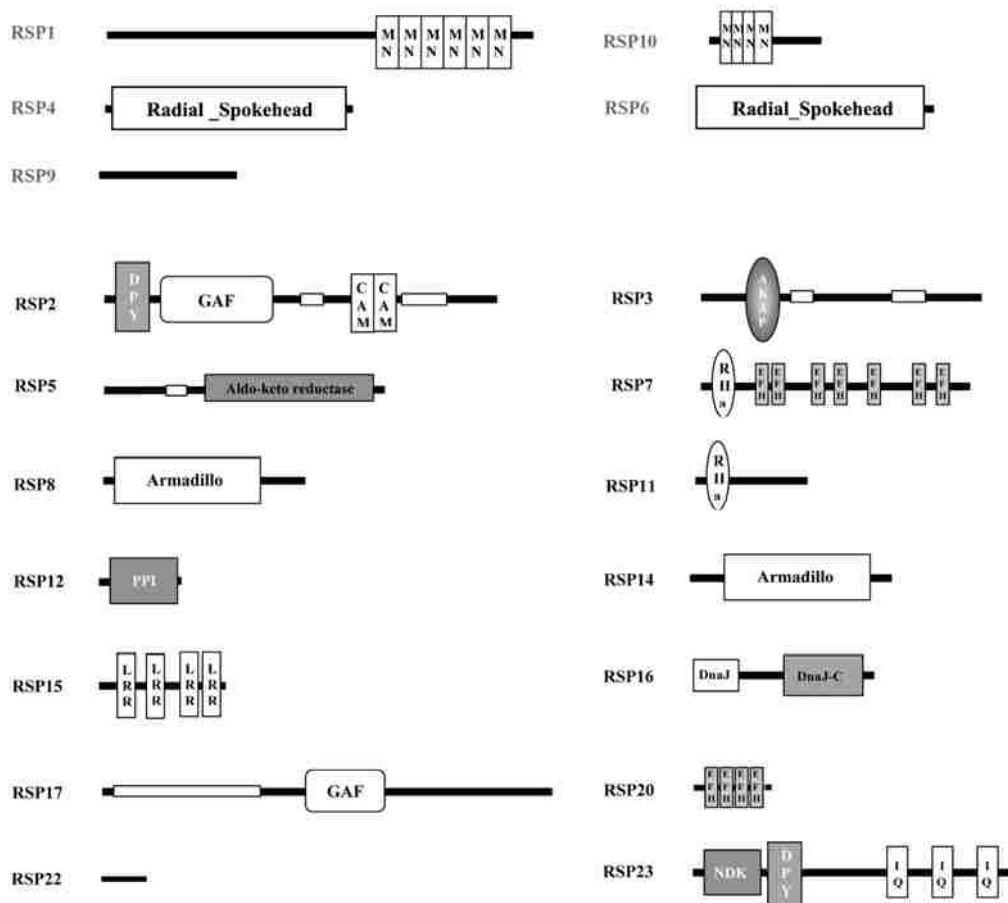
Figure 1-4. Predicted functional domains of radial spoke proteins.
The five spoke head proteins (RSP1, 4, 6, 9, 10) are highlighted in gray. MN, MORN domain; DPY, Dpy-30 motif; GAF, cyclic GMP, Adenylyl cyclase, FhlA domain; CAM, 1-8-14 calmodulin-binding motif; AKAP, A-Kinase Anchoring Protein motif; RIIa, RII alpha motif; EFH, EF-hand domain; PP1, peptidyl prolyl isomerase motif; LRR, leucine-rich repeat; DnaJ and DnaJ-C, DnaJ-J and DnaJ-C molecular chaperone homology domains; NDK, NDK domain; IQ, IQ calmodulin-binding motif. Coiled-coil domains are indicated by an open bar. The figure was modified from Yang and Smith, 2009.

central apparatus while the spoke stalk contains regulatory domains for the modulation of flagella motility.

Like other axonemal proteins, radial spoke proteins are synthesized in the cell body and transported into the flagella by an intraflagellar transport (IFT). Qin et al., 2004 demonstrated that the radial spoke proteins are largely preassembled as 12S precursor particles in the cell body. Anterograde IFT delivers the precursor to the flagellar tip where it is converted into the 20S mature radial spoke complex that is ultimately incorporated into microtubules. Moreover, the 20S radial spoke complex are disassembled from the axoneme and transported back to the cell body by retrograde IFT.

1.7 *Chlamydomonas* **Mutants with Defective Radial Spoke**

Chlamydomonas cells swim with a breast stroke-like beat. Mutagenesis studies have been conducted to select for strains displaying motilities that deviate from this typical movement, such as reduced beat frequencies, reduced bend amplitude, twitching and complete paralysis. Flagella from these mutants were found to be defective in dynein motors, central apparatus or radial spokes (Kamiya, 2002). Existing radial spoke mutants are summarized in Table 1-2.

Studies on radial spoke mutants have revealed important information about radial spokes. The majority of mutants are defective in more than one radial spoke protein, suggesting that radial spokes and other axonemal complexes are assembled into a sub-complex and missing one molecule will result in the absence of the sub-complex. For example, in the two radial spoke head mutants *pf1* and *pf17* which are defective in the genes encoding RSP4 and RSP9 respectively, absence of one spoke head protein leads to

Table 1-2. *Chlamydomonas* **radial spoke mutants.**

Mutants	Gene Product	Motility phenotype	Morphological defect	Protein missing	Proteins in reduced amount
pf1	4	Paralyzed	Headless	1,4,6,9,10	None
pf17	9	Paralyzed	Headless	1,4,6,9,10	None
pf26ts	6	Paralyzed at 32°C	None	None	1,4,6*, 9,10
pf14	3	Paralyzed	Spokeless	All spoke proteins	None
pf25	11	Swimming/Paralyzed	None	11	8
pf24	2	Paralyzed	Less spokeheads and stalks	None	1,4,6,9,10,2,16,23
pf5	?	Paralyzed	?	RSP13,15 Inner dynein protein 1 An unknown protein	?
pf27	?	Paralyzed	Less spokeheads and stalks	None	All spoke proteins

the absence of the other four spoke head proteins, and cells are completely paralyzed (Huang et al., 1981). In the two conditional mutants, *Pf25* and *pf26$_{ts}$* which are defective in the genes encoding RPS11 and RSP6 respectively, their motility deficiencies are less severe. The cells are motile under certain conditions.

The motility of *pf26$_{ts}$* is affected by the temperature during flagella elongation. Shifting temperature afterwards does not affect motility (Huang et al., 1981). When cells generate flagella at the permissive temperature and are then shifted to the restrictive temperature, cells still exhibit WT motility. However, cells are paralyzed if flagella elongation occurs at the restrictive temperature. The flagella contain normal or reduced amounts of spoke head proteins, including mutated RSP6, that is slightly smaller and has a more basic isoelectric point (pI). This result suggests that at the restrictive temperature, the mutation in RSP6 causes a conformational change, interfering with the assembly of the radial spoke head.

The motility of *pf25* is sensitive to the culture conditions (Yang and Yang, 2006). The mutant is defective in RSP11 gene. The mutant axonemes lack RSP11 and have reduced amount of RSP8, an armadillo repeat protein. The mutant cells in the log phase culture appear WT-like but become entirely paralyzed in spent media. After being cultured in fresh media for 2 days, the culture is teeming with swimmers again. The reason for this dramatic swing in *pf25* motility during the regular culture period is not known.

The first aim of the dissertation is to understand the mechanisms underlying this reversible paralysis. Toward this goal, I investigated two *Chlamydomonas* mutants that also displayed this motility change. Surprisingly, both mutants were allelic with *pf26$_{ts}$,*

but with rather different deficiencies in assembly and motility. The second aim is to use chemical cross-linking to reveal the molecular interactions in radial spokes that are critical for the oscillatory beating. Together, these findings revealed new insight in motility mechanism, assembly of axonemal complexes and the potential spectrum of cilia dyskinesia.

Chapter 2: Materials and Methods

Chemical, medium, oligonucleotides, antibodies used in the study are summarized in tables at the end of this chapter.

2.1 Cell Strains

2.1.1 *Chlamydomonas* Strains and Culture Conditions

Chlamydomonas reinhardtii WT strain *cc124(-), cc620(+), cc621(-)* and radial spoke mutant *pf26$_{ts}$* were acquired from the *Chlamydomonas* Resource Center (Duke University, Durham, NC). Two novel radial spoke head mutants 1C12 and 45G7 were obtained from Dr. David R Mitchell at Upstate Medical University, Syracuse, NY. The 1C12 strain was recovered from screening for motility mutants following exposure to ultraviolet radiation. The 45G7 strain was identified from a screen of insertional mutagenesis using pMN24 plasmid with the nitrogen reductase gene (*NIT1*) for metabolic selection (Mitchell and Sale, 1999).

All cells were grown on Tris-Acetate-Phosphate (TAP) agar plates for 6-7 days. A loop of cells was inoculated into ~300 ml TAP or Sager's liquid medium and cultured under aerated photoheterotrophic growth in 14/10 light/dark cycle (Harris, 2009).

2.1.2 Strain Maintenance

Chlamydomonas strains were maintained in TAP-agar stabs under light at room temperature. Bacterial stains were stored at -80°C in 50% glycerol (V/V).

2.2 Molecular Biology and Genetics

2.2.1 Polymerase Chain Reaction (PCR)

The 50-µl aliquot of PCR reaction mixture included 0.2 mM dNTPs, 10% DMSO, 0.2

pmol/µl of each primer, DNA template (either ~0.1 ng/µl plasmids or 1-3 µl supernatant

from boiled *Chlamydomonas* cells), 1.25 unit of pfu DNA polymerase and 1X pfu buffer.

The cycling reactions were performed using a thermocycler (Minicycler, MJ research).

The conditions, including 35 cycles between step 2-4 were as followed: step 1, 95°C for 3

minutes; step 2, 95°C for 90 seconds; step 3, 55°C -68°C, depending on the annealing

temperature of primers, for 90 seconds; step 4, 70°C for 3 minutes; step 5, 70°C for 10

minutes; step 6, 4°C.

2.2.2 Electrophoresis and Purification of DNA

DNA samples with 1X loading buffer (0.04% bromphenol blue and 2.5% ficoll 400) were

fractionated using 0.7-1% agarose gels made with 1X TAE buffer (0.04 M Tris base,

0.1% acetic acid, 1 mM Na_2EDTA, pH 8.5) and a trace amount of ethidium bromide.

Electrophoresis in 1X TAE running buffer was carried out at 100 V. Hi Lo DNA marker

(Bionexus) was included for the estimation of molecular weight and amount. DNA was

visualized by a UV transilluminator (UVP). For cloning the DNA fragment of interest

revealed by long-wavelength hand-held UV illuminator was excised from agarose gels

and purified using a gel extraction kit as described by manufacture (Qiagen).

2.2.3 Quantification of DNA

DNA concentration was measured by the absorbance at 260 nm using a Nano Drop

spectrophotometer (Thermo Scientific).

2.2.4 Digestion of DNA with Restriction Enzymes

DNA was digested at a ratio of 2 µl restriction enzymes (5-20 units from New England Biolabs) per 1 µg DNA in respective buffers at 37°C for 2 hours. Enzymes were inactivated by incubating the mixture at 65°C for 20 minutes.

2.2.5 DNA Ligation

Plasmid DNA was digested with the appropriate restriction enzymes and then dephosphorylated by treatment with shrimp alkaline phosphatase (Prche Applied Science) for 1 hour at 37°C followed by heat inactivation. The linear plasmid DNA and band-purified DNA inserts at a 1: 3 molar ratio were ligated with T4 DNA ligase (New England Biolabs) for 2 hours at room temperature. The ligation mixture was then used for transformation.

2.2.6 Transformation of *E.coli*

1 µl ligation mixture was added to 25 µl GC5 or GC10 competent cells (Gene Choice). After 30-minute incubation on ice, the mixture was heat shocked at 42°C for 45 seconds and returned to ice for additional 2 minutes. Following the addition of 1 ml LB medium and 1 hour recovery at 37°C, the mixture was evenly distributed to two LB agar plates containing appropriate selection antibiotics (50 µg/ml carbenicillin or 100 µg/ml kanamycin). For blue-white selection, a mixture containing 0.5 mg IPTG and 1 mg X-gal was spread on a LB plate first. The agar plates were then incubated at 37°C overnight and single colonies were transferred to new plates for screening.

2.2.7 Slot Lysis Electrophoresis

Slot lysis electrophoresis was performed to compare the size of plasmids in the transformants. Each bacterial colony was resuspended in 16 µl protoplasting buffer (30 mM Tris-HCl pH 8, 20% sucrose, 5 mM EDTA, 50 mM NaCl, 50 µg/ml RNAase) and

the suspension was loaded into a lane containing 4 µl lysis buffer (89 mM Tris-HCl, pH 8.0, 2.5 mM Na₂EDTA, 89 mM boric acid, 0.04% bromphenol blue, 5% sucrose, 2% SDS) in 0.7% agarose gel containing 0.05% SDS. Electrophoresis was conducted at 20 V for 30 minutes and 120 V for 1 hour in 1X TAE buffer with 0.05% SDS. The gel was then stained with 0.5 µg/ml ethidium bromide. Plasmids containing the inserted fragment migrated slower than control plasmid without the cloned fragment. These candidate colonies were re-plated and inoculated into 5 ml LB medium with appropriate antibiotics and incubated overnight at 37°C. Plasmid DNA was isolated using a plasmid prep kit (Qiagen) and further analyzed by enzymatic digestion or PCR.

2.2.8 Crude *Chlamydomonas* Genomic DNA Preparation

A *Chlamydomonas* colony of approximately 5-10 µl was resuspended in 50 µl 10 mM EDTA and then incubated at 100°C for 5 minutes. The mixture was vortexed and centrifuged at 12,000 g for 1 minute. 1-3 µl of the supernatant was used in PCR reactions.

2.2.9 Cloning of RSP6 Gene

The DNA from BAC clones (Clemson University, Clemson, SC) was purified using Phase Prep BAC kit (Sigma-Aldrich) and digested with NotI restriction enzyme. A ~5.5 kb fragment containing the RSP6 gene, the untranslational regions and additional ~1 kb flanking sequences was band-purified and cloned into pBluescript KS(+) vector (Stratagene).

2.2.10 Constructions of His-tagged RSP6 Transgenes

PCR and a three-piece ligation strategy were taken to insert 6His codons at the C-terminus of RSP6 gene. First, PCR with the sense primer upstream of the NcoI site (#6S in Table 2-3) and anti-sense primer (#6A) with a built-in SpeI restriction site was

performed to generate a 2.7 kb fragment upstream to the stop codon (Figure 2-1, left

column). The downstream fragment with 6His codons were generated by two consecutive

PCR (Figure 2-1, middle column). In the first round PCR, a 1.4 kb fragment was

amplified using sense primer (S#6) containing 4His codons and the stop codon as well as

the adjacent 18 non-coding sequence and anti-sense primer downstream with a SphI

convenient restriction site (A#7). The PCR product was used as the template in the

second round PCR using a new primer (A#8) that included a SpeI restriction site and 2

additional His codons. The final two 2.7 kb and 1.4 kb PCR products were cloned in

PGEMT Easy and pBluescript vectors respectively. The N-terminal NcoI/SpeI fragment

and the SpeI/SphI fragment were released to replace the NcoI-SphI fragments in RSP6

gene to generate the construct expressing the C-terminus-tagged RSP6 (pRSP6-6His).

To engineer the construct expressing 2Gly-6His tagged RSP6 (pRSP6-2Gly-

6His), identical procedure was applied except that nucleotides encoding 2 glycines were

added to the sense primer (A#9) for the second-round PCR of the SpeI-SphI fragment.

To create a 3HA-18His tagged RSP6 construct (pRSP6-3HA-18His), a 3HA-

12His fragment was released by SpeI digest from a plasmid p3HA-12His in the lab and

ligated into the SpeI site of the pRSP6-6His plasmid.

2.2.11 Preparation of Autolysin

Autolysin is a protease produced by mating gametes. It was used to remove the

cell wall prior to transformation. To prepare the lytic enzyme, *cc620(+)* and *cc621(-)* of

opposite mating types were grown on TAP plates for at least 5 days until cells became

confluent. 25 ml TAP(-N) media was then added to each plate and cells were scraped off

using sterile spatula and transferred to 50 ml conical tubes. After cell densities were
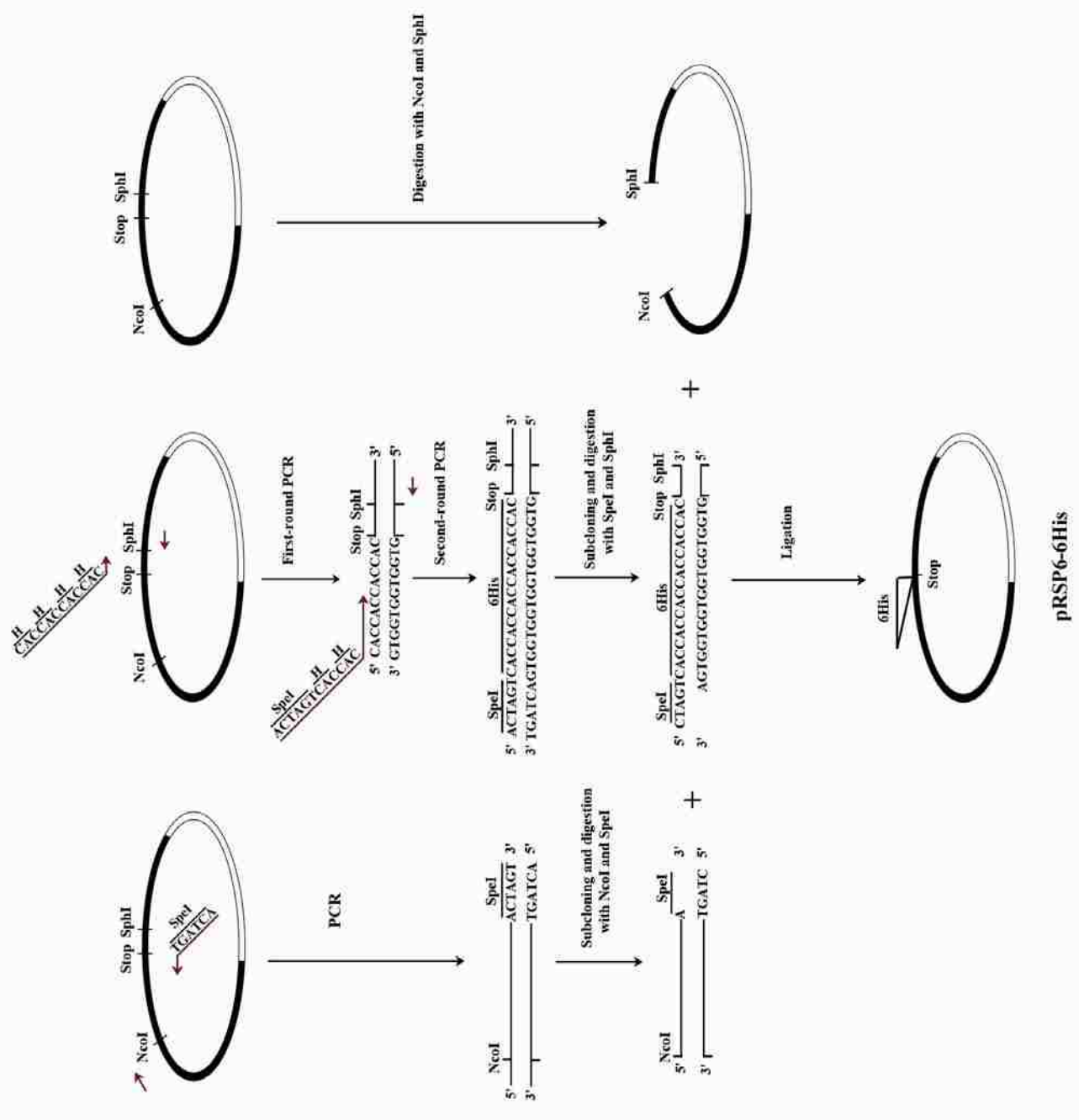
pRSP6-6His

Figure 2-1. Three-piece cloning strategy for generation of 6His tagged RSP6 genomic construct (pRSP6-6His).
The fragment upstream to the stop codon (NcoI/ SpeI) was amplified by PCR with an anti-sense primer containing a built-in SpeI site (left column). The 3' end fragment (SpeI-SphI) was generated by two consecutive PCR using sense primers with His codons and a SpeI site (middle column). These two fragments were cloned into in PGEMT Easy and pBluescript vectors and released with NcoI/ SpeI and SpeI/SphI respectively. The band-purified fragments were ligated into the corresponding sites in the RSP6 gene (right column). The double-stranded ellipse depicted the RSP6 gene (black) in pBluescript. Red arrows represented primers.

determined using a hemocytomer, the cell resuspensions were centrifuged at 2200 rpm

for 10 minutes with IEC clinical centrifuge. The pellets were resuspended in TAP(-N) to

a final concentration of $1x10^8$ cells/ml. The cell suspensions were placed in a sterile Petri

dish on a shaker under light. After 3-4 hours, small amounts of the two mating-type

cultures were mixed and the mating efficiency was assessed under light microscopy

based on the numbers of quadriflagellates. If mating occurred effectively, equal cell

numbers of opposite mating types were mixed and incubated under light for 1 hour until

more than 80% cells were quadriflagellates. The mating mixture was then transferred to a

50 ml conical tube and centrifuged at 2200 rpm for 15 minutes. Aliquots of the

supernatant were stored at -80°C for future usage.

2.2.12 Transformation of *Chlamydomonas*

Cells were grown in ~300 ml liquid medium under 14/10 light/dark cycle for two days

and under constant light for additional 24 hours. Cells were harvested with centrifugation

at 1500 rpm for 5 minutes and then treated with autolysin at $1X10^7$ cells/ml for 1-2 hours

until >50% of cells were lysed by 0.5% Nonidet-P40. Aliquots of ~$0.3X10^8$ cells were

then pelleted in 15-ml conical tubes at 1000 rpm for 5 minutes and resuspended in TAP

medium at $1X10^8$ cells/ml. 1.5-3 µg of plasmid containing RSP6 gene (or plasmid

containing His tagged RSP6 gene), 0.5-1 µg of pSI103, 100 µl of 20% PEG 8000 and

300 mg of glass beads were added into the cell suspension. The mixture was vortexed at

speed 8 (Mini-Vortexer, VWR) for 45 seconds followed by dilution with 10 ml TAP

medium. The supernatant was decanted to a new tube was spun in a clinical centrifuge

with speed 3 for 5 minutes. Cell pellets were gently resuspended in 5 ml TAP medium

and shaken slowly under constant light. After 24 hours, cells were harvested, resuspended

in 500 µl TAP medium and plated on TAP plates with 10 µg/ml paromomycin. Plates were placed under constant light for 4 days when colonies became visible. For screening transformants, cells from single colonies were transferred to a fresh plate. Upon confluence in 3-4 days, a fraction of cells were resuspended in TAP medium in 96-well plates for motility analysis. The transformation rate is about 10-15%.

2.3 Cell Biology

2.3.1 Motility Analysis

The percentage of swimming cells was determined by observing aliquots of the cell culture at 200X magnification with an Olympus BH-2 compound microscope. The light source was filtered through a 62-mm filter with a 625-nm cutoff (HOYA, Japan) to prevent light induced motility anomalies. At least 200 cells from more than 6 randomly selected fields were counted. Swimmers were defined as cells that actively translocated from the original spot. Immotile cells that were obviously stuck to glass surfaces were excluded. The number of swimmers divided by the total cells was the percentage of swimmers. As motile cells moved in and out of fields quickly, the number of swimmers was an estimate and thus standard deviations were not included in the percentage. To reveal swimming trajectories and determine velocity, time-lapse microscopy was performed at 200X magnification with the red filter. The images were captured with a CoolSnap CCD camera (Photometrics) at a rate of 20 frame/sec for 5 seconds (Yang and Yang, 2006). Individual cells were tracked by MetaMorph software and the mean velocity was derived from 20 swimmers tracked from at least 30 sequential images.

2.3.2 Reactivation of Cell Model

Cells were gently spun down with an IEC clinical centrifuge at speed #3 for 1 minute. The cell pellet was resuspended in wash buffer (10 mM Hepes, 4% sucrose, 0.5 mM EGTA) to a final concentration of 3×10^6 cells/ml. Aliquots of 75 µl were removed and added to 500 µl of demembranation buffer (30 mM Hepes, 5 mM MgSO4, 1 mM dithiothreitol (DTT), 1 mM EGTA, 50 mM potassium acetate, 1% PEG 8000, 0.1% Nonidet-P40). After 30-60 seconds, the cessation of motility was confirmed by light microscopy. To reactivate the motility, 500 µl of the reactivation buffer (30 mM Hepes, 5 mM $MgSO_4$, 1 mM DTT, 2 mM EGTA, 50 mM potassium acetate, 1% PEG 8000, 1 mM ATP) was added to the demembranated cells. The reactivated mixture was observed immediately under a light microscope and the motile cells were quantified.

2.3.3 Electron Microscopy

Axonemes were collected by centrifugation at 15,000 rpm for 20 minutes. The pellet was fixed with a primary fixative (1% tannic acid, 1% glutaraldehyde, 0.1 M cacodylate pH 7.4) for 1 hour on ice. The supernatant was removed and the pellet was washed with 0.1 M cacodylate buffer twice for 5 minutes each. The pellet was then fixed with a secondary fixative (1% osmium tetroxide, 0.1 M cacodylate pH 7.4) on ice for 1 hour and washed twice again with 0.1 M cacodylate buffer. Afterwards the pellet was dehydrated sequentially, 2 times 5 minutes /each with 50, 70, 80, 95 and 100% ethanol. The pellet was then infiltrated with a mixture containing 10 ml epoxy resin (5 ml EMBed-812, 2.25 ml DDSA, 3 ml NMA and 0.18 ml DMP-30) and 1 ml propylene oxide for 24 hours at room temperature. Subsequently, the pellet was transferred to fresh epoxy resin in a mold for incubation at 60°C for 48 hours. The polymerized blocks were sectioned and processed and the images were taken as described (Yang et al., 2008).

2.4 Biochemistry

2.4.1 Extraction and Fractionation of Axonemal Proteins

Chlamydomonas cells were harvested by centrifugation at 1,500 g for 5 minutes using a TA10 rotor and Allegra" 25R centrifuge (Beckman Coulter). Cell pellets were resuspended in 20 ml HMDS (10 mM Hepes, 5 mM $MgSO_4$, 1 mM DTT, 4% sucrose). Cells were deflagellated with 50 mM dibucaine, at a ratio of 1 ml/L cell culture, followed by the addition of protease inhibitors, including 0.1 mM PMSF, 0.5 TIU/ml aprotinin, and 0.5 mM EGTA. Flagella and cell bodies were separated by centrifugation with the clinical centrifuge at speed #4 for 7 minutes. To remove the residual cell bodies, the supernatant was underlayed with 5 ml 20% sucrose and centrifuged at 1500 g for 7 minutes. The supernatant at the upper layer was centrifuged at 12,000 g for 10 minutes using TA14 rotor and Allegra 25R centrifuge. The flagella were resuspended in Buffer A (10 mM Hepes, 5 mM $MgSO_4$, 1 mM DTT, 0.5 mM EDTA, 30 mM NaCl, 0.1 mM PMSF and 0.5 TIU/ml aprotinin) and demembranated with 0.5% Nonidet-P40 for 20 minutes. The axonemes were recovered by centrifugation at 12,000 g centrifugation for 10 minutes. The pellet was resuspended in Buffer A and a small fraction was tested with Protein Assay Reagent (Bio-Rad) to determine the protein concentration. For SDS-PAGE, axonemes were resuspended in buffer A at 2-5 mg/ml.

To extract radial spoke complexes, axonemes were resuspended in 0.6 M potassium iodide (KI) in buffer A at a protein concentration of 5 mg/ml for 30 minutes on ice. The mixture was centrifuged at 12,000 g for 10 minutes and the supernatant was dialyzed in buffer A for 30 minutes on ice and then clarified by centrifugation at 12,000g for 10 minutes. An aliquot of 0.7 ml supernatant was overlayed on an 11-ml 5-20%

continuous sucrose gradient. Following velocity sedimentation at 36,000 rpm (SW41 rotor, Beckman Coulter) for 10-16 hours at 4°C, fractions were collected using the Econo peristaltic pump (Bio-Rad). Aliquots of fractions were fixed with 5X sample buffer for SDS-PAGE.

2.4.2 Chemical Cross-linking

Axonemes, 2 mg/ml in buffer A, were incubated with crosslinkers with final concentrations 0.05-5 mM for 1 hour at room temperature. In the case of bis(maleimido)ethane (BMOE), the reaction was terminated by 20 mM DTT or L-cysteine for 15 minutes. For the rest of the crosslinkers the reactions were terminated by 20 mM Tris, pH 8. The cross-linked axonemes were mixed with 5X sample buffer for western analyses or further processed for Ni-NTA affinity purification.

2.4.3 Ni-NTA Affinity Purification

Axonemes treated with crosslinkers were harvested at 12,000 g centrifugation for 10 minutes and then resuspended in 1 ml denaturing lysis buffer (8 M urea, 100 mM NaH_2PO_4, 10 mM Tris base, pH 8). The soluble fraction was incubated with 50-100 μl Ni-NTA (Qiagen) in a 1.5 ml purification column (Bio-Rad) for 1 hour at room temperature. The flow through was collected and the matrix was washed extensively with washing buffer (8 M urea, 100 mM NaH_2PO_4, 10 mM Tris base, 20 mM imidazole, pH 6.3). The His-tagged proteins were eluted with 50 μl elution buffer (8 M urea, 100 mM NaH_2PO_4, 10 mM Tris base, 250 mM imidazole, pH 4.5) five times.

2.4.4 SDS-PAGE

SDS-Polyacrylamide Gel Electrophoresis (SDS-PAGE) was performed using 1X running buffer (27 mM Tris base, 0.1% SDS, 170 mM glycine) as described by Laemmli (1970,

1973). Unless specified, 8 cm X 7 cm mini-gels were used to fractionate a 5 µl aliquot of molecular weight marker (Fermentas) and samples that were mixed with 5X electrophoresis sample buffer (10% SDS, 50% glycerol, 0.3 M Tris pH 6.8, 5% β-mercaptoethanol, 0.05% bromophenol blue) and boiled at 100°C for 5 minutes. Electrophoresis with Protean III mini-gel apparatus (Bio-Rad) was carried out at 190 V, for 0.5-1.5 hours.

2.4.5 Western Blotting

After SDS-PAGE, the molecules were transferred to nitrocellulose membrane with 0.45 µm pore size (Pall Corporation) using transfer buffer (0.38 M glycine, 50 mM Tris base, 10% SDS, 20% methanol) at 100 V for 30-60 minutes in a mini-gel transfer apparatus (Bio-Rad). The membrane was then stained with Ponceau S solution (0.2% Ponceau S, 3% trichloroacetic acid, 3% sulfosalicylic acid) for 2 minutes followed by destaining in double distilled water (ddH$_2$O). Subsequently, the membrane was blocked with blotto, 5% non-fat milk pH 7.4 in 1X TBS (0.14 M NaCl, 2.6 mM KCl, 25 mM Tris base) for 2 hours at room temperature. The blot was then incubated with a primary antibody at room temperature or 37°C for 2 hours. The concentration of antibodies varied depending on the titer. The blot was washed three times with 1X TBS, 5 minutes each, followed by incubation with appropriate secondary antibodies (1: 5000 dilution in blotto), depending on the animals that generate the primary antibody. After incubation for 2 hours, the blot was washed again with 1X TBS as mentioned above.

The protein bands decorated by antibodies were revealed by the enhanced chemiluminescence (ECL). The blot was immerged in the mixture of equal volume solution 1 (0.5 ml 1 M Tris base pH 8.8, 50 µl 44 mg/ml luminol, 22 µl 15 mg/ml *p*-

coumaric acid, 4.4 ml H_2O) and solution 2 (0.5 ml 1 M Tris base pH 8.8, 3 μl H_2O_2, 4.5 ml H_2O) for 1 minute and then exposed to autoradiography film (Denville scientific) for various durations and developed with an automatic film processor CP1000 (AGFA healthcare).

2.4.6 Silver Staining

To reveal all protein bands, the gels were fixed in 45% methanol and 7% acetic acid for 30 minutes and rinsed in ddH$_2$O three times, five minutes each. The gels were then sensitized for 3 minutes in 0.2 g/L sodium thiosulfate pentahydrate and rinsed again in ddH$_2$O three times, 30 seconds each. The gels were then impregnated in 0.2 g/100ml silver nitrate for 1 hour followed by washing with ddH$_2$O three times, 1 minute each. The gels were developed in 6% sodium carbonate, 0.018% formaldehyde and 4 mg/L sodium thiosulfate. When the adequate intensity of staining was achieved, the gels were transferred to a stop solution containing 45% methanol and 7% acetic acid for at least 10 minutes.

2.4.7 Two-dimensional Gel Electrophoresis

SDS and β-mercaptoethanol were added to axoneme samples to final concentrations of 2 and 1% respectively. After boiling for 5 minutes, 15 μl of the samples was mixed with 5 μl 10% Nonidet-P40 and 30 μl first-dimensional sample buffer (9.5 M ultrapure urea, 8% Nonidet-P40, 0.8% ampholine pH 3.5-9.5, 5% β-mercaptoethanol) and loaded on top of the 14-mm tube gels from the mixture containing 0.5 ml acrylamide (28.3% acrylamide and 1.62% bisacrylamide), 0.75 ml 10% Nonidet-P40, 0.24 ml ampholine pH 3.5-9.5, 0.8 ml H_2O, 2.06 g ultrapure urea, 5 μl 12.5% ammonium persulfate and 3 μl TEMED. The tubes were inserted into a Protean II xi electrophoresis cell (Bio-Rad). After overlaying

the sample with buffer containing 5 M urea, 1% ampholine pH 3.5-9.5, the upper and

lower chambers were filled with acidic running buffer (0.01 M H_3PO_4) and basic running

buffer (0.02 M NaOH) respectively. Electrophoresis was run at 200 V for 2 hours, 500 V

for 2 hours and 800 V for 16 hours. After isoelectric focusing, the tube gel was ejected

into 2X SDS-PAGE sample buffer for at least 30 minutes. The acidic half of the tube gel

was loaded into a 1.5-mm thick mini-gel for regular SDS-PAGE.

2.4.8 Protein Concentration Determination

A Bradford-based method was used to determine protein concentrations. To establish the

standard curve, 0, 2, 4, 6, 8, 10 µl of 1 mg/ml bovine serum albumin (BSA) was added to

1 ml 1:5 diluted Protein Assay Reagent (Bio-Rad). Unknown samples of 2 µl each was

treated identically. The absorbance of each sample was measured at 595 nm using a

spectrophotometer (Thermo Spectronic). The absorbance of BSA standards was plotted

as a function of its concentration and the standard graph was used to determine the

concentration of unknown samples.

Table 2-1: Chemicals used in this study.

Vendor	Chemical
Amresco	Yeast extract
	Dithiothreitol (DTT)
	Isopropyl-β-D-thio-galactoside (IPTG)
Bio-Rad	Acrylamide
Biolab Inc.	dNTPs
Calbiochem	Nonidet-P40
Celliance	Aprotinin
EM Sciences	Osmium tetroxide
	Propylene oxide
	2,4,6-(Tri(Dimethylaminoethyl)phenol) (DMP30)
	Dodecenyl succinic anhydride (DDSA)
	Nadic methyl anhydride (NMA)
	EMBed-812
Invitrogen	Urea
JT Baker	Methanol
	Potassium hydrogen phosphate (K_2HPO_4)
	Potassium dihydrogen phosphate (KH_2PO_4)
	Tris base
Fisher Scientific	Potassium iodide (KI)
Mallinckrodt	Sucrose
Midwest Sci.	Agarose
	Tryptone
MP Biomedicals	Paromomycin
Shelton Scientific	Bromphenol blue
Spectrum Chemical Mfg. Corp.	Dibucaine
Stratagene	Pfu DNA polymerase
TCI America	Luminol

Sigma	Acetic acid
	Adenosine triphosphate (ATP)
	Agar
	Ammonium chloride (NH_4Cl)
	Ammonium heptamolybdate ($(NH_4)_6Mo_7O_{24}$)
	Ammonium Persulfate
	Ammonium nitrate (NH_4NO_3)
	Bisacrylamide
	Boric acid (H_3BO_3)
	Bovine serum albumin (BSA)
	Calcium chloride dehydrate ($CaCl_2$-$2H_2O$)
	Cobalt chloride hexahydreate ($CoCl_2$-$6H_2O$)
	Coumaric acid
	Cupric sulfate pentahydrate ($CuSO_4$-$5H_2O$)
	L-Cysteine
	Dimethyl sulfoxide (DMSO)
	Ethidium bromide
	Ethylenediaminetetraacetic Acid (EDTA)
	Ethylene glycol tetraacetic acid (EGTA)
	Ferric chloride hexadhydrate ($FeCl_3$-$6H_2O$)
	Ferrous sulfate ($FeSO_4$)
	Ficoll 400
	Formaldehyde
	Glycerol
	Glycine
	Glutaraldehyde
	4-(2-hydroxyethyl)-1-piperazineethanesulfonic acid (Hepes)
	Hydrogen peroxide (H_2O_2)
	Imidazole
	β-mercaptoethanol (BME)
	Manganese sulfate ($MnSO_4$)
	Manganese chloride ($MnCl_2$)
	Magnesium Sulfate Heptahydrate ($MgSO_4$-$7H_2O$)

Magnesium Chloride Hexahydrate (MgCl$_2$-6H$_2$O)

Phenylmethanesulfonylfluoride (PMSF)

Phosphoric acid (H$_3$PO$_4$)

Polyethylene glycol (PEG 8000)

Ponceau S

Potassium acetate (KCH$_3$COO)

Potassium chloride (KCl)

Ribonuclease

Sodium citrate (Na$_3$C$_6$H$_5$O$_7$·2H$_2$O)

Sodium Dodecyl Sulfate (SDS)

Sodium chloride (NaCl)

Sodium hydroxide (NaOH)

Sodium acetate (NaCH$_3$COO)

Silver nitrate (AgNO$_3$)

Sodium carbonate (Na$_2$CO$_3$)

Sodium phosphate (NaH$_2$PO$_4$)

Sodium thiosulfate pentahydrate (Na$_2$S$_2$O$_3$)

Sulfosalicylic acid

Tannic acid

Tetramethylethylenediamine (TEMED)

Trichloroacetic acid

Zinc sulfate heptahydrate (ZnSO$_4$-7H$_2$O)

Table 2-2: Composition of medium used in this study.

Medium	Composition
TAP medium (Tris-acetate-phosphate)	20 mM Tris base, 0.6 mM K_2HPO_4, 0.4 mM KH_2PO_4, 7.5 mM NH_4Cl, 0.34 mM $CaCl_2$-$2H_2O$, 0.41 mM $MgSO_4$-$7H_2O$, 76.5 µM $ZnSO_4$-$7H_2O$, 184 µM H_3BO_3, 25.6 µM $MnCl_2$-$4H_2O$, 6.8 µM $CoCl_2$-$6H_2O$, 6.3 µM $CuSO_4$-$5H_2O$, 17.9 µM $FeSO_4$-$7H_2O$, 6.2 µM $(NH_4)_6Mo_7O_{24}$, pH 7 For plates, 1.5% agar was added.
TAP-N medium (Nitrogen-free TAP)	Same recipe as TAP medium except NH_4Cl was not added
Sager medium	1.7 mM Na citrate, 0.37 mM $FeCl_3$-$6H_2O$, 0.36 mM $CaCl_2$-$2H_2O$, 0.08 mM $MgSO_4$-$7H_2O$, 0.34 mM $MgCl_2$-$6H_2O$, 0.9 mM K_2HPO_4, 0.7 mM KH_2PO_4, 3.7 mM NH_4NO_3, 12 mM Na acetate, 16 µM H_3BO_3, 3.5 µM $ZnSO_4$-$7H_2O$, 2 µM $MnSO_4$, 0.84 µM $CoCl_2$-$6H_2O$, 0.25 µM $CuSO_4$-$5H_2O$, 0.82 µM $(NH_4)_6Mo_7O_{24}$
LB medium	1% tryptone, 0.5% yeast extract, 1% NaCl, pH 7.4 For plates, 1.5% agar was added.

Table 2-3: Oligonucleotides used in this study.

Name	Sequences
#1S	CAGTCATTTCTGGACAGAATCGCTGC
#1A	GTCAGGCAGGCTGCAGGTACGTGAG
#2S	CTCACGTACCTGCAGCCTGCCTGAC
#2A	CCTCGCACTCGAACTGGATTAAGCACG
#3S	CGTGCTTAATCCAGTTCGAGTGCGAGG
#3A	CCTCTAGCACCGCTGTAGGCCTAAGC
#4S	CGAGCTGTCCGCCAACGACGAGTGG
#4A	GCTCCTCAGCCTCAGCTAACCACACC
#5S	CCAGCACTATAGGCATGTTCATGCACTGC
#5A	GCAGCGATTCTGTCCAGAAATGACTG
NIT-S	GCTTAGGCCTACAGCGGTGCTAGAGG
NIT-3'	GTCAAAGCACCTGTGTACCTCGCGAG
NIT-5'	GCACCTGTACATGTACCCATTCACTG
#6A	AGTAGCCTAGACTTCTAGACATCTTACCAGGC
#6S	TAACTAGTCTCGTCCTCCTCCTCCGGC
#7A	CACCACCACCAC TAG GCAAGCCCAGGAGGGAAG
#7S	TACGGTATCCAGACGCAGGTCG
#8A	AACTAGTCACCACCACCACCACCACTAGGCAAGC
#9A	AACTAGTGGCGGCCACCACCACCACCACCACTAGGCAAG

S: Sense primer; A: Anti-sense primer

Table 2-4: Antibodies used in this study.

Antigen	Host	Reference
RSP1	Rabbit	Yang et al., 2008
RSP2	Rabbit	Yang et al., 2001
RSP3	Rabbit	Yang et al., 2001
RSP5	Rabbit	Qin et al., 2004
RSP6	Rabbit	Yang et al., 2008
RSP7	Rabbit	Yang et al., 2006
RSP8	Rabbit	Yang et al., 2006
RSP9	Rabbit	Yang et al., 2006
RSP10	Rabbit	Yang et al., 2006
RSP11	Rabbit	Yang et al., 2006
RSP12	Rabbit	Yang et al., 2006
RSP16	Rabbit	Yang et al., 2005
RSP23	Rabbit	Yang et al., 2008
IC140	Rabbit	Yang and Sale, 1998
HA	Rabbit	Covance Inc.
Radial Spoke	Chicken	Yang et al., 2005
His	Rabbit	Qiagen
Secondary antibodies		
Anti-chicken IgY-peroxidase	Rabbit	Sigma
Anti-rabbit IgG-peroxidase	Goat	Sigma

Chapter 3: *Chlamydomonas* Mutants Display Reversible Deficiencies in Flagellar Beating and Axonemal Assembly

3.1 Introduction

The anomalies of most flagellar mutants are described and considered as irreversible and irreparable. The only way known to partially restore the motility of live mutant cells is through extragenic suppressor mutations (Huang et al., 1982) or direct mechanical stimulation (Hayashibe et al., 1997). Yet the phenotypes of a few *Chlamydomonas* mutant strains are not so cut-and-dried. The vegetative cells of the dynein arm mutant *pf13* are paralyzed while the gametic ones are motile (Huang et al., 1979; Brokaw and Kamiya, 1987). Some strains with subtle biochemical and morphological deficiencies in radial spokes contain mixed populations of swimmers and paralyzed cells (Huang et al., 1982; Frey et al., 1997; Gaillard et al., 2006; Yang and Yang, 2006). Notably, it was demonstrated that in *pf25*, which is defective in RSP11 and RSP8, the ratio of swimmers and paralyzed cells fluctuates according to the culture conditions. Cells in a log phase culture can appear WT-like but become entirely paralyzed in spent media. After being cultured in fresh media for 1-2 days, the culture is teeming with swimmers again. Thus, certain types of dyskinesia appear reversible. Biochemical differences are not evident in motile or immotile populations of *pf13* or *pf25* strains (Luck and Piperno, 1988; Yang and Yang, 2006).

In vitro studies have shown that phosphorylation can modulate the motility level of axonemes. Inhibition of cAMP-dependent protein kinase (PKA) increases the reactivation rate of WT axonemes (Hasegawa et al., 1987). In the same fashion, a motile

mutant with two a. a. residues replaced in RSP3 has an equal ratio of swimmers and paralyzed cells. A similar ratio is found in the reactivated cell model while inhibition of PKA increases the motile fraction of cell models (Gaillard et al., 2006). However, inhibition of kinase activity cannot mobilize the paralyzed *pf25* cells in the spent media (Yang and Yang, 2006), suggesting that distinct mechanisms influence the reversible paralysis of *pf25* in vivo.

The cultures of two new mutants also contain cells displaying a range of motility defects. This study found that both strains displayed reversible paralysis and revealed the genetic defects and the cause underlying reversible paralysis.

Results

3.2 RSP6 is a Nonessential Paralogue in the Radial Spoke Head

3.2.1 Discovery of Two Novel Radial Spoke Head Mutants

Screening of ultraviolet radiation mutagenesis and insertional mutagenesis respectively recovered two strains, 1C12 and 45G7, with abnormal motility. The cells, when resuspended from agar plates into liquid medium, were largely paralyzed with few cells moving locally. To test if the severe motility deficiency was due to defective radial spokes or the central apparatus, mutants were crossed with the suppressor mutant *sup-pf1* defective in outer dynein arms by Dr. David R. Mitchell. The paralysis was rescued, suggesting that the strains were defective in radial spokes or central apparatus.

3.2.2 Protein Deficiency in 1C12 Flagella

To test if 1C12 was a radial spoke mutant, axonemes for western blots were harvested from the mutant and WT cells from aerated stationary phase liquid cultures. Curiously,

some mutant cells swam quite well. Among the radial spoke proteins tested, only RSP6 was absent in 1C12 axonemes but other radial spoke proteins including spoke head proteins were present (Figure 3-1A). Although the spoke head proteins (RSP1, 9 and 10) and the spoke chaperone in the stalk (RSP16) of 1C12 were less abundant than those in the wild type (WT) control as shown in Figure 3-1A, the reduction in most preparations was not evident. This finding was unexpected because the only other spoke head mutants, *pf1*, defective in RSP4, and *pf17*, defective in RSP9, lacked all 5 proteins in the radial spoke head and were entirely paralyzed (Table 3-1). On the other hand, in the axonemes of the RSP6 temperature sensitive mutant *pf26$_{ts}$*, spoke head components, including the mutated RSP6 were present. This reduction in spoke head amounts also occurred in *pf26$_{ts}$* (Huang et al. 1981).

The RSP4/6 molecules are much bigger than RSP9 and 10, two of the other three spoke head components. We reasoned that if the bulbous spoke head only consisted of the 5 molecules (Table 3-1) as postulated (Curry and Rosenbaum, 1993), morphological defects due to loss of RSP6 should be visible by electron microscopy (EM). To test this, axonemes of WT and 1C12 from liquid cultures were processed for EM. However, the bulbous spoke head did not appear smaller but seemed less defined in the cross section (Figure 3-1B). The presence of spoke head is consistent with the motile RSP6-minus cells, yet missing RSP6 did not result in deformed radial spokes. This could be due to the insufficient resolution of EM for radial spokes or that the bulbous spoke head actually consists of more than the 5 radial spoke proteins defined based on mutants (Curry and Rosenbaum, 1993).

A
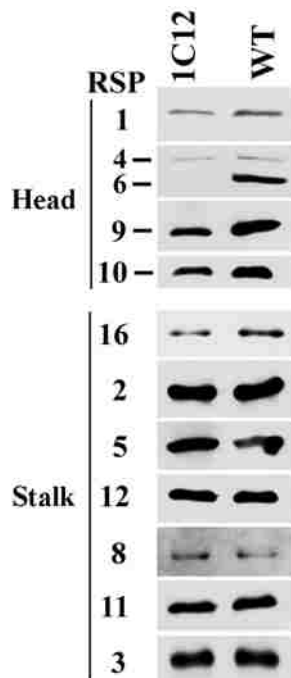
B
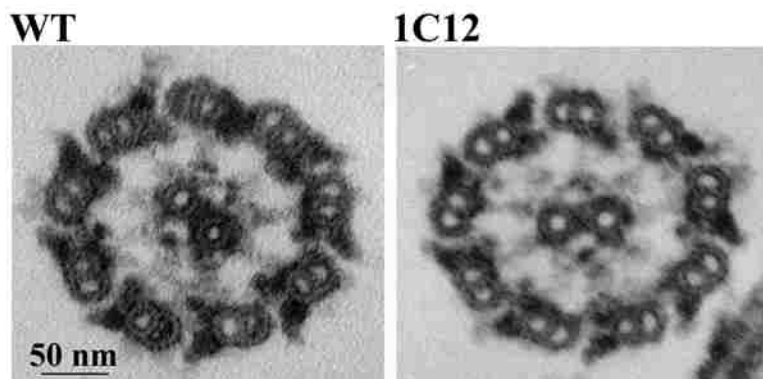
Figure 3-1. Characterization of a new mutant strain 1C12.
(A) Western analyses of axonemes revealed that radial spokes in 1C12
axonemes lacked RSP6 only. Each protein was revealed by antibodies raised
against individual molecules. Anti-RSP6 antibody cross-reacted with RSP4 and
hence RSP4 band appeared weaker than RSP6. In this particular preparation, the
spoke head proteins, RSP 1, 9 and 10 and the stalk chaperone HSP40 (RSP16)
were less abundant in the 1C12 axonemes than those in the WT control. This
difference was not evident in most preparations. (B) Cross section of WT and
1C12 axonemes by EM. No obvious morphological defect can be found in any
radial spoke in the 1C12 axoneme. The samples were prepared from the early
stationary phase liquid culture.

Table 3-1. The molecules in the head module of *Chlamydomonas* radial spoke and the available mutants.

	Molecular Domain[a]	MW(kDa)[b]	Mutant[c]	Spokehead[c]	Motility[c]
RSP1[d]	———————[MN]—	123	N/A		
RSP10[d]	▪MN▪—	24	N/A		
RSP4	—[RS]—	76	*pf1*	−	−
RSP6	—[RS]—	67	*pf26$_{ts}$*	+	+/−
RSP9	———	26	*pf17*	−	−

a. Yang et al., 2006.
b. Piperno et al., 1981.
c. Huang et al., 1981.
d. Each box represents a MORN (MN) motif.

3.2.3 Genetic Defect of 1C12

To test if the RSP6 gene was defective in 1C12, RSP6 genomic DNA was amplified by PCR from 1C12 cells. Sequencing of the amplified RSP6 gene fragments from 1C12 showed that AC at #141-142 coding sequence in the first exon was replaced by T (Figure 3-2A). The elimination of 1 bp caused a frame shift after the 47th a.a. and a premature termination after a.a. #58 (Figure 3-3). Considering that the entire molecule is 459 a.a. long and is highly similar to RSP4, the new polypeptide of only the first 47 a.a. is most likely nonfunctional.

To test whether the motility and genetic defect of 1C12 was due to the mutated RSP6 gene, transformation rescue of 1C12 with WT RSP6 gene was carried out. To recover RSP6 genomic DNA, the DNA end sequences of BAC clones that were mapped to the region of the RSP6 gene in *Chlamydomonas* genome v.2.0 (http://genome.jgi-psf.org/Chlre2/Chlre2.home.html) were first analyzed. From all of the clones that included the entire RSP6 gene, the shortest clone, #7P14, was chosen. A 5.5 kb fragment that included the untranslated regions and additional ~1 kb flanking sequence at 5' and 3' ends was subcloned into a pBluescript vector. The recombinant plasmid containing the RSP6 gene was co-transformed into mutant 1C12 cells with the plasmid pSI103 that confers paromomycin (PMM) resistance (Yang et al., 2008). Transformants were first grown on PMM agar plates to select colonies that contain the pSI103 plasmids. The PMM-resistant transformants were resuspended from agar plates into liquid medium for motility analysis. Among 126 colonies examined, 12 contained mostly motile cells, a 10% rescue rate. In contrast, the parental 1C12 cells were paralyzed. The fact that most colonies contained paralyzed cells suggests most colonies only contained pSI103.

A
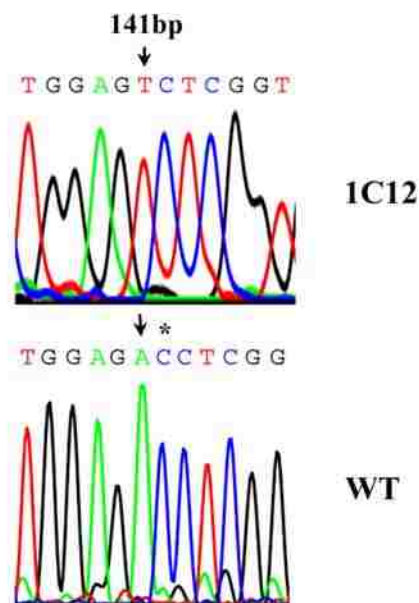
B
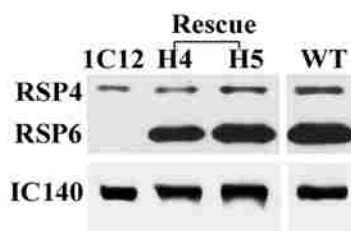
Figure 3-2. The deficiencies of 1C12 flagella were caused by mutations in the RSP6 gene.

(A) A representative result revealed the mutation in 1C12. Sequence comparison of RSP6 genomic DNA amplified by WT and 1C12 revealed that there was a A to T single base pair replacement and a deletion in the following C in the first exon of RSP6 gene in 1C12. The nucleotides shown in the figure is from 136 bp to 147 bp. (B) Western analyses revealed that RSP6 was restored in two representative transformants (H4 and H5) to the WT level. The positive and negative controls were WT and 1C12 respectively. The protein loading control was dynein intermediate chain, IC140.

A

```
DNA: ATGGCCGCGGATGTGGGCCAGGCTCTGGCCTTCCTGCAGCAAGTGAAGACAACACAAGGCGCATCAATCTATGAAGGCCTTAAAGCAGCGTTGGCGAAGGT
+1: M  A  A  D  V  G  Q  A  L  A  F  L  Q  Q  V  K  T  T  Q  G  A  S  I  Y  E  G  L  K  A  A  L  A  K  V
```
                                                    AC to T in 1C12
```
DNA: CTGGAGGATCGGCCTGTGAACGCGGTCGAGGCGCTGGAGACCTCGGTGCTGTCGACACCCCCGCAGCGAACCTGAGTGTGCCCCTTGTTCCCGCAGCTTC
+1: L  E  D  R  P  V  N  A  V  E  A  L  E  T  S  V  L  S  T  P  P  A  A  N  L  S  V  P  L  V  P  A  A  S
              E  S  R  C  C  R  H  P  P  Q  R  T  *
```
```
DNA: GCTGCAGCTGCGGCAGCTGCCGTGGCGAAGGCGAGCCTATTCGGGGACCCAGAGCCAGTGCTTGACCCCGAGTCAGGGGAACCTATCGATCCGGATGCTCC
+1: A  A  A  A  A  A  A  V  A  K  A  S  L  F  G  D  P  E  P  V  L  D  P  E  S  G  E  P  I  D  P  D  A  P
```
```
DNA: AACGAGTTCGAGTGCGAGGACGTGGAGGGCGACGGTGACCTGCTGGACGGCCTGGGTGTGGGGCTGGGCCGGCAGGAGATGTACGCGGCCATGCTGGCGGT
+1: N  E  F  E  C  E  D  V  E  G  D  G  D  L  L  D  G  L  G  V  G  L  G  R  Q  E  M  Y  A  A  M  L  A  V
```
```
DNA: AAGAGGCTGGGGGAGGACGCCAAGAGGGGCGTATCTACGGTGCGCTTCTTCGGCAAGTTCTTCGGCACGCAGGCCGACTACTACGTGTTTGAGACCACGCT
+1: K  R  L  G  E  D  A  K  R  G  V  S  T  V  R  F  F  G  K  F  F  G  T  Q  A  D  Y  Y  V  F  E  T  T  L
```
                          ↓Insertion of 3' *NIT* plasmid in 45G7
```
DNA: CAGAGCAACCCGGACATGCCCGAGGCACCAGAGGGCACCATCCCCTTGGAGCCGTACGGCGAGGGCGTCAACGCCTACATCTACTTTGTGTCCAACACGCT
+1: Q  S  N  P  D  M  P  E  A  P  E  G  T  I  P  L  E  P  Y  G  E  G  V  N  A  Y  I  Y  F  V  S  N  T  L
```
```
DNA: GGCGGCCCGCTGCAGCAGCTGCCCTACGTCACGCCCGAGCAGATCAAGGCCAGCCGCCTGCTGCGGCCGCTACCTGACCGGCCGCCTGGACGCGCCCGTGTC
+1: G  G  P  L  Q  Q  L  P  Y  V  T  P  E  Q  I  K  A  S  R  L  L  R  R  Y  L  T  G  R  L  D  A  P  V  S
```
```
DNA: GCCCTTCCCAGCCTTCCCCCGGCAACGAGGCCAACTACCTGCGCGCCCTCATTGCGCGCATCAGCGCCGCCACCGTGTGCTGCCCCGCGCGGCTTCTTCACCGC
+1: A  F  P  A  F  P  G  N  E  A  N  Y  L  R  A  L  I  A  R  I  S  A  A  T  V  C  C  P  R  G  F  F  T  A
```
```
DNA: GACGACGACAGCGCCGAGCTGTCCGCCAACGACGAGTGGGTGCCGCTCAAGGGTCGCGAGATGGCGCTGCCCGTCAACTGGTCGCACCGCTACGCGCACCT
+1: D  D  D  S  A  E  L  S  A  N  D  E  W  V  P  L  K  G  R  E  M  A  L  P  V  N  W  S  H  R  Y  A  H  L
```
```
DNA: AAGGGCCAGGGCCGCCACCGTGACGCACAAGCGCGACCCGCCCGACGAGGAGGAGGAGCCGGAGAAGAACTTCTGGACGGCCGAGGAGATGGAGGCCGGCCC
+1: K  G  Q  G  R  T  V  T  H  K  R  D  P  P  D  E  E  E  E  P  E  K  N  F  W  T  A  E  E  M  E  A  G  P
```
```
DNA: CCGCCGCTGGCCACCCTGGACACGGACGCGCCGCTGCCGGCCGCCACTGGCGACAAGGTGCCACCGCCCGCCTGGAGCCCCGTGTTCGCCAGCGCCTCGGT
+1: P  P  L  A  T  L  D  T  D  A  P  L  P  A  A  T  G  D  K  V  P  P  P  A  W  S  P  V  F  A  S  A  S  V
```
                          G to A in *pf26ts*
```
DNA: ACCACGCGCAACCAGGTGGCGGGCGTGCGCTCCAACCGCTGGCCGGGCGCGGTGTGCGCCTGCGCGGGCCGCCACTTCACGTCCATGTACGTGGGCTGGGG
+1: T  T  R  N  Q  V  A  G  V  R  S  N  R  W  P  G  A  V  C  A  C  A  G  R  H  F  T  S  M  Y  V  G  W  G
              M                                              G addition in *pf26ts*
```
```
DNA: ATCAAGGCCGGCGGCGAGTGGTCGCCCTGCCCGCCGCCGCCGCCCGTGCCGCAGTGGGCGGCCCCCGCTGCTGGCGTCGAGGGCGGGCAGCAGCTGCTGCT
+1: I  K  A  G  G  E  W  S  P  C  P  P  P  P  P  V  P  Q  W  G  A  P  A  A  G  V  E  G  G  Q  Q  L  L  L
                                                        G  R  P  R  C  W  R  R  G  R  A  A  A  A  A
```
```
DNA: GAGTGCAACGACCTGCCGCCCAAGCCCGCCGCCGCCGGAGGAGGAGGACGAGTAG
+1: E  C  N  D  L  P  P  K  P  A  P  P  E  E  E  D  E  *
     R  V  Q  R  P  A  A  Q  A  R  A  A  G  G  G  G  R  V  G  K  P  R  R  E  E  R  I  R  A  V  W  L  A  E
     A  E  E  L  G  E  G  *
```

B
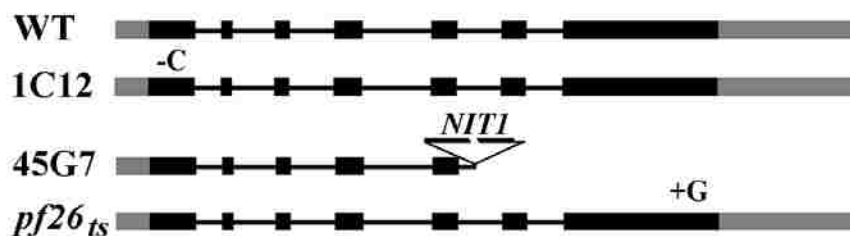
Figure 3-3. Summary of the mutations in the three RSP6 mutants.
A single-nucleotide deletion in the first exon in 1C12 resulted in premature
termination after 58 a.a. In the case of 45G7, insertion of nitrate reductase gene
(*NIT1*) in the fifth intron resulted in deletion of three fifth of the 3' end. An
additional G in the last exon in the *pf26ts* RSP6 gene caused frame shift of the
C-terminus and a more basic RSP6 in *pf26ts* axoneme (Huang et al., 1981). The
results were obtained by PCR of RSP6 genomic DNA, followed by cloning in
some cases and sequencing. The mutations were confirmed by repeated PCR
and sequencing. The black bars in (B) depict exons and the two gray bars
represent 5' and 3' UTR respectively. The lines between black bars represent
introns.

The rescue rate is about 10%. To confirm the presence of RSP6 in the rescued colonies, axonemes were prepared from two representative transformants (H4 and H5, Figure 3-2B), 1C12, and WT control for western blot analysis. As expected, RSP6 amounts in the transformants' flagella were restored to WT levels. Therefore, 1C12 is a spoke head mutant defective in RSP6. H4 and H5 transformants were used as WT control (WT*) for motility analysis. Characterization of this mutant revealed that despite high sequence similarity, the functions of RSP4 and RSP6 differ: RSP4 is essential for assembly while RSP6 is not.

3.2.4 Protein Deficiency in 45G7 Flagella

Like 1C12, 45G7 axonemes also only lacked RSP6 in the spoke head. The rest of the radial spoke proteins, including spoke head proteins, were present but in reduced amounts in some preparations (Figure 3-4).

3.2.5 Genetic Defect of 45G7

45G7 strain was recovered from random insertional mutagenesis using the plasmid pMN24 with the nitrogen reductase gene (*NIT1*) for metabolic selection. To test if the absence of RSP6 was directly due to the disruption of the gene by the insertion of pMN24, the entire RSP6 gene was PCR-amplified (Figure 3-5A). All of the PCR products were obtained from the reactions using WT genomic DNA and 5 primer pairs (Figure 3-5B). In contrast, the PCR reactions using 45G7 genomic DNA generated the fragments only from the #1, #2 and #3 primer pairs. This suggested that pMN24 inserted either in the sense or antisense direction after the fifth exon.

As 45G7 grew in nitrogen-minus media, the *NIT-1* gene in pMN24 at the insertional site must be functional. To reveal the precise insertional site, PCR was carried
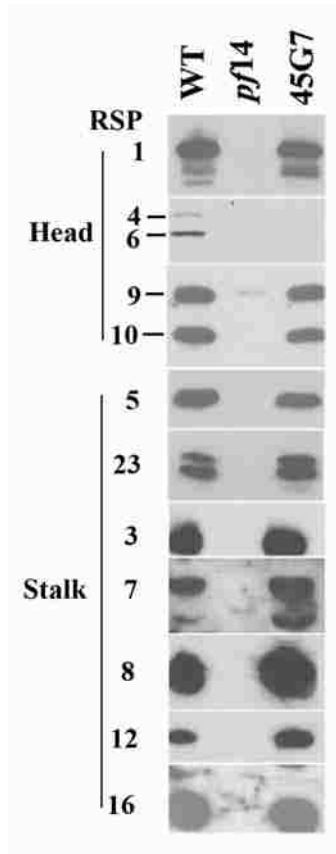
Figure 3-4. Western analyses of axonemes showed that RSP6 was absent in 45G7.
Axonemes were isolated from 45G7 and probed with antibodies against different radial spoke proteins. Controls were from WT and *pf14* lacking radial spokes. Compared to WT control, RSP4 in 45G7 was not detected in this particular preparation. And the rest of the radial spoke head proteins RSP1, 9, and 10 in the 45G 7 axonemes were present but may be reduced in this blot.

A
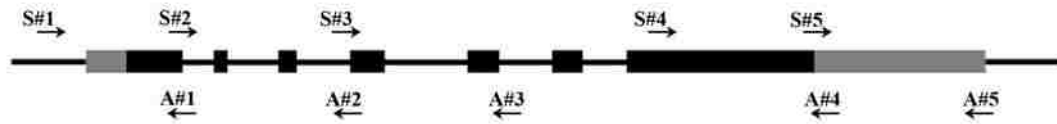
B
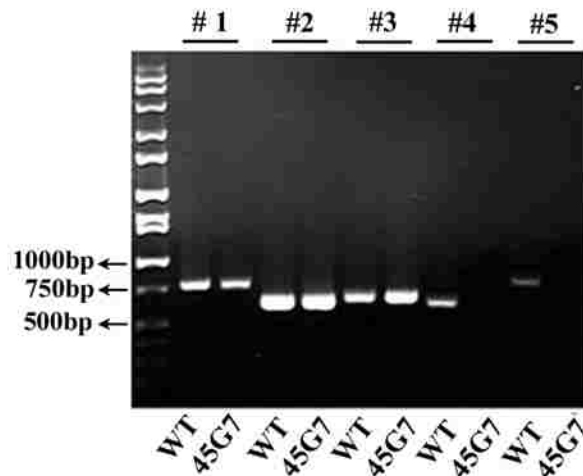
Figure 3-5. Mapping the insertional site of pMN24 in 45G7.
(A) Diagram depicts primer pairs #1- #5 for PCR of RSP6 gene. The black bars represented exons and black lines between black bars represented introns. The two gray bars represent 5' and 3' UTR and black lines at the two ends represent flanking sequences. S, sense primers and A, antisense primers. (B) PCR revealed the insertional site of the selection plasmid at the C-terminus of RSP6 gene in 45G7. 45G7 and WT genomic DNA were used as templates for PCR amplification with primer pairs #1- #5. Note PCR using #4 and #5 primer pairs and 45G7 genomic DNA failed to generate the expected fragments.

out using a sense primer in the fifth exon of the RSP6 gene (NIT-S) and primer on the 3'
end (NIT-3') or 5' end (NIT-5') of the *NIT1* gene using 45G7 genomic DNA as the
template (Figure 3-6A). A 300-bp product was amplified from the reaction using the
NIT-3' primer (Figure 3-6B), suggesting that *NIT-1* and RSP6 genes were oriented in
opposite orientations. Sequencing of this 300 bp fragment revealed the 3' end of *NIT1*
gene on the fifth intron of the RSP6 gene (Figure 3-6C). The insertion at this position
disrupted the RSP6 gene and likely resulted in the deletion of the downstream sequences
(Figure 3-5B).

An in-frame stop codon in the fifth intron upstream of the insertional site could
terminate translation. The truncated protein, if expressed, is predicted to be 21 kDa with
pI 4.44. Western blot analyses with anti-RSP6 failed to detect any truncated RSP6.
Independently, 2-D gel electrophoresis was performed to compare axonemes from 45G7
and WT. RSP11, which has a similar molecular weight (MW) and an isoelectric point (pI)
with the predicted truncated RSP6, served as a marker. Protein staining of the 2-D gel did
not reveal any new polypeptides around RSP11 in 45G7 axonemes (Figure 3-7),
suggesting that truncated RSP6 was not present in 45G7 axonemes and cannot account
for the assembly of the partial spoke head in motile 45G7 flagella (Figure 3-4).

To test if a mutation in RSP6 gene resulted in the phenotype of 45G7, the mutant
was transformed with WT RSP6 genomic DNA and the selection plasmid pSI103 that
contains a paromomycin (PMM)-resistant cassette. The antibiotic-resistant colonies were
resuspended in liquid medium and screened for motility. Among 136 colonies, the
motility of 16 colonies was rescued to WT level. The rest colonies were still paralyzed.

To test whether RSP6 was restored, axonemes were prepared from the three

A

B

C
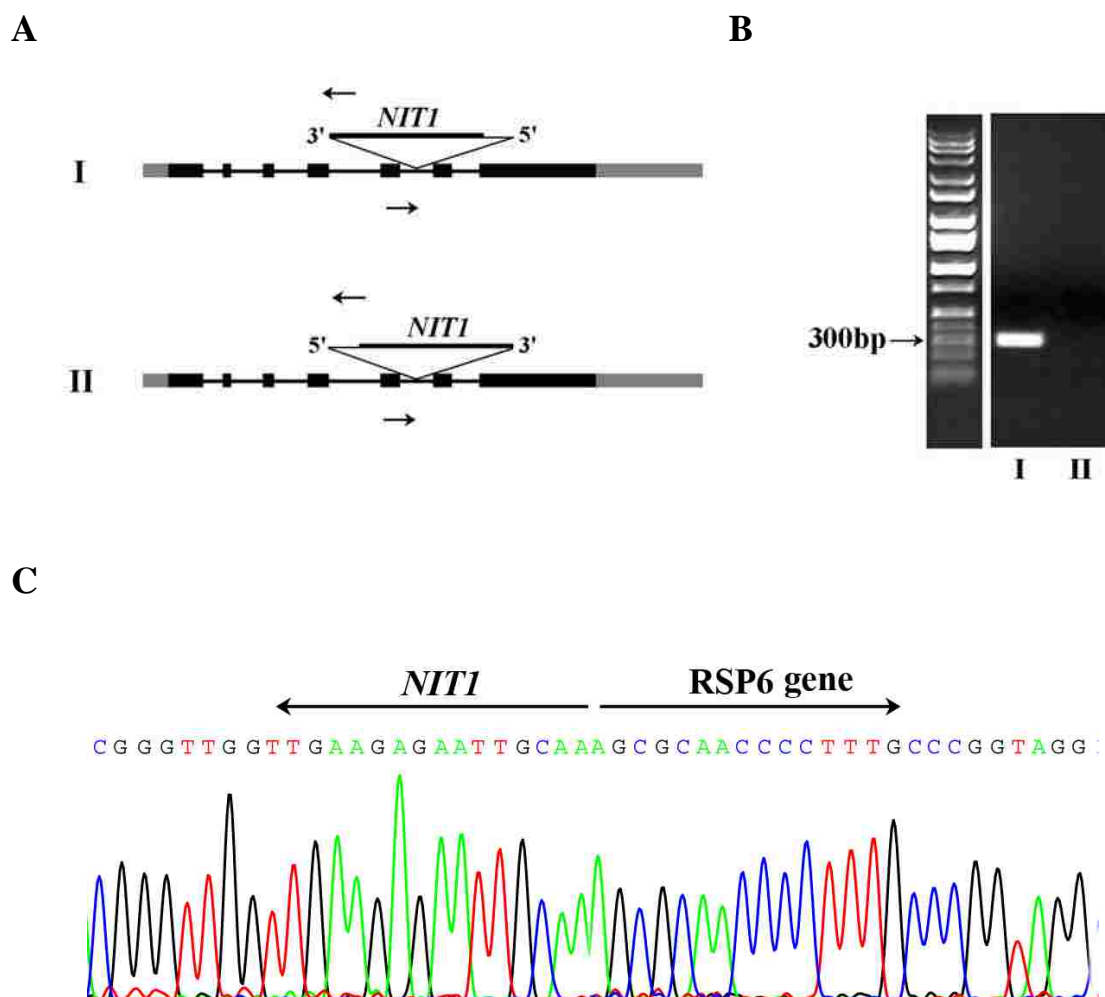
Figure 3-6. The selective plasmid pMN24 was inserted into the fifth intron of RSP6 gene in 45G7.

(A) Schematic diagrams depict two possible orientations of pMN24 in the RSP6 gene, (I) 3'-5', (II) 5'-3' direction. Black bars on the triangles represented the selective gene *NIT1*. The two arrows in each diagram represent the primer pair used in PCR experiment. (B) PCR showed that the primers at 3' end of *NIT-1* generated a 300 bp product, indicating that the selection gene was inserted in 3'-5' direction (I). (C) Sequencing of the 300 bp PCR product confirmed the disruption of the RSP6 gene by the insertion of *NIT1* gene in 45G7 strain.
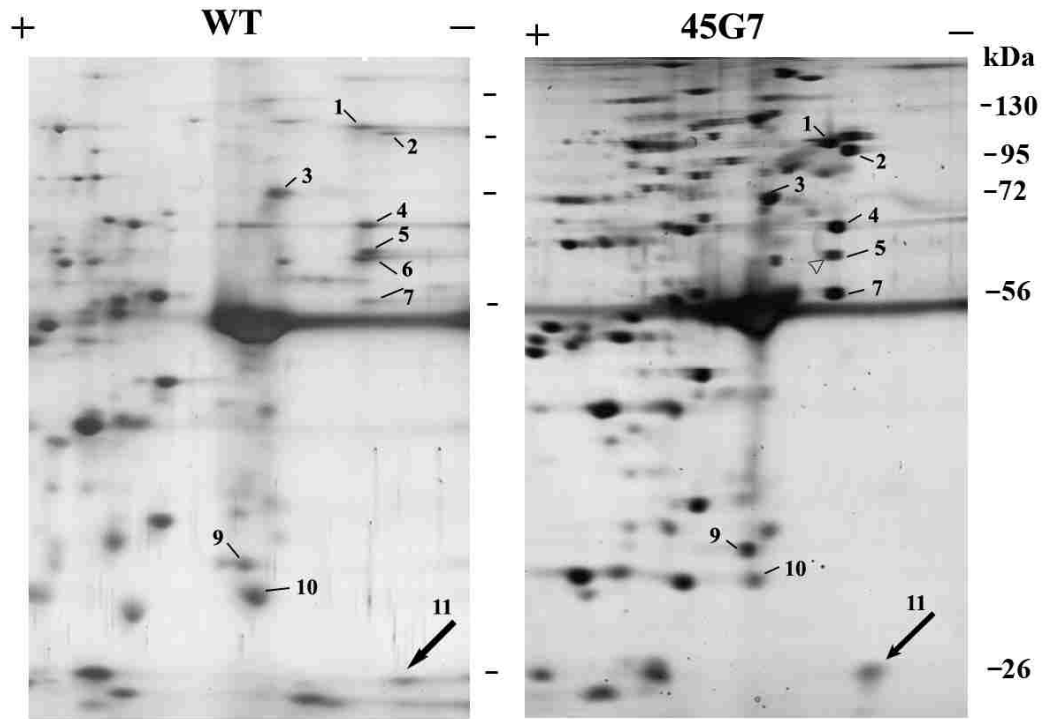
Figure 3-7. Two-dimensional gel electrophoresis showed the profile of radial spoke proteins in 45G7.
Axonemal proteins from WT (left) and 45G7 (right) were separated by two-dimensional gel electrophoresis according to pI and MW, and then revealed by silver staining. Radial spoke proteins (RSP1-7, 9-11) are numbered. If truncated RSP6 was present, it would have migrated near RSP11 (arrow). RSP6 was absent in 45G7 (empty arrowhead). "+" indicates the basic end and "-" indicates the acidic end. Horizontal bars indicate molecular markers of 130, 95, 72, 56, 26 kDa from top to bottom.

motile transformants (A11, B5 and C6) and 45G7. Axonemes of WT and *pf14* served as positive and negative controls, respectively. Western blots showed that RSP6, absent in 45G7 and *pf14*, was present in the three transformants at a level similar to that in WT (Figure 3-8).

3.2.6 Characterization of *pf26$_{ts}$*

To determine the genetic defect of the RSP6 temperature sensitive mutant *pf26$_{ts}$*, the RSP6 gene in this mutant was PCR-amplified for sequencing. Sequencing of PCR products from two separate reactions revealed an additional G in the last exon of the RSP6 gene (Figure 3-9). The frame shift resulted in the replacement of the last 31 a.a. of pI 3.8 with 55 mis-sense residues of pI 11.8 (Figure 3-3), consistent with the more basic mutated RSP6. This suggested that the altered C-termini interfered with the conformation of the spoke head at the restrictive temperature.

Examination of *pf26$_{ts}$* from two laboratories showed distinct motility phenotypes. The cells from one strain were largely motile while cells from the other strain contained mixed population of swimmers and immotile cells. Neither exhibited temperature sensitive phenotypes. The changes of phenotypes were either due to different culture conditions or additional mutations accumulated during storage. This strain was not analyzed further.

Taken together, characterization of the three strains showed that although RSP4 and RSP6 are highly similar in sequence and length, only RSP4 is essential for the assembly of spoke head and motility whereas the requirement for RSP6 is not as absolute.
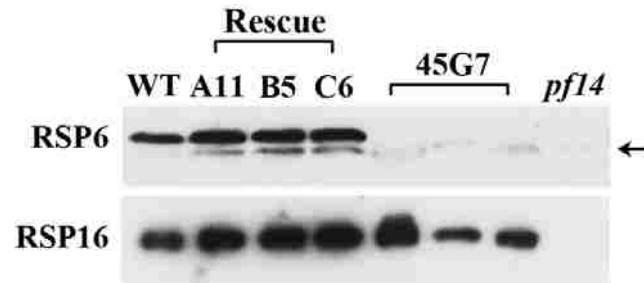
Figure 3-8. Transformation of the RSP6 gene restored RSP6 to the 45G7 axonemes.
Axonemes were prepared from three transformants, *45G7*, *pf14* and WT and probed for RSP6 and RSP16, which served as a positive control. Three different amounts of 45G7 axonemes were loaded. As shown by the arrow, anti-RSP6 sometimes recognized an unknown protein that was also present in radial spokeless mutant *pf14*.
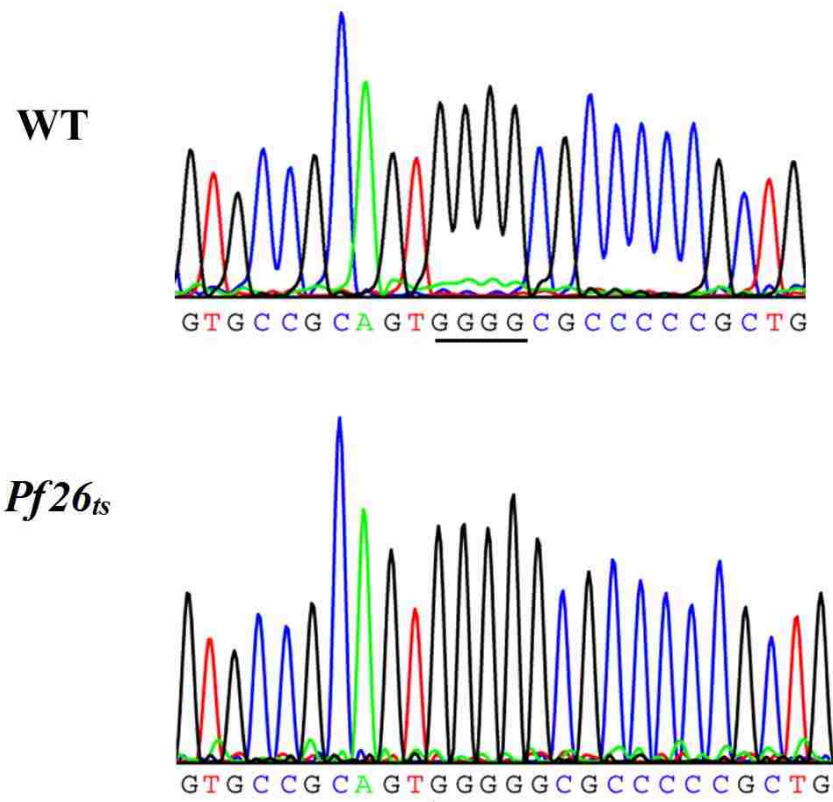
Figure 3-9. Sequencing of the 3' end of RSP6 gene revealed the mutation in *pf26ts*.
Sequencing of the 3' end PCR products revealed an additional G at the 3' end of RSP6 gene in the *pf26ts* mutant.

3.3 Duplicated RSP4/6 Genes are not Universal

Chlamydomonas RSP4 and RSP6 are encoded by two duplicated genes tandemly aligned in linkage group V. They share 48% identical a.a. residues distributed throughout the molecules (Curry et al., 1992). Two copies of highly conserved RSP4/6 genes are also present in human and mouse (Eriksson et al., 2001; Castleman et al., 2009). As the significance of the two duplicated genes appeared different, we questioned if duplicated RSP4/6 is universal after all. To test this, the BLASP program at National Center for Biotechnology Information (NCBI) was used to conduct a search using the essential *Chlamydomonas* RSP4 as a query. Although only the genomes of selected organisms were analyzed, it is evident that mammals (Figure 3-10, brackets) and many protists harbor two or more copies. The branches of phylogeny trees and multiple sequence alignment showed that the two genes from *Chlamydomonas* (arrowheads) were much more similar to each other than to any one of the human orthologues. Crucially, only one RSP4/6 gene was found in the other branches of eukaryotes, including zebrafish, beetle, *Drosophila* and sea urchin. As the *Drosophila* genome is sequenced, it is clear that the duplicated RSP4/6 gene is not universal and not essential. Consistently, only a single RSP4/6 protein is present in the purified Ciona radial spoke complex (Satouh et al., 2005). Thus the ancestral eukaryote likely only had a single RSP4/6 gene. It is possible that two identical proteins are assembled into the spoke head. For the organisms that contain the duplicated RSP4/6 gene, one copy may have diverged resulting in a slightly different function.
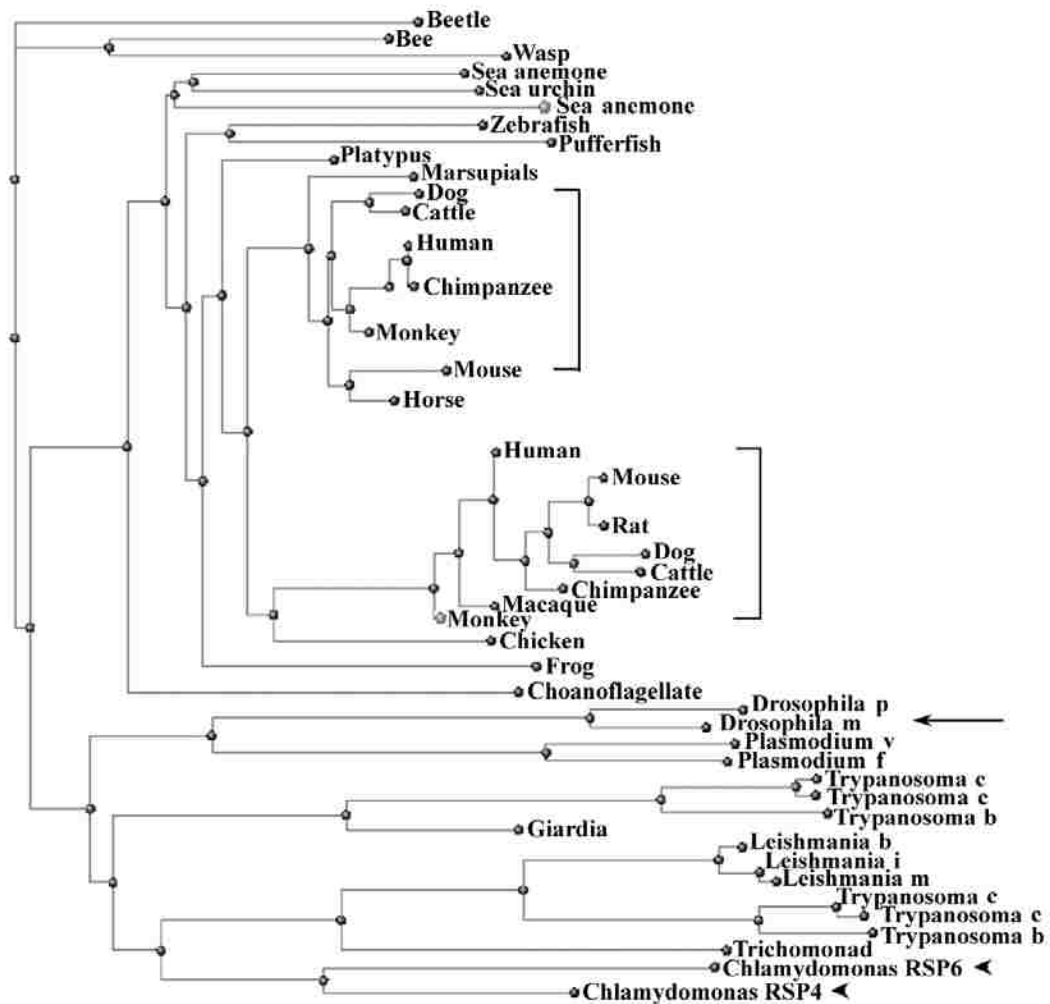
Figure 3-10. Phylogeny tree revealed that two duplicated genes for RSP4 and RSP6 are not present in every organism with motile cilia and flagella. For example, *Drosophila melanogaster* (arrow) only contains one RSP4/6 gene, while the two RSP4/6 orthologous genes in mammals form two distinct sub-trees (brackets). Notably, *Chlamydomonas* RSP4 and RSP6 (arrowheads) are most homologous to each other rather than to either of the mammalian sub-trees. For clarity, redundant sequences were deleted and scientific names for organisms were replaced by common names.

3.4 The Motility of RSP6 Mutants is Overtly Sensitive to Culture Conditions

Liquid cultures for axoneme preparation and EM were usually harvested from early stationary phase with a density of ~2 X 10^7 cells/ml 4 days after inoculation from agar plates. A small number of RSP6-minus cells swam. Strikingly, the culture harvested two days earlier for transformation appeared almost like WT culture. We postulated that the motility of the RSP6-minus cells was overtly sensitive to the culture condition, like *pf25*, which is deficient in RSP11 and RSP8 (Yang and Yang, 2006). To test this, 1C12 cells were inoculated from the 7-day old algal plate stock to liquid medium and the motility (Figure 3-11A) and cell density (Figure 3-11B) were measured for 4 consecutive days (D1-D4). The rescued 1C12 transformants served as a control (WT*). As predicted, 1C12 cells generated full-length flagella within 1 hour after resuspension but the cells were paralyzed (D0, Figure 3-11A). Occasionally, several cells jiggled or moved locally. The motility level did not change significantly within the same day. The percentage of swimmers gradually increased in the next two days during early log phase as shown by the cell density plot (D1 and D2, Figure 3-11B) and then declined as the culture approached or reached the stationary phase (D3 and D4). Although the absolute percentages and density plots varied in each preparation, all exhibited a similar bell-shape curve in motility changes. Replacing exhausted medium with fresh medium reduced the deterioration level in the next day, similar to the result using *pf 25* cells (Yang and Yang, 2006), suggesting that the motility of 1C12 cells was sensitive to media conditions. In contrast, flagellated WT* cells were always motile.

To clarify if the mixed populations of distinct motility were due to additional mutations, the 1C12 cell cultures was placed under light for 1 hour to separate

A
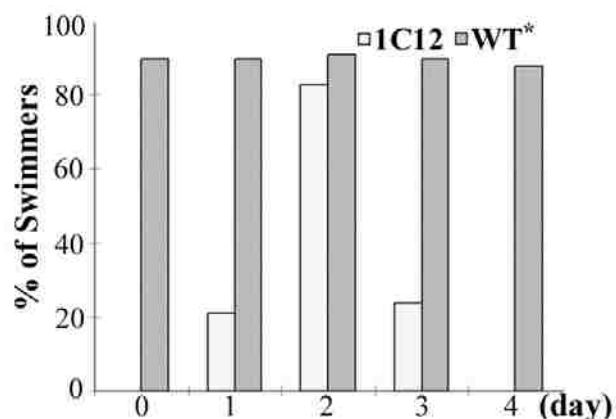
B
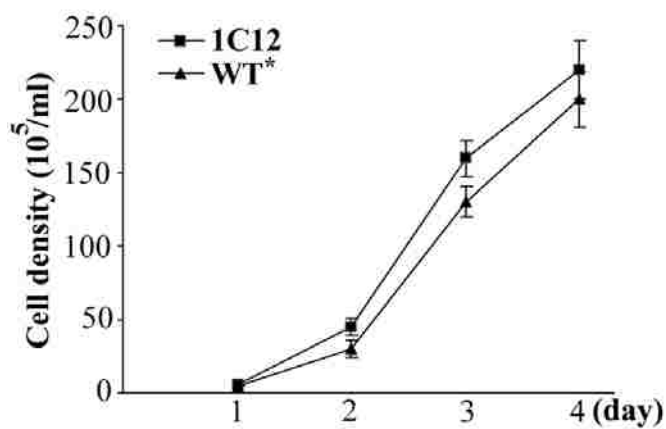
Figure 3-11. The changing motility phenotypes of 1C12 cells.
(A) Representative histogram demonstrating changes in the percentage of swimmers during 5 consecutive days of the liquid culture of 1C12 (open bars) and rescued 1C12 control (WT*, gray bars). Freshly resuspended 1C12 cells from agar plates (Day 0) were paralyzed. Motility improved during the early log phase and then declined as the culture reached the stationary phase. The percentages of 1C12 swimmers during the culture period were lower than WT swimmers ($p<0.05$, student's t test). (B) A representative plot of cell densities of WT* (triangle) and 1C12 cells (square). The density at the inoculation date was too low to determine. At the fourth day, the culture reached stationary phase. Each data point was the average from four measurements.

motile and immotile cells. The top fraction that was enriched with motile cells and the bottom fraction that contained more paralyzed cells were separated and replated on agar plates. The suspension of single colonies from both fractions still exhibited similar bell-shape curves in motility changes, similar to the result using *pf25* cells (Yang and Yang, 2006) . Thus, the mixed motility was an inherent phenotype caused by the absence of RSP6 molecule in the radial spoke.

The velocity of motile 1C12 cells that can translocate significantly in a lateral direction was measured as well using the MetaMorph software. Surprisingly, the velocity was only slightly slower than WT* cells (Figure 3-12). Moreover, the velocity of both 1C12 and WT swimmers did not fluctuate dramatically over the three days. Therefore, absence of RSP6 did not significantly affect the velocity of motile 1C12 cells.

Interestingly, the motility level of 1C12 cells was sensitive to temperature. The motility of $pf26_{ts}$ was determined by the temperature at which flagellar assembly occurred. Shifting temperature afterwards did not affect motility (Huang et al., 1981). In contrast, the 1C12 swimmers with motile flagella generated at room temperature (~24°C) became completely paralyzed within 1 hour at 32°C (Table 3-2). The motile fraction decreased at 28°C as well. Paralysis did not recover on the same day after the temperature returned to 24°C. Thus, although RSP6 is not essential, the RSP6-minus cells easily become paralyzed at higher temperature or in spent media.

3.5 Motile RSP6 Mutant Cells Cannot Maintain a Helical Trajectory

As 1C12 swimmers at the permissive temperature and in the early log phase appeared almost like WT* control, video microscopy and image analyses were performed to
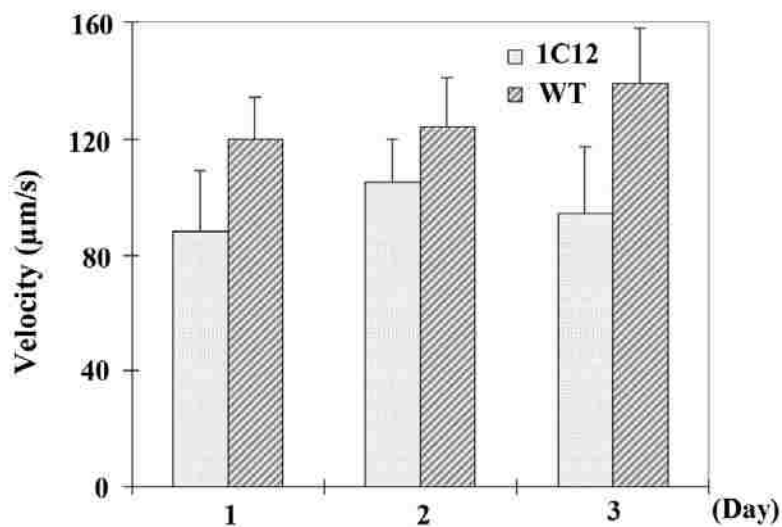
Figure 3-12. 1C12 swimmers were only slightly slower than WT cells.
The velocity of 1C12 (open bars) and WT* (gray bars) was measured on three consecutive days. The swimming velocity of 1C12 cells was slower than WT cells on the three days ($p < 0.05$, student's *t* test). Each data point was obtained from the average of 20-30 individual cells.

Table 3-2. Temperature-sensitive paralysis of 1C12 swimmers.

	Log phase	Stationary phase
24 °C	80%	20%
28 °C	40%	5%
32 °C	0%	0%

The percentage of swimmers showed temperature-sensitive paralysis of RSP6-minus cells. 1C12 swimmers, either from the log-phase or stationary-phase culture, became completely paralyzed within 1 hour after transferring to the water bath at 32°C. The motile fraction was greatly reduced at 28°C as well. Each number was obtained from the average of six randomly chosen fields.

analyze their movement. Both WT rescue (WT*) and 1C12 were very light sensitive,

turning toward the illumination source and thus sticking to the glass slide or cover slip.

To prevent the light-induced movement, a 625 nm-cutoff filter was inserted in the optic

path to remove short wavelength stimulating light and the image was recorded by a light-

sensitive CCD camera. As shown by the tracked motion, most WT* cells maintained

helical trajectories fairly well under the filtered illumination (Figure 3-13, left panel).

Contrarily, except the few cells that move locally, the 1C12 processive swimmers in the

log phase actually changed direction frequently, failing to maintain helical trajectories

(right panel). Consistently, the velocity was only slightly slower (compare the length of

the tracks). The light sensitivity of WT* and 1C12 precluded the possibility of waveform

analysis as high-speed video-microscopy requires bright light to compensate short

exposure durations (Yang et al., 2008).

3.6 The Axonemal Defect of 1C12 Cells is Exacerbated in Spent Media

To further assess motility, in vitro reactivation of cell models was conducted. WT* and

1C12 cells from the early log-phase (day 2, D2) and early stationary-phase (day 4, D4)

culture were first permeabilized with a detergent. Cells became completely paralyzed

after the removal of flagellar membrane and intraflagellar fractions. The cell models were

reactivated with 0.5 mM MgATP. Without flagellar membrane and intraflagellar

fractions, the axonemal structure can be directly assessed in this experiment. For the day

2 culture, the percentages of motile reactivated cells for mutant and WT* control

prepared from the log-phase culture were similar, although the mutant group evidently

contained more spinners (Figure 3-14). Interestingly, although 1C12 cells were all
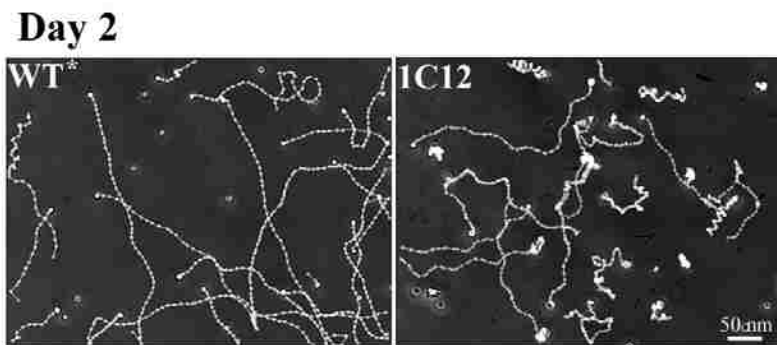
Figure 3-13. 1C12 cells failed to maintain helical trajectories.
Many WT* cells display helical trajectory. In contrast, the 1C12
swimmers from log-phase culture changed directions frequently
without a discernable trajectory. Yet the distance that processive
1C12 swimmers transversed was not significantly different from that
of WT* cells.
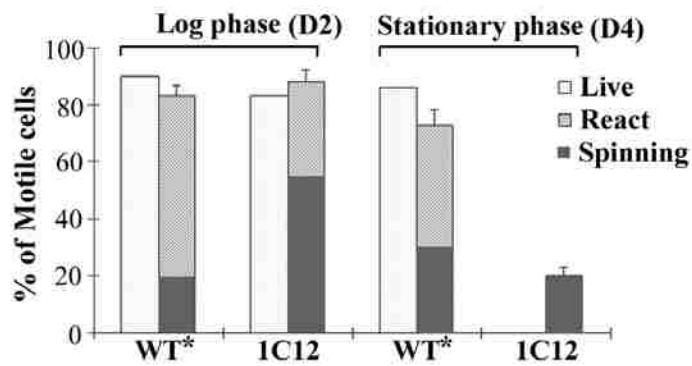
Figure 3-14. The effect of media on the motility of WT and 1C12 mutant cells.
Motile fractions of live cells and reactivated cell with a buffer containing detergent and 0.5-mM ATP were determined for the log phase and stationary phase cultures. The reactivated motile cells were further classified into swimmers that transverse processively and spinners that rotated around a fixed spot. Spinners were more prominent in 1C12 cell model and in older cultures of WT*. Notably, despite complete paralysis in early stationary phase, a fraction of reactivated 1C12 cell models still can spin. Each data point was the average from four measurements.

paralyzed at D4, 20% of the cell models were motile, albeit spinning only. The motile

fraction of reactivated WT* cell model from the log phase was slightly lower but the ratio

of spinners increased significantly. Thus, RSP6-minus cells have a higher propensity to

spin while their axonemes in paralyzed cells could enable cell models to swim but could

not allow live cells to move at all. Furthermore, there were more spinners of WT cells at

stationary phase than those in log-phase, suggesting that spent media also reduced the

reactivation level of WT* axonemes albeit less prominently as 1C12 axonemes.

This in vitro reactivation system was also used to test if the reversible paralysis is

caused by phosphorylation. Previous research shows that PKA inhibitors (PKI) enhance

the dynein-driven sliding velocity and increased the motile permeabilized cells upon

reactivation (Hasegawa et al., 1987; Gaillard et al., 2006). However, the percentage of

reactive 1C12 cells was similar between the group with or without PKI (Figure 3-15).

Thus, the paralysis of 1C12 cells in spent media appeared unrelated to mis-regulated

PKA activity.

3.7 Drastic Reduction of Spoke Heads in Flagella from Spent Media Cultures

To test whether the paralysis of RSP6-minus spoke heads was due to an exacerbated

assembly defect of the spoke head, spokes were extracted from axonemes with 0.6 M KI

buffer and separated by velocity sedimentation through a 5-20% sucrose gradient. Since a

major fraction of WT radial spokes precipitated following a routine 16-hour

centrifugation (Yang et al., 2005), a shorter centrifugation period was tested. As expected,

the peaks of radial spokes sedimented in fractions #5 and #7 respectively following a 12-

or 10-hour centrifugation (Fig. 3-16). The 12-hour centrifugation period was chosen for
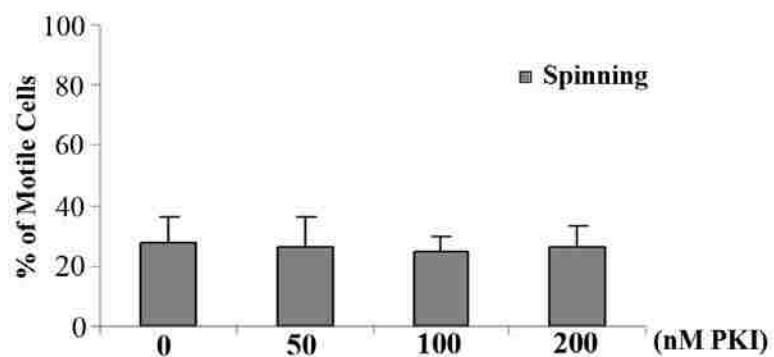
Figure 3-15. The effect of PKI on the reactivated cell model.
Paralyzed 1C12 cells at the stationary phase were demembranated and then reactivated in the presence of 0.5 mM ATP or ATP+PKI of indicated concentrations. Each data point was the average from four measurements.
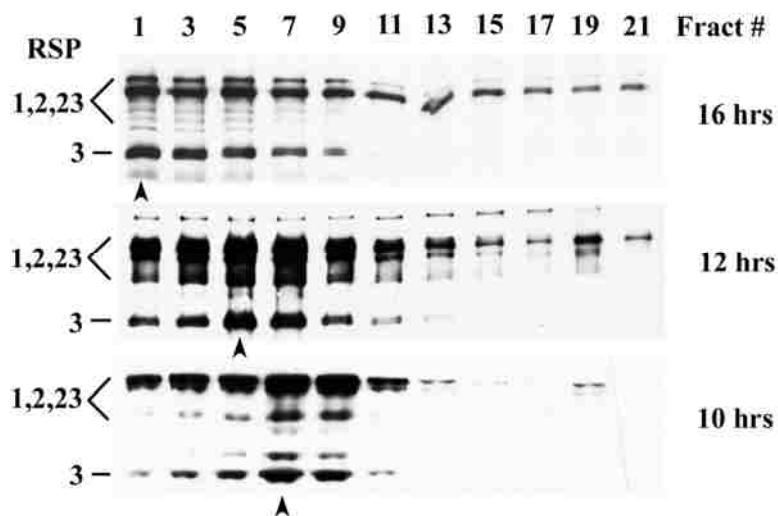
Figure 3-16. The duration of centrifugation significantly influenced the sedimentation profile of the radial spoke particles.
Western blots of sucrose gradient fractions (1-21, bottom to top) of KI extracts from WT axonemes following centrifugation for 16, 12, or 10 hours were probed with the antibody raised against the isolated radial spoke complex. The radial spoke peak (arrowhead) sedimented deeper into the gradient after longer centrifugation. Note that this polyclonal antibody recognized multiple large radial spoke proteins including RSP1, RSP2, and RSP23 that migrated at similar positions in SDS-PAGE.

the presence of the entire radial spoke peak in the gradient and a better separation among peaks.

To prepare a large quantity of flagella for sucrose gradient, the cells were harvested from 8-liter stationary phase cultures after 6 days in liquid culture. The cells were entirely paralyzed. The fractions were probed for RSP1, 4, 6 in the spoke head and RSP3 in the stalk as a control. As anticipated, all four radial spoke proteins in the rescued 1C12 (WT*) gradient sedimented as 20S particles with the peak in fraction #7 (Figure 3-17A). Surprisingly, RSP4 and RSP1 were barely detectable in the gradient of the mutant (upper panel, compare with WT* #7 fraction). Furthermore, the major fraction of the residual RSP1 and RSP4 sedimented near the top of the gradient (fraction #19), indicative of dissociation. On the contrary, the stalk protein RSP3 was not reduced and sedimented as a slightly smaller particle (compare two arrowheads in the two gradients). Thus, RSP6-minus spoke heads in such preparations decreased drastically and were unstable.

We reasoned that the diminished spoke head content was an extended scenario of the reduced spoke head that was observed occasionally from the 4-day-old small liquid culture (Figure 3-1A) at the stationary phase and the deficiency revealed by western blots might be more prominent and reproducible if axonemes were prepared from older cultures. To test this, axonemes were prepared one day later, from the late stationary phase (Day 5) liquid culture, and from 7-day old agar plates (the stock that were usually used for inoculation of liquid cultures). The cells from both preparations were entirely paralyzed. The controls were the early log-phase 1C12 liquid culture with about 80% swimmers and WT* cultures. RSP3, a stalk protein, provided a loading control. The spoke contents in WT* axonemes prepared from the three types of cultures were not
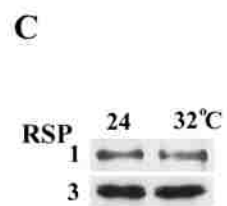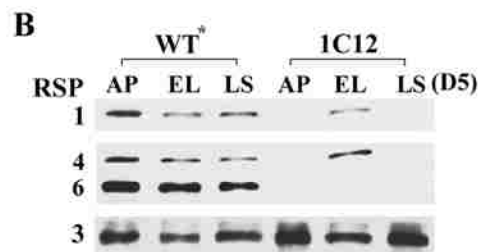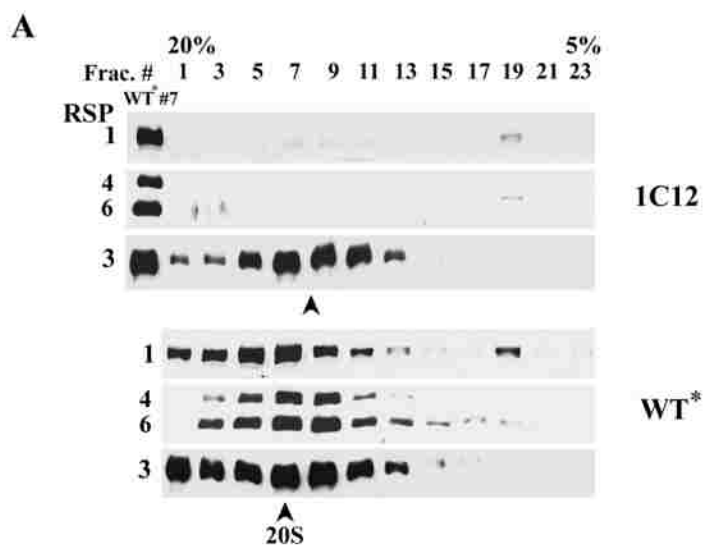
Figure 3-17. Western blots showed drastic reduction of radial spoke head domain in flagella of mutant cells grown in spent medium.
(A) Radial spoke extracted from WT* axonemes, as shown by the bands of RSP1, 3, 4 and 6 sedimented around fraction 7 as 20S intact particles (arrowhead) in the sucrose gradient. Compared to fraction 7, RSP1 and 4 from the 1C12 gradient were drastically reduced. Furthermore, a major fraction of these two proteins sedimented near the top of the gradient, indicative of dissociation. In contrast, stalk proteins in 1C12, represented by RSP3, were not reduced and sedimented as a slightly smaller particle (compare the two arrowheads). (B) The spoke head proteins were drastically reduced in the axonemes from 1C12 harvested from 7-d old agar plates (AP) and late stationary phase liquid culture (LS, Day 5). All cells were entirely paralyzed. However, these proteins from the early log phase (EL) with many swimmers were comparable with WT* samples that were not notably affected by the media conditions. (C) Temperature-induced paralysis was not caused by drastic dissociation of radial spoke heads. 1C12 axonemes were prepared from the log-phase culture, either maintained at 24°C or shifted to 32°C for 1 hour.

obviously affected. In contrast, as predicted, the amount of head proteins RSP1 and RSP4 were barely detectable in mutant axonemes prepared either from agar plates (AP, Figure 3-17B) or the late stationary phase culture (LS), but appeared normal in the early log phase culture (EL) with an abundance of swimmers. Thus the motility as well as the spoke head assembly of RSP6 mutants was much more sensitive to media conditions than was WT.

To test if the paralysis at the restrictive temperature was also due to dissociation of the spoke head, we compared axonemes prepared from duplicated early log-phase 1C12 cultures, one maintained at 24°C and the other placed at 32°C for 1 hour in which cells were entirely paralyzed. Western blots showed that spoke head amounts, represented by RSP1, were similar (Figure 3-17C), indicating that the temperature-induced paralysis was not due to a drastic dissociation of the RSP6-minus spoke head.

Collectively, these results showed that RSP6, unlike its paralogue RSP4, is nonessential for the assembly of the spoke head or motility. However, it promotes the assembly of the spoke head when the media become exhausted and enables the swimmers to maintain the typical helical trajectory. The irregular trajectory of RSP6-minus cells strongly suggests frequent asynchrony of these cells is due to a dysfunctional RSP6-minus spoke head module that can not interact with the central apparatus consistently during oscillatory beating.

Chapter 4: Molecular Interactions of Radial Spoke Head Proteins

4.1 Introduction

Recent studies strongly support the hypothesis that the transient engagement between the radial spokes and central apparatus coordinate the sequential activation of subsets of dynein motors distributed throughout the axonemes (Yang et al., 2008). Lacking the entire spoke head abolishes the direct interactions leading to paralyzed flagella. Yet missing only RSP6 in the radial spoke results in irregular trajectories. To elucidate the underlying defective machinery and thus the normal transient interaction, it will require the identification of the molecules that are directly involved in the engagement and the topography of the interacting moieties. The molecules involved in the interaction will be critical for oscillatory beating and human candidate genes of primary ciliary dyskinesia.

Toward this goal, we tested the approach of chemical cross-linking to identify candidate proteins involved in the interaction. The results show the limitations of this approach and a new chemical crosslinker that is suitable for the study of axonemal complexes.

Results

4.2 C-terminal Tagged RSP6 Successfully Rescued the Defect in 1C12

To improve the detection of cross-linked products in the spoke head region, the strategy was to express 3HA-6His tagged RSP6. In theory, the His tag will allow Ni-NTA enrichment of the cross-linked products that are often of low abundance. Secondly, the 3HA tag, with 3 epitopes for the high affinitive HA antibody could help to detect cross-linked products if the cross-linking abolishes the antibody epitopes. The potential

downside is that the tag sequence, if positioned inappropriately, may interfere with the translational machinery or the assembly of the tagged protein.

The tag sequence was first added to the N-terminus of RSP6 since the C-terminus is more conserved among the orthologues than the N-terminus. In addition, the human RSP6 orthologue contains an additional 45 a.a. at the N-terminus, suggesting that a N-terminal tag to *Chlamydomonas* RSP6 will be tolerated (Figure 1-2). Lastly, the temperature sensitive mutant *pf26ts* has a mutation at the C-terminus leading to an additional 23 a.a. at the C-terminus (Figure 3-3) and motility defects at the restrictive temperature.

The coding sequence for 3HA-6His tag was amplified by PCR and inserted into the NcoI site at the start codon of the RSP6 genomic construct (Figure 4-1A). The plasmid containing the 3HA-6His tagged RSP6 gene was confirmed by restriction digest and sequencing. The plasmid was transformed into 1C12 along with the selection plasmid pSI103. PMM-resistant transformants were then resuspended into liquid medium for motility analysis. Among 200 colonies from three transformations, none exhibited a higher percentage of motile cells than the parental 1C12 strain, contrary to the expected 10-20 clones.

To differentiate if the tag interferes with the production or assembly of RSP6, PCR was performed first to identify the transformants harboring the tagged RSP6 gene. In theory, two PCR products will be obtained from transformants receiving the tagged RSP6 gene, one from the endogenous gene and one from the tagged RSP6 gene, respectively. Among 40 transformants tested, 28 transformants incorporated tagged RSP6 gene into the genomes. However, western blots did not reveal any tagged RSP6 in these

A
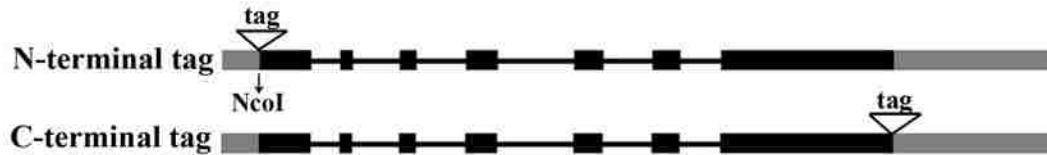
B
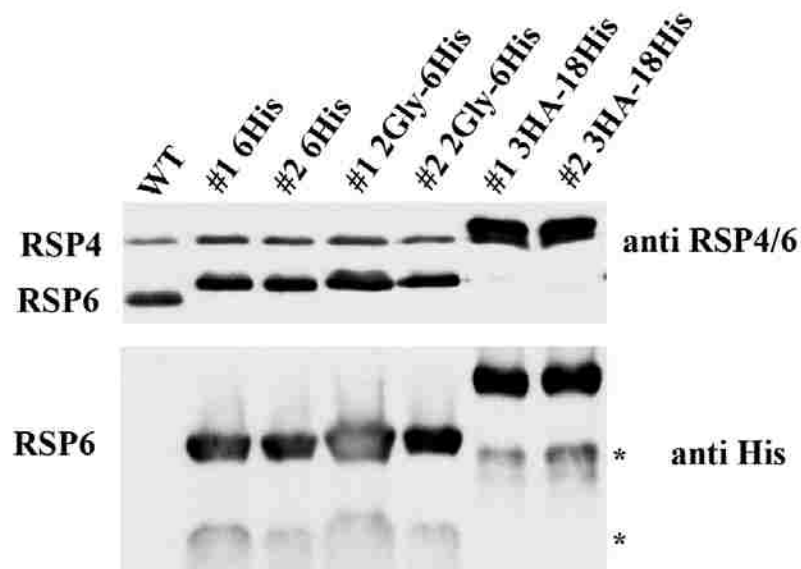
Figure 4-1. C-terminal tagged RSP6 was restored to 1C12 axoneme.
(A) The strategies for tagging RSP6 genes. The black bars represent exons and the two gray bars represent 5' and 3' UTR respectively. The lines between black bars represent introns. (B) Western analyses of axonemes prepared from motile 1C12 transformants rescued by the three different C-terminal tagged RSP6 genes. Note the tagged RSP6 was present in the three groups of transformants. Anti-RSP6 cross-reacted with RSP4 with identical sizes in all strains (upper panel). However, the three different tagged RSP6 molecules were larger than WT RSP6. The tagged RSP6 molecules were confirmed by anti-His western blot (bottom panel). The smaller bands (asterisk) were likely generated from an in-frame ATG downstream to the start codon.

transformants regardless of axonemes or cell bodies. Thus, the addition of a tag sequence at the very N-terminus of RSP6 gene likely interfered with the translation of the tagged RSP6 gene. This tag sequence may not be suitable for N-terminal tagging.

We then generated three RSP6 genes tagged at the C-terminus. The first one expressed RSP6-6His. In case the positively charged tag interferes with the assembly of the acidic RSP6, the second construct expressed an additional two glycine (Gly) residues preceding the 6His tag. The additional small neutral amino acids were predicted to position the positive tag farther away from RSP6 molecule. The third plasmid contained a 3HA-18His tag sequence. The long tag may improve the sensitivity of western blots and Ni-NTA affinity purification.

The three tagged RSP6 constructs were individually co-transformed with the selection plasmid pSI103 into the 1C12 strain respectively. The PMM-resistant clones were screened for motility first. Interestingly, many clones from all of the three groups exhibited ~100% swimmers like WT strains (Table 4-1). Thus, the C-terminus is suitable for tagging.

To show that the tagged RSP6 was restored, axonemes were prepared from two representative transformants from each group and an untagged WT strain. Western blots probed with anti-RSP6 and anti-His showed that the tagged RSP6 was present in all tested transformants (Figure 4-1B). As expected, RSP6-6His was larger than untagged RSP6 (Figure 4-1B, upper panel). The additional two glycines did not increase the protein size significantly, whereas RSP6-3HA-18His appeared much larger, co-migrating with RSP4.

Anti-His also revealed a weak smaller band in all transformants, but not the WT

Table 4-1: Transformation of 1C12 cells with RSP6 gene carrying one of the three tags at the C-terminus.

	6His	2Gly-6His	3HA-18His
Total Clones	145	70	130
*Rescued Clones	12	13	9
Rescue rate	8%	18%	7%

*, the clones containing ~ 100% motile cells were designated as rescued clones.

(Figure 4-1B, lower panel). The one from 3HA-18His clones was larger than those
 from the other two groups. Based on the size of these second products, they were likely
generated from an alternate in-frame ATG encoding M128 residue. These smaller bands
were not recognized by anti-RSP6. Thus the epitope of anti-RSP6 that did not detect any
N-terminal truncated RSP6 in 45G7 and 1C12 axonemes was near the N-terminus. This
finding supported the prediction that the axonemes in these RSP6 mutants do not contain
truncated RSP6 polypeptides (Chapter 3).

4.3 BMOE Successfully Cross-linked RSP6 to Axonemal Proteins

The strain containing RSP6-3HA-18His was chosen for cross-linking because using this
strain, the cross-linked complexes can be detected by anti-HA. Several crosslinkers with
different arm lengths and reactive groups were tested (Table 4-2). In general, the cross-
linking from the long-arm crosslinkers (e.g., EGS, DTSSP) is less selective than those
with a short space arm (e.g., EDC, DFDNB) that were often used in cross-linking studies
of axonemes. However, the long-arm crosslinker may cross-link RSP6 to central pair
proteins. BMOE that only reacts with the sulfhydryl group in cysteine could be useful for
RSP6 that contains 7 cysteine residues (Figure 4-2). Moreover, products cross-linked
with reversible crosslinkers (DTSSP and EGS) could be cleaved, allowing the separation
of individual cross-linked proteins.

Axonemes containing RSP6-3HA-18His were treated with each crosslinker of
increasing concentrations. Cross-linking was assessed by western analyses probed for
RSP6, His or HA. Six crosslinkers (Table 4-2) did not generate distinct cross-linked
RSP6 bands in SDS-PAGE at the concentrations examined. Two examples were shown

Table 4-2. Crosslinkers used in the study.

Crosslinker	Arm length	Reactive groups	Cleavable
EDC	0	$-NH_2$, $-COOH$	**-**
DFDNB	0.3 nm	$-NH_2$, $-NH_2$	**-**
DTSSP	1.2 nm	$-NH_2$, $-NH_2$	$+$
DSS	1.1 nm	$-NH_2$, $-NH_2$	**-**
MBS	0.9 nm	$-NH_2$, $-SH$	**-**
EGS	1.6 nm	$-NH_2$, $-NH_2$	$+$
*BMOE	0.8 nm	$-SH$, $-SH$	**-**

*, the only crosslinker that cross-linked RSP6 into resolvable products in SDS-PAGE.

```
MAADVGQALAFLQQVKTTQGASIYEGLKAALAKVLED
RPVNAVEALETSVLSTPPAANLSVPLVPAASAAAAAA
AVAKASLFGDPEPVLDPESGEPIDPDAPNEFECEDVE
GDGDLLDGLGVGLGRQEMYAAMLAVKRLGEDAKRGVS
TVRFFGKFFGTQADYYVFETTLQSNPDMPEAPEGTIP
LEPYGEGVNAYIYFVSNTLGGPLQQLPYVTPEQIKAS
RLLRRYLTGRLDAPVSAFPAFPGNEANYLRALIARIS
AATVCCPRGFFTADDDSAELSANDEWVPLKGREMALP
VNWSHRYAHLKGQGRTVTHKRDPPDEEEEPEKNFWTA
EEMEAGPPPLATLDTDAPLPAATGDKVPPPAWSPVFA
SASVTTRNQVAGVRSNRWPGAVCACAGRHFTSMYVGW
GIKAGGEWSPCPPPPPVPQWGAPAAGVEGGQQLLLEC
NDLPPKPAPPEEEDE
```

Figure 4-2. Amino acid sequence of *Chlamydomonas* RSP6.
The seven cysteine (C) residues are highlighted in red.

A

B

RSP6

0 0.05 0.1 0.2 0.4 (mM DFDNB)

RSP6

0 0.2 0.4 0.8 (mM DTSSP)

C

kDa

#5
#4
#3
#2

—170
—130

#1

RSP6
—95
—72

0 0.2 0.4 (mM BMOE)
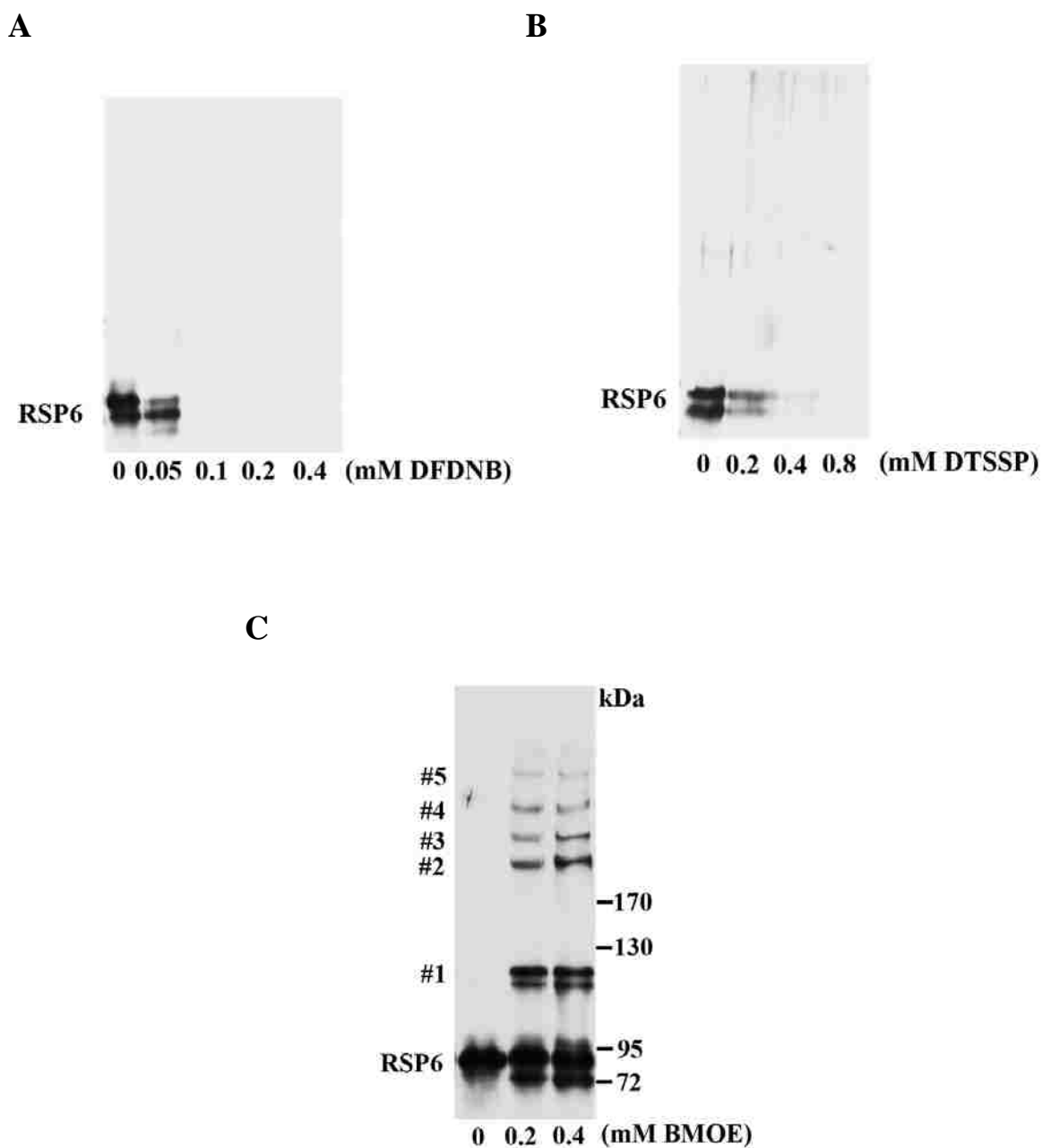
Figure 4-3. Western blots revealed distinct tagged RSP6 oligomers cross-linked by BMOE.
Axonemes from RSP6-3HA-18His strain were incubated with crosslinkers including DFDNB (A), DTSSP (B) or BMOE (C) with increasing concentrations. The blots of cross-linked axonemes were probed for -HA. Note, BMOE cross-linked RSP6 into 5 products of distinct sizes, "#1-#5" while the other two did not generate discernable products in the SDS-PAGE. The molecular weights were indicated on the right of the C panel.

in Figure 4-3A and B. As the concentrations of DFDNB and DTSSP were increased, the

intensity of RSP6 band, revealed by anti-HA, decreased while no larger bands emerged.

The absence of resolvable cross-linked product from these crosslinkers appears to be due

to cross-linking of multiple molecules instead of abolished epitope, since none of the

three antibodies can detect any RSP6 cross-linked complex.

Nonetheless, DTSSP-cross-linked axonemes containing tagged RSP6 or untagged

RSP6 (control) were denatured and the supernatant was subjected to Ni-NTA purification.

The rationale is that this reducible crosslinker can be cleaved, thus the cross-linked

proteins can then be separated by SDS-PAGE and revealed by silver stain. The proteins

specifically cross-linked to RSP6 were supposed to be present in tagged RSP6 axonemal

sample but absent in the control. However, silver protein gels failed to identify distinct

bands that were cross-linked and pulled down specifically (Figure 4-4).

Interestingly, the sulfhydryl crosslinker BMOE, as revealed by HA antibody,

generated at least 5 distinct cross-linked products larger than RSP6 (Figure 4-3C). The

cross-linking level largely plateaued at 0.4 mM BMOE (Figure 4-5A). A band smaller

than RSP6 was possibly generated from intra-molecular cross-linking (Figure 4-3C). The

multiple cross-linked products were consistent with the 7 cysteine residues in RSP6. The

tag does not contain any cysteine residue. Therefore, BMOE selectively cross-linked

RSP6 to individual proteins while the other compounds cross-linked RSP6 to a huge

multi-protein complex.

Contrary to the HA antibody, anti-RSP6 only recognized two of the five cross-

linked bands (#1 and #2, Figure 4-5B) and the band intensity was rather low. Anti-His

failed to detect any RSP6 cross-linked product. The lower sensitivity of anti-His and anti-
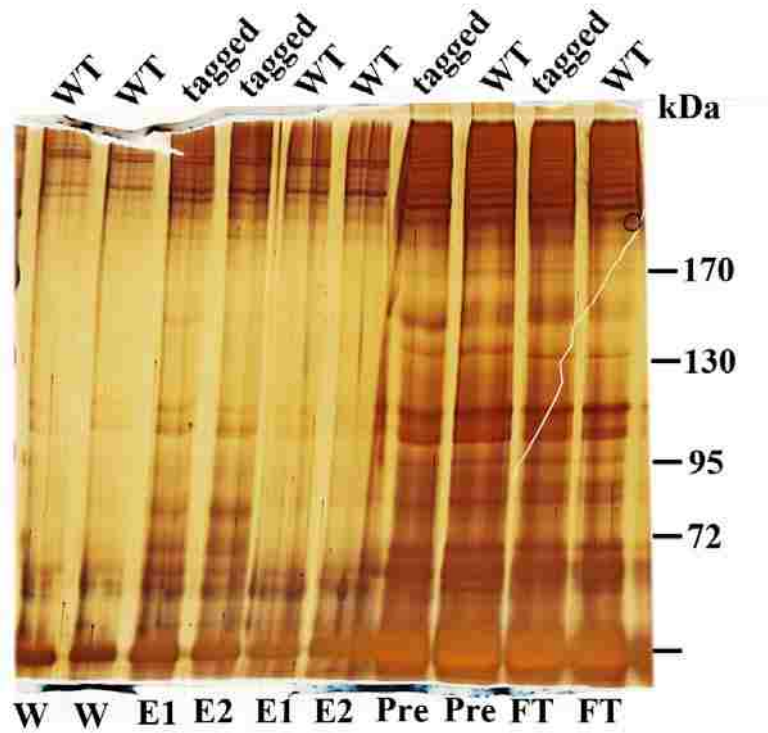
Figure 4-4. Ni-NTA purification of cross-linked tagged RSP6 under denatured conditions.
DTSSP-cross-linked axonemes were solubilized in denature buffer. The extract was processed for Ni-NTA affinity. The samples were assessed by silver stained SDS-PAGE. Control was untagged WT strain. Pre, extract of cross-linked axonemes; FT, flow through; W, wash; E, elute.

A
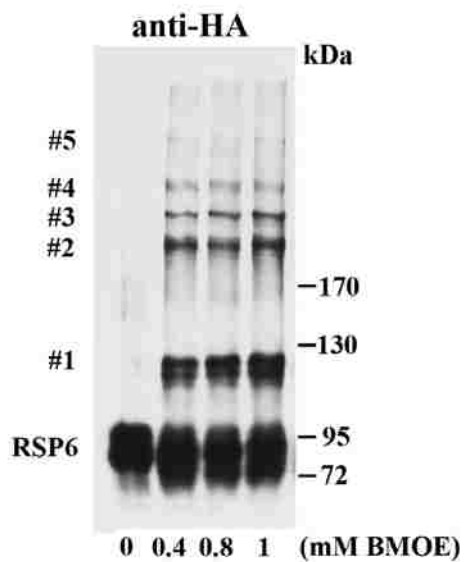
B
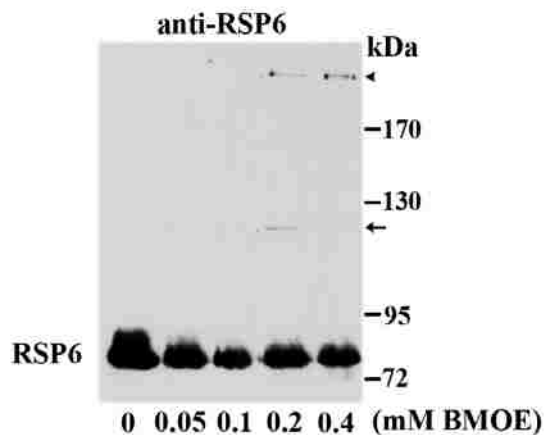
Figure 4-5. HA antibody (A) is more sensitive than anti-RSP6 (B) in detecting cross-linked products.
Axonemes containing RSP6-3HA-18His were incubated with BMOE of increasing concentrations. HA blots revealed 5 cross-linked products while RSP6 antibody only detected the #1 (arrow) and #2 (arrowhead) products. The molecular weights were indicated on the right.

RSP6 in revealing RSP6 cross-linked products are likely due to lower affinity, loss of epitopes or smaller amounts of cross-linked products. This shows the value of a 3HA tag for this approach.

4.4 Intra-molecular Complex Cross-linking

Considering the close proximity of radial spokes to the central apparatus, RSP6 may be cross-linked to proteins in the central apparatus or the radial spokes. If the cross-linking occurs within radial spokes, cross-linking of isolated radial spokes may result in the same bands. To test this, axonemes from RSP6-3HA-18His were extracted with 0.6 M KI. The extract containing solubilized radial spoke complex was sedimented through a sucrose gradient and the 20S radial spoke fractions were treated with BMOE. HA western blots revealed only cross-linked product #1 in the isolated radial spokes (Figure 4-6). Thus, this band likely contained another radial spoke protein. The rest of the cross-linked bands (#2-#5 in Figure 4-5A) may contain the central pair proteins. Alternatively, KI extraction may alter the conformation of the radial spokes.

To differentiate these two possibilities, axonemes of the central apparatus mutant *pf18* and the control, untagged WT, were treated with BMOE and the cross-linking result was revealed by anti-RSP6 instead (Figure 4-7). In theory, any band from cross-linked RSP6 and central pair protein will be absent in the cross-linked axoneme missing the central apparatus.

However, none of the central apparatus mutants actually lacks all central pair proteins. Electron microscopy (EM) revealed that amorphous material remained in the center of *pf18* axonemes. Since detergents during flagellar demembranation destabilize
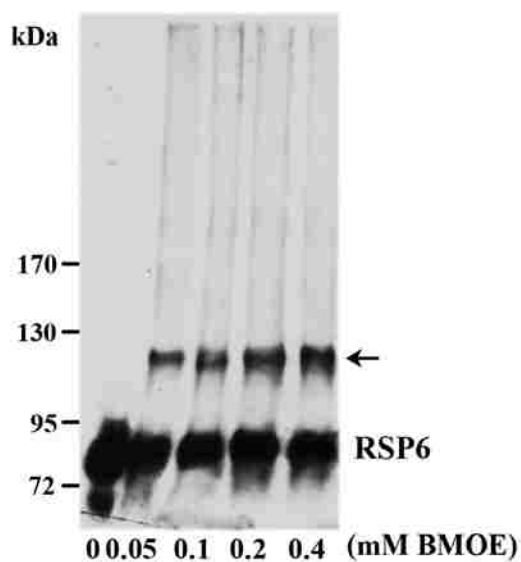
Figure 4-6. The #1 cross-linked product was resulted from intra-radial spoke cross-linking.
Isolated radial spokes from sucrose gradient fractions of KI extract from RSP6-3HA-18His axonemes were treated with increasing concentrations of BMOE. The cross-linked products were revealed by western blot probed with anti-HA. Only one cross-linked product (#1, by arrow) was generated in significant amount.

A
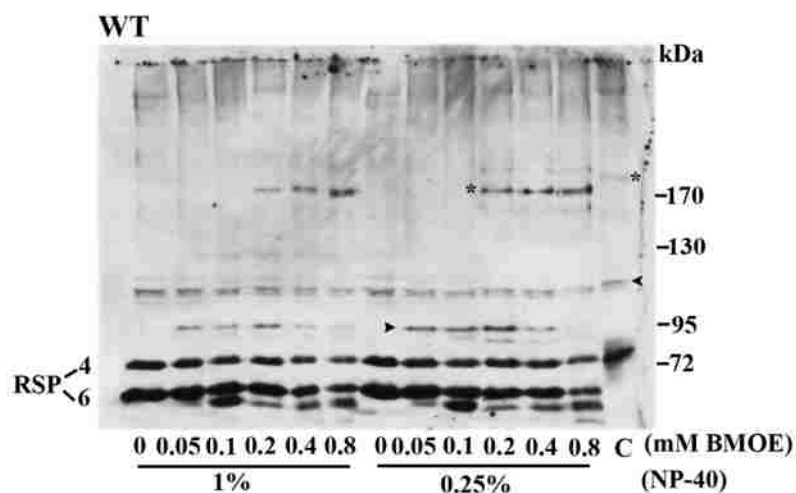
B
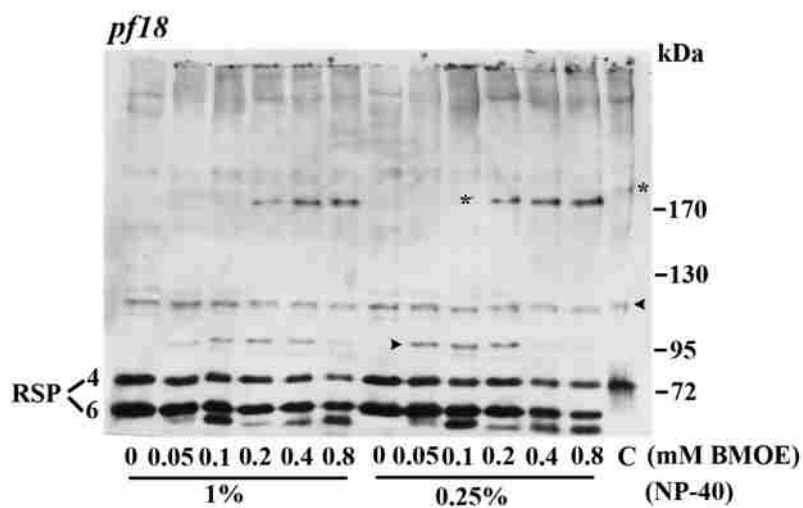
Figure 4-7. Similar cross-linked RSP6 products in BMOE-treated axonemes of WT (A) and *pf18* (B) strain that lacks the central apparatus. Axonemes, after treatment with 0.25% and 1% NP-40, were reacted with BMOE of indicated concentrations and the cross-linked products were identified by RSP6 western blots. Note Anti-RSP6 cross-reacted with RSP4. Control (C) was cross-linked axonemes containing RSP6-3HA-18His. Tagged RSP6 in the control co-migrated with RSP4. The #1 (arrowhead) and #2 (asterisk) cross-linked products from tagged axoneme appeared slightly larger than those from untagged WT axonemes. Cross-linking results in WT and *pf18* axonemes prepared from two detergent concentrations were similar, suggesting that both bands were from intra-radial spoke cross-linking. The molecular weights are indicated on the right.

central pair components (Mitchell, 2009), flagella were treated with 0.25% and 1% detergent (Nonidet-P40) respectively. An additional control was cross-linked tagged axonemes (Figure 4-7, lane C). Two BMOE-cross-linked complexes in WT axoneme corresponded to the slightly larger #1 and #2 cross-linked tagged RSP6 in the control (arrowhead and asterisk in Figure 4-7A). These two RSP6 cross-linked bands in WT were also present in *pf18* (Figure 4-7B). These results suggest that at least #1 and #2 bands resulted from intra-radial spoke cross-linking and show the limitation without the tag.

To identify the rarer #3-#5 cross-linked products, tagged and untagged WT axonemes (control) were treated with 0.4 mM BMOE and then denatured by urea-containing buffer. The supernatant was subjected to Ni-NTA purifications. The samples were separated by SDS-PAGE. Silver stain showed that Ni-NTA purification indeed enriched RSP6 and #2 cross-linked complex (Figure 4-8, arrowhead and asterisk). However, many additional bands prevent unequivocal identifications of the other cross-linked complex. Most bands also appeared in the WT axoneme albeit with lower intensities. Our previous experience suggested that radial spoke proteins exhibited affinity to Ni-NTA possibly because of the acidic pI (Table 1-1) and thus some of these non-specific bands may actually be radial spoke proteins. Because of difficulties in identifying cross-linked products and possible intra-radial spoke cross-linking, mass spectrometry will not be performed to identify the unknown proteins in #3-5.

4.5 Identification of Unknown Proteins Cross-linked to RSP6 with Western Blots

The candidate protein approach was taken to reveal the proteins cross-linked to RSP6. The blots of cross-linked axoneme were probed with other radial spoke antibodies. The
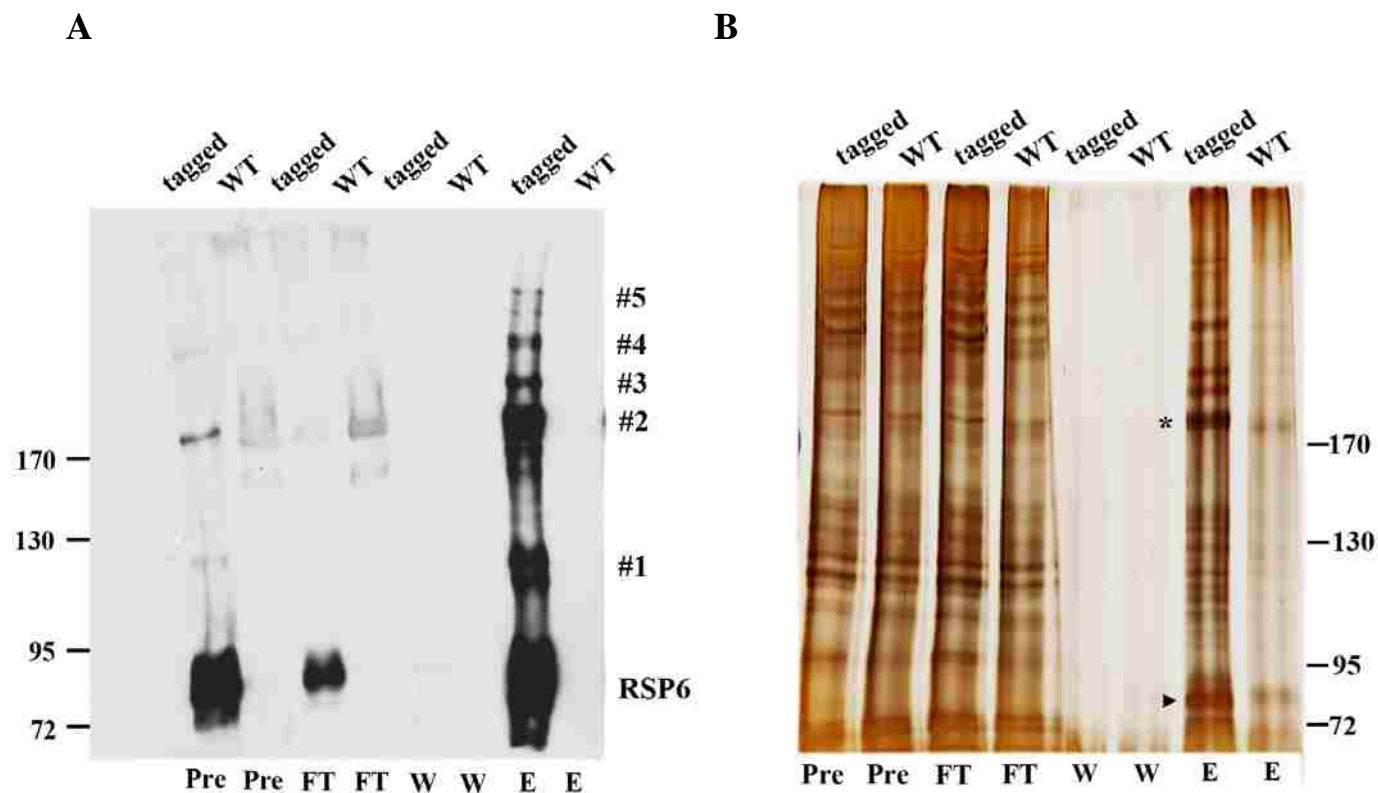
Figure 4-8. Ni-NTA purification of cross-linked tagged RSP6 under denatured conditions.
Protein samples were assessed by HA western blot (A) and silver stain (B). Only RSP6 (arrowhead) and #2 cross-linked RSP6 (asterisk) can be unequivocally identified in the elute. Control was untagged WT strain. Pre, extract of cross-linked axonemes; FT, flow through; W, wash; E, elute.

antibody was chosen based on the sizes of these cross-linked complexes derived from the log plot (Table 4-3). The log of a protein's molecular mass is proportional to the distance it will migrate (Neville, 1971).

Candidate proteins that could be cross-linked to RSP6 are spoke head proteins (RSP1, 4, 9, 10) and stalk proteins that are predicted to be adjacent to the spoke head (RSP2, 5, 16, 23). Note all these proteins contain at least two cysteine residues (Table 4-4). In contrast, RSP3 that is essential for the assembly of the entire spoke (Diener et al., 1993), does not contain any cysteine.

Cross-linked axoneme blots were first probed with the RSP5 antibody (Figure 4-9A and B). This antibody recognized a band (labeled with arrow) of the same size of tagged RSP6 in tagged axonemes, regardless if treated with crosslinker or not. But it was absent in the untagged WT axoneme (Figure 4-9B). Since anti-RSP5 was raised against His-tagged RSP5 recombinant protein, the band was actually the RSP6-3HA-18His detected by anti-His in the RSP5 serum. Similarly, anti-RSP16 that was also raised against His tagged RSP16 recognized the tagged RSP6 as well. Thus although His tag is supposed to be of low antigenicity, it is still antigenic and poses unexpected problems in this approach.

BMOE cross-linked the 120 kDa RSP2 into a 150 kDa product (asterisk, Figure 4-9C). The band did not appear to contain RPS6 or RSP10 (see below). The other possibility is RSP9. However, the affinity of RSP9 antibody was too low to detect any cross-linked band (not shown).

4.6 RSP6 was cross-linked to RSP10 and RSP1

Table 4-3: Estimated molecular masses of the five cross-linked RSP6 complexes and involved partners.

	Size of Cross-linked product (kDa)	Size of partners (kDa)
RSP6	67	
RSP6-3HA-18His	85	
#1	115	30
#2	185	100
#3	205	120
#4	220	135
#5	280	195

Table 4-4: The molecular masses and the numbers of cysteines in the radial spoke proteins.

	Molecular Mass (kDa)	Cysteines
RSP6	67	7
RSP6-3HA-18His	85	7
RSP4	76	5
RSP1	123	6
RSP10	24	2
RSP9	26	3
RSP2	118	3
RSP5	69	6
RSP16	34	3
RSP23	102	1
RSP3	86	0
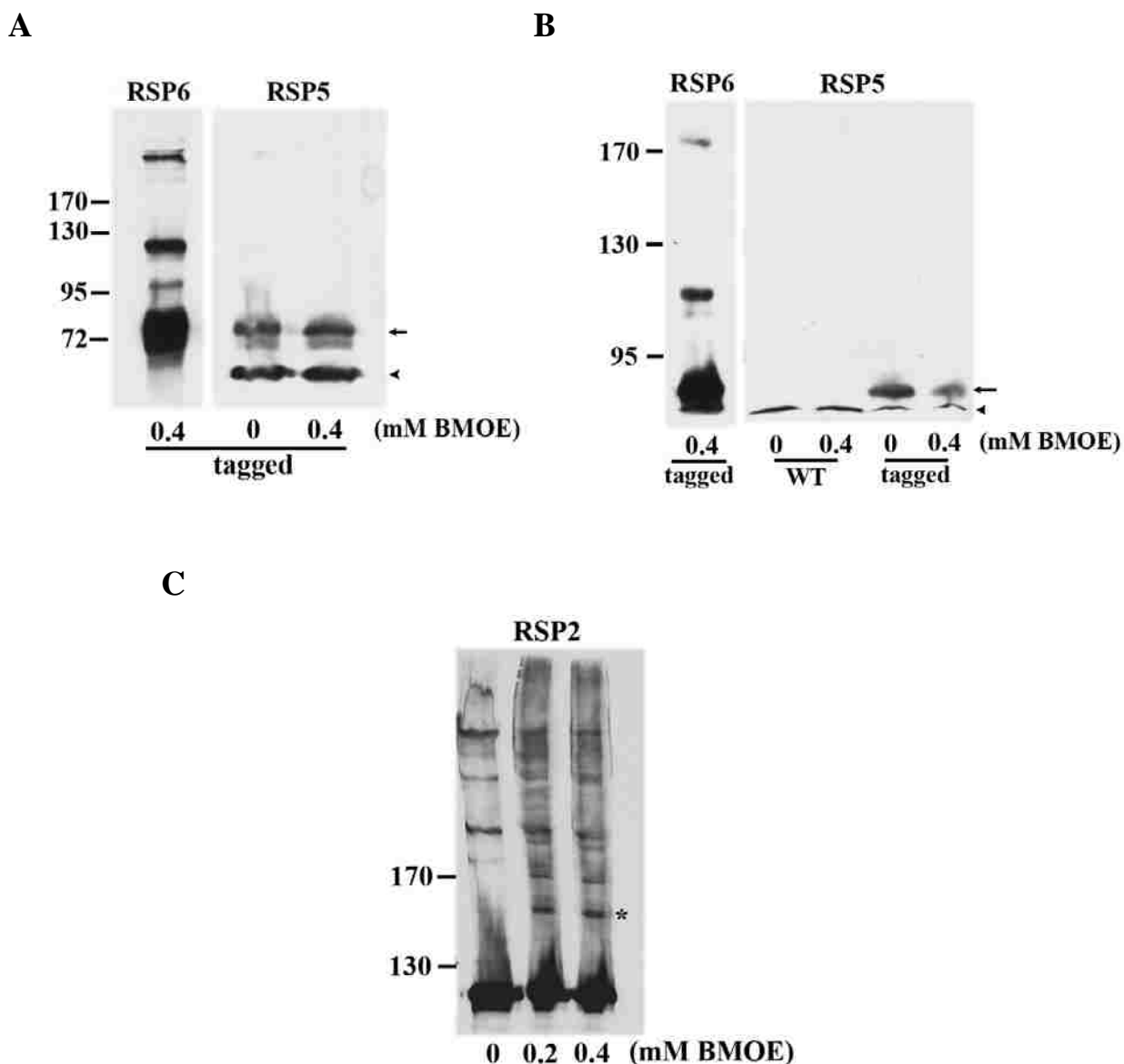
Figure 4-9. RSP5 and RSP2 antibodies did not definitively recognize any of the RSP6 cross-linked products.
WT and tagged axonemes treated with BMOE were subjected to 16% (A), 7% (B) and 8% (C) SDS-PAGE and probed for HA (left panel in A and B), RSP5 (right panel in A and B) and RSP2 (C). Arrow, tagged RSP6; Arrowhead, RSP5; Asterisk, one possible RSP2 cross-linked complex. Anti-RSP5, that was raised against His-tagged RSP5 fusion protein, recognized RSP5 (arrowhead) as well as the His-tagged RSP6 (arrow). The non-specific bands from RSP2 in non-crosslinked sample prevented the interpretation of the other cross-linked products. The molecular weights were indicated on the left.

To determine if BMOE cross-linked RSP10 to RSP6, cross-linked axonemes were

subjected to western analyses (Figure 4-10). A ~120 kDa RSP10-containing complex

appeared in cross-linked tagged axoneme (asterisk on the 4th lane, Figure 4-10A),

corresponding to the #1 RSP6 cross-linked band (arrowhead). Consistently, the cross-

linked WT axoneme contained a smaller 95 kDa cross-linked band that included RSP10

and untagged RSP6 (asterisk on the 2th lane in Figure 4-10A, Figure 4-7A). Aside from

the RSP10-RSP6 complex, the RSP10 antibody also revealed a ~130 kDa complex

(diamond, Figure 4-10A) in cross-linked axonemes, either with tag or untagged RSP6.

Thus, BMOE also crosslinked RSP10 to a non-RSP6 protein, possibly the RSP6

paralogue, RSP4.

To test whether RSP6 was cross-linked to RSP1, different concentrations of

BMOE were added to axoneme with RSP6-3HA-18His and the cross-linking result was

detected by western blot with anti-HA and anti-RSP1. Interestingly, several RSP1 cross-

linked complexes appeared after addition of BMOE and one of these band co-migrated

with the #3 RSP6 cross-linked band (Figure 4-11). It suggested that RSP6 is in close

proximity to RSP1.

4.7 Discussion

In summary, the 0.8-nm long BMOE cross-linked RSP6 to at least RSP10 and RSP1.

Note RSP4 and RSP6 are paralogues while both RSP1 and RSP10 contain MORN motifs.

The cross-linking of these molecules supports a topographic model that will be discussed

further in the next chapter. As no unequivocal evidence implicating central pair proteins

in the rest RSP6 cross-linked products, the urgency of identify them with mass

A
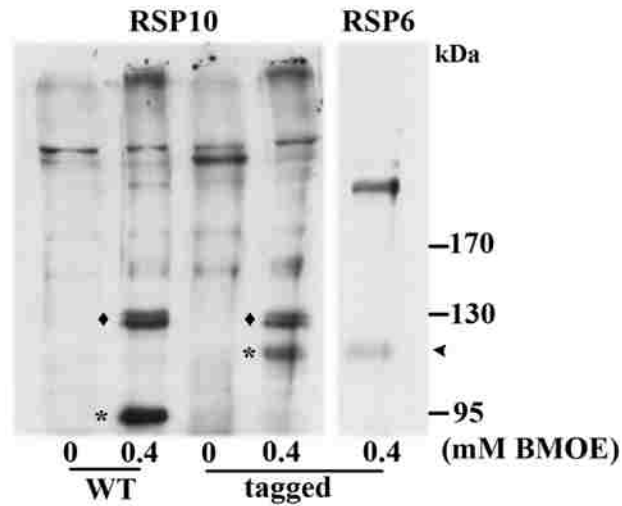
B
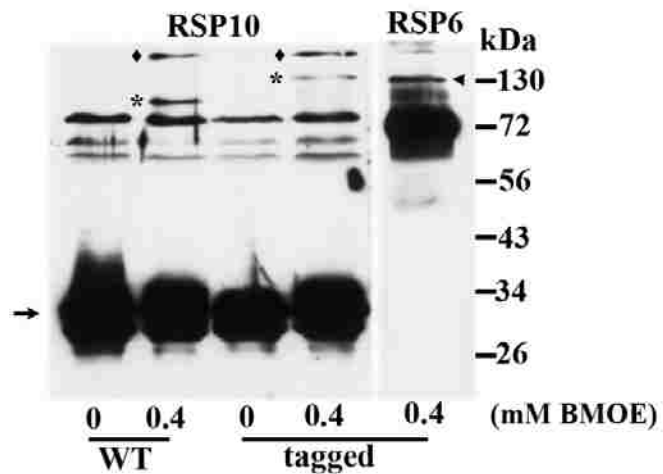
Figure 4-10. RSP6 and RSP10 were cross-linked by BMOE.
BMOE-treated axonemes were fractionated by 7% (A) and 14% (B) SDS-PAGE respectively and probed for the 27 kDa RSP10 (arrow, left panels) and HA (right panels). Asterisks, cross-linked 95 kDa complex containing RSP10 and untagged RSP6 in WT axonemes vs the 120 kDa complex in the cross-linked axonemes with tagged RSP6; arrowhead, #1 tagged RSP6 cross-linked product; diamond, a cross-linked 130-kDcomplex containing RSP10 and a non-RSP6 protein. The molecular weights were indicated on the right.
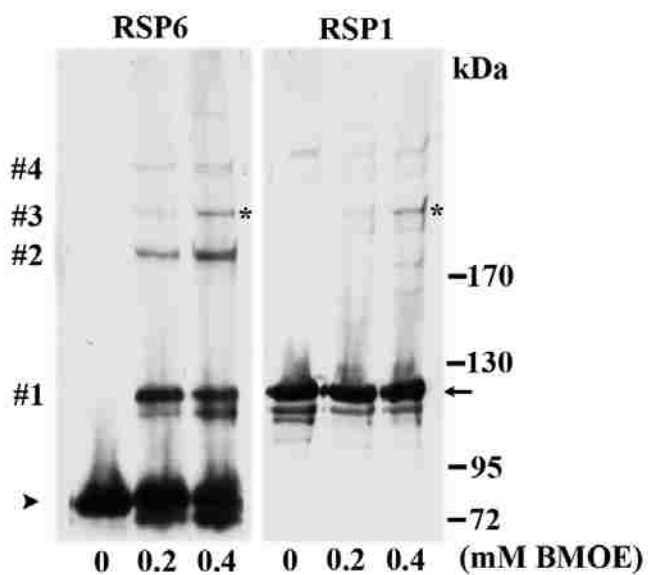
Figure 4-11. The #3 RSP6 cross-linked product contains RSP1.
BMOE-treated tagged RSP6 axonemes were probed for HA (left panel) and RSP1 (right panel). Asterisk, the co-migrated bands; arrowhead, tagged RSP6; arrow, RSP1. The molecular weights were indicated on the right.

spectrometry is low.

Several factors may explain this problem. Despite the proximity between the central apparatus and radial spokes under EM, it is possible only a fraction of radial spokes actually contact the central apparatus at any moment. Furthermore, the preparation of axonemes may dislocate the interacting proteins. Moreover, cysteine residues in both molecules may not be properly positioned near each other and antibodies are not sensitive enough to detect the presence of RSP6 cross-linked complexes by western analyses. Moreover, cross-linking preferentially occurs within the structural modules first rendering huge inter-cross-linking products too large to resolve in SDS-PAGE. Lastly, Ni-NTA purification of cross-linked axonemal samples was not as specific as desired and did not enrich the larger cross-linked products.

The short crosslinkers, EDC and DFDNB, are the most commonly used crosslinkers for the study of axonemes. However, they failed to cross-link RSP6 into resolvable products in SDS-PAGE. In contrast, long-arm length crosslinker resulted in large axonemal complexes that cannot be resolved in SDS-PAGE. Yet BMOE succeeded to cross-link proteins within the spoke head module, indicating that this rather long crosslinker is effective and selective because of its specific interaction with cysteine residues. On the other hand, this specificity excludes its usage in proteins that don't have cysteines.

Chapter 5: Discussion

The study on the mutants and molecular interactions of the spoke head shed light on the the 9+2 axoneme and primary ciliary dyskinesia.

5.1 Distinct Roles of RSP4 and RSP6

The phenotypes of two new RSP6 mutants are different from the typical motility mutants that display steady-state deficiencies in motility, morphology and composition. They also differ from the first RSP6 mutant, *pf26ts*, whose flagella contain the mutated RSP6 and the other spoke head proteins and whose motility will not change once flagella have assembled. The flagella of the new RSP6 mutants most likely do not contain any RSP6 polypeptides as shown by the nature of their mutations, transformation rescue (Figure 3-2) and western analyses of axonemes (Figure 3-1). Yet the rest of the spoke head components can still assemble and the flagella are motile when cells are in the log phase and at room temperature. Hence, despite the high similarity of RSP4 and RSP6, only RSP4 is essential for spoke head assembly and motility.

In line with this conclusion, the duplicated RSP4/6 genes found in green algae and mammals are not universal (Figure 3-10). Several organisms, including *Drosophila melanogaster*, sea urchin and *Ciona intestinalis* have only one copy of the RSP4/6 gene. Interestingly, the fly genome sequence has been completed and the purified radial spoke in *Ciona intestinals* also only contains a single RSP4/6 band (Satouh et al., 2005). For those organisms that have only a single RSP4/6 gene, the gene product may function as a homodimer, since RSP4 and RSP6 extracted by concentrated KI buffer do not associate

with RSP1 but remain co-sedimenting with each other, likely as a heterodimer (Kelekar et al., in press).

The 2nd RSP4/6 paralogue is used differently in different organisms. Although nonessential for the motility of green algae in the ideal laboratory condition, RSP6 ensures motility when the conditions deviate, at slightly higher temperature or in spent media. In fact, such deviations, not the laboratory condition, are the norm in the natural habitat. In this sense, the second paralogue is essential to confer a competitive edge against evolutionary pressure. For human and mouse, both northern blots (Eriksson et al., 2001) and EST profiles showed that one of the two RSP4/6 genes, RSHL1, is only expressed in testis. Contrarily, the other gene encoding RSPH4A is expressed in all tissues with motile cilia and flagella and is a causative gene for primary ciliary dyskinesia (Castleman et al., 2009). Thus RSPH4A, likely equivalent to RSP4, is essential for all motile cilia and flagella in mammals while RSHL1 may enhance fertility.

The distinct roles of RSP4 and RSP6 suggested that the two paralogues are not interchangeable and RSP4 cannot substitute for RSP6. Consistently, the amount of RSP4 in 1C12 axoneme was not more abundant than that in WT (Figure 3-1; 3-17). The tight control of translation may also prevent the paralogues from replacement. Radial spoke proteins are synthesized with similar kinetics (Remillard and Witman, 1982). Moreover, the existing protein pool in the cell body is maintained at a level sufficient to generate flagella of half the normal length (Rosenbaum et al., 1969). Therefore, there may not be redundant RSP4 molecules in 1C12, either in rich or spent media, to replace RSP6.

5.2 The Reversible Paralysis and Media-dependent Spoke Head Assembly Deficiency of RSP6-minus Mutants

The most perplexing phenotypes of RSP6 mutants and the RSP11 mutant *pf25* are mixed

populations of cells with drastically different motility despite identical genetic

backgrounds, and a 2-day lag to reach maximal percentage of swimmers. Although

axonemal protein kinase inhibits the dynein-driven sliding of radial spoke mutant

axonemes (reviewed by Wirschell et al., 2007) and inhibition of PKA activity enhances

the reactivation rate of WT axonemes (Hasegawa et al., 1987) and the reactivated cell

model of a motile RSP3 mutant (Gaillard et al., 2006), paralyzed *pf25* or *pf26* cells will

not become motile after treatment with the kinase inhibitor staurosporine, which is

effective in vivo (e.g. Zhang and Snell, 1994). The possibilities of preferential selection

of motile cells or second mutations have also been ruled out (Yang and Yang, 2006).

It is not due to the progression of cell cycles either, since replacement of the exhaust

culture with fresh media can prevent the paralysis of 1C12 cells. Therefore, the motility

swing can be best explained by the varied assembly deficiencies detected by western

blots (Figures 3-1 and 3-17B), with reductions of spoke head proteins being apparent

when most mutant cells become immotile. We reason that the lag of obvious assembly

defects is because of the stringent requirement of radial spokes for oscillatory beating and

the limited sensitivity of western analyses.

One question is how media affect the radial spoke assembly of RSP6-minus

mutant but not WT (Figure 3-17B). The availability of nutrients and the reduced

assembly efficiency of the defective complexes can adequately explain different facets of

the changing phenotypes. One possibility is that the spoke head without RSP6 are less

stable. However it is hard to explain that the instability increases only in the spent media

and there is no evidence that the general disassembling rate increases in such a condition

either. We postulate that without RSP6, the other spoke head components assemble at a reduced rate. The inefficiency is negligible in healthy cells but becomes evident when nutrients are restricted, in spent media or on agar plates in which nutrients diffuse passively. Under the deprived conditions, a myriad of cellular reactions are critically reduced and yet the assembly of all components into WT radial spokes remains coupled, albeit slower. However, the assembly of spoke heads without RSP6 becomes even slower than that of spoke stalks, leading to the delivery of a mixed population of spokes, with or without the spoke head content, into flagella. The stalk by itself, once assembled into the axonemes, can not be repaired as spoke head by itself may not be delivered into the flagella. Consequently, the motility does not improve until next day when new flagella generate after cell division and flagellar components are replenished. One day in rich media is insufficient for starved cells to recover fully and thus the percentage of swimmers does not reach the peak level until 2 days after resuspension (Fig 3-11A). Furthermore, as vegetative algal cells usually multiply four fold each day during the log phase and then the rate tapers toward the stationary phase (Harris, 2009), the cell density, the available nutrients and the nutritional state of every cell may vary after logarithmic growth.

The media-dependent assembly deficiency likely is not unique to RSP6 or radial spoke mutants. Although western blots are not adequate to reveal changes in the axonemal content of WT (Figure 3-17) or *pf25* (Yang and Yang, 2006), reactivation rates of WT cells at different culture ages are not the same. The motile fraction prepared from older WT culture (D4) is only slightly lower than that from earlier culture (D2) but the fraction of spinners is significantly higher (Figure 3-14). It was noted that helical-

swimming cell models gradually became spinning as one axoneme tend to become

inactivated until eventual quiescence (Kamiya and Witman, 1984), even though the cause

of the transition was unknown. As reactivated cell models that lack RSP6 tend to spin,

the increased reactivated spinners from older WT culture (WT at D2 and D4, Figure 3-14)

may reflect subtle axonemal defects. Likewise, structural defects may underlie the

ineffectiveness of the kinase inhibitor to enhance reactivation of damaged WT axonemes

(Hasegawa et al., 1987) and RSP6-minus cell models. By the same token, the subtle

axonemal defects in conjunction with the deficiency in two radial spoke proteins may be

sufficient to paralyze old *pf25* cells.

It is quite interesting that immotile mutant cells can be reactivated to spin,

consistent with the fact that sufficient radial spokes are still present. Apparently, some

factors in vivo hinder the residual motility of a defective axoneme. Ample ATP in vitro

or removal of the hydrated flagellar glycoproteins that increase the stroke load

(Nakamura et al., 1996) are the two possibilities.

5.3 Molecular Model of the Spoke head Module

Studies of *Chlamydomonas* radial spoke mutants strongly suggest that the head module is

assembled as a subcomplex which then associates with the stalk via RSP2 and possibly

RSP2-coassembled molecule, like spoke HSP40 (RSP16) or RSP23. The connection

between these two modules of a complex that transduce force is rather intriguing.

Interestingly, spoke HSP40 and the other spoke head proteins decrease in RSP6-minus

axonemes (Figure 3-1). Perhaps, this chaperone directly interacts with RSP2 on one end

(Yang et al., 2008) and spoke head molecules on the other.

Note, the planar waveform of reactivated sea-urchin axonemes became three dimensional after incubation with anti-RSP4/6 antibody (Gingras et al., 1998), while twitching RSP16-minus flagella resemble that of various central pair mutants (Randall et al., 1964; Witman et al., 1978; Dutcher et al., 1984; Yokoyama et al., 2004). These phenotypes support the current model that bend propagation of a planar waveform, typical of the 9+2 axoneme, is founded on a mechanical feedback transduced between the central apparatus, radial spokes and 9 outer doublets that inherently beat in three dimensions (Yang et al., 2008). The failure of RSP6-minus mutant cells to maintain helical trajectories further underscores the importance of a precise feedback system in maintaining rhythmic beating and thus a helical trajectory. The question is why RSP6-minus radial spoke cannot support persistent helical trajectories.

Based on previous studies on the morphology of *Tetrahymena* radial spokes (Figure 1-3) as well as the cross-linking results from *Chlamydomonas* (Chapter 4), we postulate a symmetric topographic model for the spoke head, with RSP4/6 and RSP1/10 opposing to its paralogues (Fig. 5-1A and B). The bulbous *Tetrahymena* spoke head is composed of two central globules and two lateral hooks (Goodenough and Heuser, 1985). Consistently, *Chlamydomonas* spoke head has two pairs of homologous proteins RSP4 and RSP6, RSP1 and RSP10. Furthermore, this study provides evidence that RSP6 is cross-linked to RSP1 and RSP10 while RSP10 seems to be cross-linked to RSP4 as well.

The symmetric arrangement with two homologous pairs of spoke head proteins may enable the radial spoke to engage the central apparatus in three dimensions reversibly and repetitively around the circumference and along the length of axonemes. We envision that one pair of the paralogues is involved in the longitudinal tilt while the

A

B

C

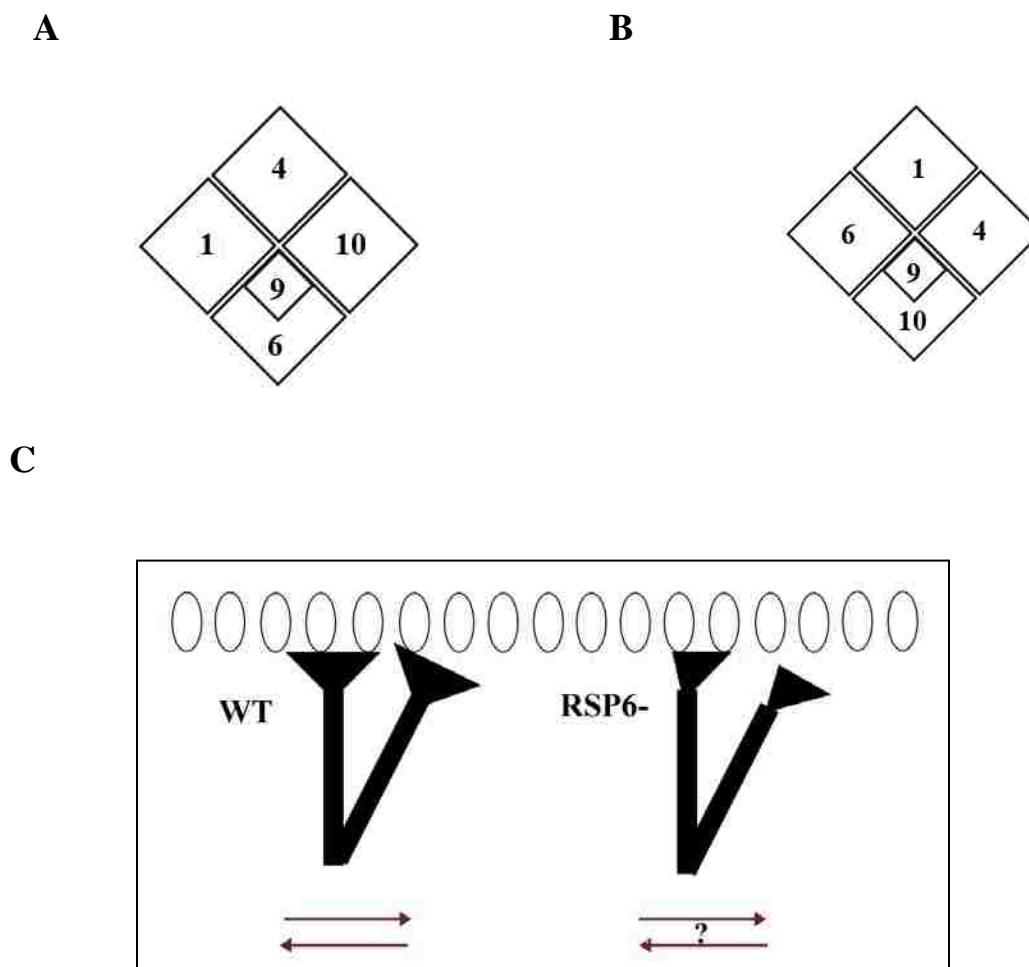**Figure 5-1. Schematic models depicting the topography of the spoke head (A and B) and the tilt-return by RSP4/6 during each beat cycle (C).**
In A and B, RSP9 is postulated to be located underneath the rest of the spoke head proteins and bundle them into a stable complex. In C, the ellipses represent different central pair projections. The black T represents the radial spoke. The red arrows represent tilt directions.

other for circumferential tilt. Flagella with intact spoke heads in place enable cells to swim in a helical trajectory. RSP6-minus radial spokes, or radial spokes lacking a few spoke heads cause glitches of this repeated movement (Figure 5-1C) leading to asynchrony and subsequent beat re-initiation and changes in trajectory directions. When media become exhausted and the metabolism is suppressed, further deficiencies result in frequent asynchrony, sporadic stalling and hence local moving cells. Those flagella in which spoke deficiencies exceed a threshold level become immotile. Yet the reduction is not significant enough to be reliably revealed in protein gels (Huang et al., 1981) or western blots that are influenced by protein loads and antigen-antibody affinities unless the axonemes are prepared from the older cultures than usually used, in which spoke heads are decreased drastically.

This progressive investigation has revealed a spectrum of phenotypes due to the defective radial spokes or central apparatus, such as paralysis, sporadic stalling in stroke initiation and propagation and reduced beat frequency. This study adds irregular trajectory and reversible paralysis to the list due to a milder defect. This study of the subtly defective radial spokes further underscores the role of the control system in orchestrating flagellar beating. Together these studies show the radial spokes and central apparatus employ critical and multiple mechanisms to regulate oscillatory beating and a subtle defect is sufficient to alter oscillatory beating. The condition-dependent drastic deterioration in assembly and motility of axonemes with mild defects appears to be a general phenomenon and should be considered in assessing the polygenic primary ciliary dyskinesia.

Chapter 6: Bibliography

Adams, G.M., Huang, B., Piperno, G., Luck, D.J. (1981). Central-pair microtubular complex of *Chlamydomonas* flagella: polypeptide composition as revealed by analysis of mutants. J Cell Biol 91(1):69-76.

Afzelius, B.A. (2004). Cilia-related diseases. J Pathol 204: 470-477.

Afzelius, B.A. (1981). Genetical and ultrastructural aspects of the immotile-cilia syndrome. Am J Hum Genet 33(6):852-864.

Bannai, H., Yoshimura, M., Takahashi, K., Shingyoji, C. (2000). Calcium regulation of microtubule sliding in reactivated sea urchin sperm flagella. J Cell Sci 113:831-839.

Bessen, M., Fay, R.B., Witman, G.B (1980). Calcium control of waveform in isolated flagellar axonemes of *Chlamydomonas*. J Cell Biol 86(2):446-455.

Brokaw, C.J., Luck, D.J., Huang, B. (1982). Analysis of the movement of *Chlamydomonas* flagella:" the function of the radial-spoke system is revealed by comparison of wild-type and mutant flagella. J Cell Biol 92(3):722-732.

Brokaw, C.J., and Kamiya, R. (1987). Bending patterns of *Chlamydomonas* flagella: IV. Mutants with defects in inner and outer dynein arms indicate differences in dynein arm function. Cell Motil Cytoskeleton 8:68-75.

Christensen, S.T., Guerra, C., Wada, Y., Valentin, T., Angeletti, R.H., Satir, P., Hamasaki, T. (2001).A regulatory light chain of ciliary outer arm dynein in *Tetrahymena thermophila*. J Biol Chem 276(23):20048-20054.

Castleman, V.H., et al., (2009). Mutations in radial spoke head protein genes RSPH9 and RSPH4A cause primary ciliary dyskinesia with central-microtubular-pair abnormalities. Am J Hum Genet 84:197-209.

Curry, A.M., and Rosenbaum, J.L. (1993). Flagellar radial spoke: a model molecular genetic system for studying organelle assembly. Cell Motil Cytoskeleton 24:224-232.

Curry, A.M., Williams, B.D., and Rosenbaum, J.L. (1992). Sequence analysis reveals homology between two proteins of the flagellar radial spoke. Mol Cell Biol 12:3967-3977.

Diener, D.R., Ang, L.H., Rosenbaum, J.L. (1993). Assembly of flagellar radial spoke proteins in *Chlamydomonas*: identification of the axoneme binding domain of radial spoke protein 3. J Cell Biol 123(1):183-190.

Dutcher, S.K., Huang, B., and Luck, D.J. (1984). Genetic dissection of the central pair microtubules of the flagella of *Chlamydomonas reinhardtii*. J Cell Biol 98:229-236.

Dymek, E., Wargo, M., Smith, E.F. (2002). Characterization of calmodulin and calmodulin binding proteins associated with the flagellar central apparatus. Mol Biol Cell 13: 328a.

Elizabeth, F., S., Yang, P. (2004). The radial spokes and central apparatus: mechano-chemical transducers that regulate flagellar motiliy. Cell Motil Cytoskeleton 57:8-17.

Eriksson, M., Ansved, T., Anvret, M., and Carey, N. (2001). A mammalian radial spokehead-like gene, RSHL1, at the myotonic dystrophy-1 locus. Biochem Biophys Res Commun 281:835-841.

Felix, H., Holzmann, D. (2000). Function and ultrastructure of cilia in primary ciliary dyskinesia. Schweiz Med Wochenschr 130(19):699-704.

Frey, E., Brokaw, C.J., and Omoto, C.K. (1997). Reactivation at low ATP distinguishes among classes of paralyzed flagella mutants. Cell Motil Cytoskeleton 38:91-99.

Gaillard, A.R., Diener, D.R., Rosenbaum, J.L., Sale, W.S. (2001). Flagellar radial spoke protein 3 is an A-kinase anchoring protein (AKAP). J Cell Biol 153(2):443-448.

Gaillard, A.R., Fox, L.A., Rhea, J.M., Craige, B., and Sale, W.S. (2006). Disruption of the A-kinase anchoring domain in flagellar radial spoke protein 3 results in unregulated axonemal cAMP-dependent protein kinase activity and abnormal flagellar motility. Mol Biol Cell 17:2626-2635.

Gingras, D., White, D., Garin, J., Cosson, J., Huitorel, P., Zingg, H., Cibert, C., and Gagnon, C. (1998). Molecular cloning and characterization of a radial spoke head protein of sea urchin sperm axonemes: involvement of the protein in the regulation of sperm motility. Mol Biol Cell 9:513-522.

Goodenough, U.W., Heuser, J.E. (1985). Substructure of inner dynein arms, radial spokes, and the central pair/projection complex of cilia and flagella. J Cell Biol 100(6):2008-2018.

Habermacher, G., Sale, W.S. (1996). Regulation of flagellar dynein by an axonemal type-1 phosphatase in *Chlamydomonas*. J Cell Sci 109:1899-1907.

Habermacher, G., Sale, W.S. (1997). Regulation of flagellar dynein by phosphorylation of a 138-KD inner arm dynein intermediate chain. J Cell Biol 136:167-176.

Harris, H.H. (2009) *Chlamydomonas* SourceBook, 2nd Ed. Chaper 8, Volume 1. Elsevier Inc., Oxford, UK

Hamasaki, T., Barkalow, K., Richmond, J., Satir, P. (1991). cAMP-stimulated phosphorylation of an axonemal polypeptide that copurifies with the 22S dynein arm

regulates microtubule translocation velocity and swimming speed in *Paramecium*. Proc Natl Acad Sci U S A 88(18):7918-7922.

Hasegawa, E., Hayashi, H., Asakura, S., and Kamiya, R. (1987). Stimulation of in vitro motility of *Chlamydomonas* axonemes by inhibition of cAMP-dependent phosphorylation. Cell Motil Cytoskeleton 8:302-311.

Howard, D.R., Habermacher, G., Glass, D.B., Smith, E.F., Sale, W.S. (1994) Regulation of *Chlamydomonas* flagellar dynein by an axonemal protein kinase. Cell Biol 127:1683-1692.

Hayashibe, K., Shingyoji, C., and Kamiya, R. (1997). Induction of temporary beating in paralyzed flagella of *Chlamydomonas* mutants by application of external force. Cell Motil Cytoskeleton 37:232-239.

Hendrickson, T.W., Perrone, C.A., Griffin, P., Wuichet, K., Mueller, J., Yang, P., Porter, M.E., Sale, W.S. (2004). IC138 is a WD-repeat dynein intermediate chain required for light chain assembly and regulation of flagellar bending. Mol Biol Cell 15(12): 5431-5442.

Huang, B., Piperno, G., and Luck, D.J. (1979). Paralyzed flagella mutants of *Chlamydomonas reinhardtii*. Defective for axonemal doublet microtubule arms. J Biol Chem 254:3091-3099.

Huang, B., Piperno, G., Ramanis, Z., and Luck, D.J. (1981). Radial spokes of *Chlamydomonas* flagella: genetic analysis of assembly and function. J Cell Biol 88: 80-88.

Huang, B., Ramanis, Z., and Luck, D.J. (1982). Suppressor mutations in *Chlamydomonas* reveal a regulatory mechanism for flagellar function. Cell 28:115-124.

Kelekar, P., Wei, M. and Yang, P. (2009). Isolation and analysis of radial spoke proteins. Methods Cell Biol Methods Cell Biol 92:181-196.

Kamiya, R. (2002). Functional diversity of axonemal dyneins as studied in *Chlamydomonas* mutants. Int Rev Cytol 219:115-155.

Kamiya, R., and Witman, G.B. (1984). Submicromolar levels of calcium control the balance of beating between the two flagella in demembranated models of *Chlamydomonas*. J Cell Biol 98:97-107.

King S.J., Dutcher S.K. (1997) Phosphoregulation of an inner dynein arm complex in *Chlamydomonas* reinhardtii is altered in phototactic mutant strains. J Cell Biol 136:177-191.

King, S.J., Inwood, W.B., O'Toole, E.T., Power, J., Dutcher, S.K. (1994). The bop2-1 mutation reveals radial asymmetry in the inner dynein arm region of *Chlamydomonas reinhardtii.* J Cell Biol 126(5):1255-1266.

Laemmli. U.K. (1970). Cleavage of structural proteins during the assembly of the head of bacteriophage T4. Nature. 227(5259):680-685.

Laemmli. U.K. and Favre. M. (1973). Maturation of the head of bacteriophase T4. I. DNA packaging events. J. Mol.Biol. 80(4):575-599.

Lie, H., Ferkol, T..(2007). Primary ciliary dyskinesia: recent advances in pathogenesis, diagnosis and treatment. Drugs 67(13):1883-1892.

Luck, R.A., and Piperno, G. (1988). Dynein arm mutants of *Chlamydomonas reinhardtii*. In Cell Movement. F. Warner, Editor. Alan R. Liss, Inc. New York.

Mitchell, B.F., Pedersen, L.B., Feely, M., Rosenbaum, J.L., and Mitchell, D.R. (2005). ATP production in *Chlamydomonas reinhardtii* flagella by glycolytic enzymes. Mol Biol Cell 16:4509-4518.

Mitchell, D.R., and Sale, W.S. (1999). Characterization of a *Chlamydomonas* insertional mutant that disrupts flagellar central pair microtubule-associated structures. J Cell Biol 144:293-304.

Mitchell, D.R. (2003). Orientation of the central pair complex during flagellar bend formation in *Chlamydomonas*. Cell Motil Cytoskeleton 56(2):120-129.

Mitchell, D.R., Rosenbaum, J.L. (1985). A motile *Chlamydomonas* flagellar mutant that lacks outer dynein arms. J Cell Biol 100(4):1228-1234.

Mitchell, D.R. (2009) *Chlamydomonas* SourceBook, 2nd Ed. Chaper 8, Volume 3. Elsevier Inc., Oxford, UK

Nakano, I., Kobayashi, T., Yoshimura, M., Shingyoji, C. (2003). Central-pair-linked regulation of microtubule sliding by calcium in flagellar axonemes. J Cell Sci 116:1627-1636.

Nakamura, S., Tanaka, G., Maeda, T., Kamiya, R., Matsunaga, T., Nikaido, O. (1996). Assembly and function of *Chlamydomonas* flagellar mastigonemes as probed with a monoclonal antibody. J Cell Sci 109: 57‑62.

Neville DM Jr. (1971). Molecular weight determination of protein-dodecyl sulfate complexes by gel electrophoresis in a discontinuous buffer system. J Biol Chem. 246: 6328-6334.

Nonaka S., Tanaka Y., Okada Y., Takeda S., Harada A., Kanai Y., Kido M., Hirokawa N. (1998). Randomization of left-right asymmetry due to loss of nodal cilia generating leftward flow of extraembryonic fluid in mice lacking KIF3B motor protein. Cell 95(6): 829-837.

Nonaka S., Shiratori H., Saijoh Y., Hamada H. (2002). Determination of left-right patterning of the mouse embryo by artifical nodal flow. Nature 418: 96-99.

Okada Y., Nonaka S, Tanaka Y., Saijoh Y., Hamada H., Hirokawa N. (1999). Abnormal nodal flow precedes situs inversus in iv and inv mice. Mol Cell 4(4):459-468.

Omoto C.K., Yagi T., Kurimoto E., Kamiya R.(1996). Ability of paralyzed flagella mutants of *Chlamydomonas* to move Cell Motil Cytoskeleton 33(2):88-94.

Omoto, C.K., Gibbons, I.R., Kamiya, R., Shingyoji, C., Takahashi, K., Witman, G.B. (1999). Rotation of the central pair microtubules in eukaryotic flagella. Mol Biol Cell 10(1):1-4.

Patel-King, R.S., Gorbatyuk, O., Takebe, S., and King, S.M. (2004). Flagellar radial spokes contain a Ca2+-stimulated nucleoside diphosphate kinase. Mol Biol Cell 15: 3891-3902.

Perrone, C.A., Myster, S.H., Bower, R., O'Toole, E.T., Porter, M.E. (2000). Insights into the structural organization of the I1 inner arm dynein from a domain analysis of the 1beta dynein heavy chain. Mol Biol Cell.11(7):2297-2313.

Piperno, G., Huang, B., Ramanis, Z., and Luck, D.J. (1981). Radial spokes of *Chlamydomonas* flagella: polypeptide composition and phosphorylation of stalk components. J Cell Biol 88:73-79.

Piperno, G., Huang, B., and Luck, D.J. (1977). Two-dimensional analysis of flagellar proteins from wild-type and paralyzed mutants of *Chlamydomonas reinhardtii*. Proc Natl Acad Sci U S A 74:1600-1604.

Piperno, G., Mead, K., Shestak, W. (1992). The inner dynein arms I2 interact with a "dynein regulatory complex" in *Chlamydomonas* flagella. J Cell Biol 118(6):1455-1463.

Piperno, G., Mead, K., LeDizet, M., Moscatelli, A. (1994). Mutations in the "dynein regulatory complex" alter the ATP-insensitive binding sites for inner arm dyneins in *Chlamydomonas* axonemes. J Cell Biol 125(5):1109-1117.

Porter, M.E., Knott, J.A., Gardner, L.C., Mitchell, D.R., Dutcher, S.K. (1994). Mutations in the SUP-PF-1 locus of *Chlamydomonas reinhardtii* identify a regulatory domain in the beta-dynein heavy chain. J Cell Biol 126(6):1495-1507.

Porter, M.E., Power, J., Dutcher, S.K. (1992). Extragenic suppressors of paralyzed flagellar mutations in *Chlamydomonas reinhardtii* identify loci that alter the inner dynein arms. J Cell Biol 118(5):1163-1176.

Porter, M.E., Sale, W.S. (2000). The 9+2 axoneme anchors multiple inner arm dyneins and a network of kinase and phosphatases that control motility. J Cell Biol 151: F37-42.

Prensier, G., Vivier, E., Goldstein, S., Schrevel, J. (1980). Motile flagellum with a "3+0" ultrastructure. Science 207:1493-1494.

Qin, H., Diener, D.R., Geimer, S., Cole, D.G., and Rosenbaum, J.L. (2004). Intraflagellar transport (IFT) cargo: IFT transports flagellar precursors to the tip and turnover products to the cell body. Journal of cell biology 164(2): 255–266.

Randall, J., Warr, J.R., Hopkins, J.M., and McVittie, A. (1964). A single-gene mutation of *Chlamydomonas reinhardtii* affecting motility: a genetic and electron microscope study. Nature 203:912-914.

Remillard, S.P. and Witman, G.B. (1982). Synthesis, transport and utilization of specific flagellar proteins during flagellar regeneration in *Chlamydomonas*. J.Cell.Biol. 93: 615-631.

Rosenbaum, J.L., Moulder, J.E., and Ringo, D.L. (1969). Flagellar elongation and shortening in *Chlamydomonas*. I. The use of cycloheximide and colchicine to study the synthesis and assembly of flagellar proteins. J. Cell Biol. 41:600-619.

Sakakibara, H.M., Takada, S., King, S.M., Witman, G.B., Kamiya, R. (1993). A *Chlamydomonas* outer arm dynein mutant with a truncated beta heavy chain. J Cell Biol 122 (3):653-661.

Sakakibara, H.M., Kunioka, Y., Yamada, T., Kamimura, S. (2004). Diameter oscillation of axonemes in sea-urchin sperm flagella. Biophys J 86:346-352.

Satouh, Y., Padma, P., Toda, T., Satoh, N., Ide, H., and Inaba, K. (2005). Molecular characterization of radial spoke subcomplex containing radial spoke protein 3 and heat shock protein 40 in sperm flagella of the ascidian *Ciona intestinalis*. Mol Biol Cell 16:626-636.

Sawamoto, K., Wichterle, H., Gonzalez-Perez, O., Cholfin, J.A., Yamada, M., Spassky, N., Murcia, N.S., Garcia-Verdugo, J.M., Marin, O., Rubenstein, J.L., Tessier-Lavigne, M., Okano, H., Alvarez-Buylla, A.(2006). New neurons follow the flow of cerebrospinal fluid in the adult brain. Science 311(5761):629-632.

Smith, E.F. (2002). Regulation of flagellar dynein by calcium and a role for an axonemal calmodulin and calmodulin-dependent kinase. Mol Biol Cell 13:3303-3313.

Smith, E.F., and Sale, W.S. (1992). Regulation of dynein-driven microtubule sliding by the radial spokes in flagella. Science 257:1557-1559.

Smith, E.F., and Yang, P. (2004). The radial spokes and central apparatus: mechano-chemical transducers that regulate flagellar motility. Cell Motil Cytoskeleton 57:8-17.

Smith, E.F., Lefebvre, P,A. (1997), The role of central pair apparatus components in flagellar motility and microtubule assembly. Cell Motil Cytoskeleton 38(1):1-8.

Summers, K.E., Gibbons, I.R. (1971), Adenosine triphosphate-induced sliding of tubules in trypsin-treated flagella of sea-urchin sperm. Proc Natl Acad Sci 68(12):3092-3096.

Tamm, S.L., Tamm, S. (1981). Ciliary reversal without rotation of axonemal structures in Ctenophore comb plates. J Cell Biol 89:495-509.

Wargo, M.J., Smith, E.F. (2003). Asymmetry of the central apparatus defines the location of active microtubule sliding in *Chlamydomonas* flagella. Proc Natl Acad Sci U S A 100(1):137-142.

Warner, F.D., and Satir, P. (1974). The structural basis of ciliary bend formation. Radial spoke positional changes accompanying microtubule sliding. J Cell Biol 63:35-63.

Warner, F.D., Satir, P. (1974). The structural basis of ciliary bend formation. Radial spoke positional changes accompanying microtubule sliding. J Cell Biol 63(1):35-63.

Wirschell, M., Hendrickson, T., and Sale, W.S. (2007). Keeping an eye on I1: I1 dynein as a model for flagellar dynein assembly and regulation. Cell Motil Cytoskeleton 64:569-579.

Witman, G.B., Plummer, J., and Sander, G. (1978). *Chlamydomonas* flagellar mutants lacking radial spokes and central tubules. Structure, composition, and function of specific axonemal components. J Cell Biol 76:729-747.

Witman G.B. (2009) *Chlamydomonas* SourceBook, 2nd Ed. Chaper 7, Volume 3. Elsevier Inc., Oxford, UK

Yagi T., Kamiya R. (2000). Vigorous beating of *Chlamydomonas* axonemes lacking central pair/radial spoke structures in the presence of salts and organic compounds. Cell Motil Cytoskeleton. 46(3):190-199.

Yang, C., Owen, H.A., and Yang, P. (2008). Dimeric heat shock protein 40 binds radial spokes for generating coupled power strokes and recovery strokes of 9 + 2 flagella. J Cell Biol 180:403-415.

Yang, C., and Yang, P. (2006). The flagellar motility of *Chlamydomonas pf25* mutant lacking an AKAP-binding protein is overtly sensitive to medium conditions. Mol

Biol Cell 17:227-238.

Yang, C., Compton, M.M., and Yang, P. (2005). Dimeric novel HSP40 is incorporated into the radial spoke complex during the assembly process in flagella. Mol Biol Cell 16: 637--648.

Yang, P., Diener, D.R., Rosenbaum, J.L., and Sale, W.S. (2001). Localization of calmodulin and dynein light chain LC8 in flagellar radial spokes. J Cell Biol 153: 1315-1326.

Yang, P., Diener, D.R., Yang, C., Kohno, T., Pazour, G.J., Dienes, J.M., Agrin, N.S., King, S.M., Sale, W.S., Kamiya, R., Rosenbaum, J.L., and Witman, G.B. (2006). Radial spoke proteins of *Chlamydomonas* flagella. J Cell Sci 119:1165-1174.

Yang, P. and Smith, E.F. (2009) *Chlamydomonas* SourceBook, 2nd Ed. Chaper 6, Volume 3. Elsevier Inc., Oxford, UK

Yang, P., Sale, W.S. (2000). Casein kinase I is anchored on axonemal doublet microtubules and regulates flagellar dynein phosphorylation and activity. J Biol Chem 275(25):18905-18912.

Yang, P. and Sale, W. S. 1998. The 140,000 Mr intermediate chain of *Chlamydomonas* flagellar inner arm dynein is a WD-repeat protein implicated in dynein arm anchoring. Mol. Biol. Cell 9:3335-3349.

Yang, P., Yang, C., Sale, W.S. (2004). Flagellar radial spoke protein 2 is a calmodulin binding protein required for motility in *Chlamydomonas reinhardtii*. Eukaryot Cell 3(1): 72-81.

Yang P., Fox L., Colbran R.J., Sale W.S. (2000). Protein phosphatases PP1 and PP2A are located in distinct positions in the *chlamydomonas* flagellar axoneme. J Crll Sci 113: 91-102.

Yang, P., and Sale, W. S. (2000). Casein kinase I is anchored on axonemal doublet microtubules and regulates flagellar dynein phosphorylation and activity. J. Biol. Chem. 275, 18905–18912.

Yokoyama, R., O'Toole, E., Ghosh, S., and Mitchell, D.R. (2004). Regulation of flagellar dynein activity by a central pair kinesin. Proc Natl Acad Sci U S A 101: 17398-17403.

Yokoyama, R., O'toole, E., Ghosh, S., Mitchell, D.R. (2004). Regulation of flagellar dynein activity by a central pair kinesin. Proc Natl Acad Sci U S A 101(50):17398-403.

Zhang, H., and Mitchell, D.R. (2004). Cpc1, a *Chlamydomonas* central pair protein with an adenylate kinase domain. J Cell Sci 117:4179-4188.

Zhang, Y., and Snell, W.J. (1994). Flagellar adhesion-dependent regulation of *Chlamydomonas* adenylyl cyclase in vitro: a possible role for protein kinases in sexual signaling. J Cell Biol 125:617-624.